JPRS L/10410

25 March 1982

Translation

SATELLITE HYDROPHYSICS

Ed. by

B.A. Nelepo

FBIS FOREIGN BROADCAST INFORMATION SERVICE

NOTE

JPRS publications contain information primarily from foreign newspapers, periodicals and books, but also from news agency transmissions and broadcasts. Materials from foreign-language sources are translated; those from English-language sources are transcribed or reprinted, with the original phrasing and other characteristics retained.

Headlines, editorial reports, and material enclosed in brackets [] are supplied by JPRS. Processing indicators such as [Text] or [Excerpt] in the first line of each item, or following the last line of a brief, indicate how the original information was processed. Where no processing indicator is given, the information was summarized or extracted.

Unfamiliar names rendered phonetically or transliterated are enclosed in parentheses. Words or names preceded by a question mark and enclosed in parentheses were not clear in the original but have been supplied as appropriate in context. Other unattributed parenthetical notes within the body of an item originate with the source. Times within items are as given by source.

The contents of this publication in no way represent the policies, views or attitudes of the U.S. Government.

JPRS L/10410

25 March 1982

SATELLITE HYDROPHYSICS

Sevastopol' SPUTNIKOVAYA GIDROFIZIKA in Russian 1980 (signed to press 4 Dec 80) pp 1-152

[Collection of articles edited by B. A. Nelepo, Izdatel'stvo Morskoy gidrofizicheskiy institut, 250 copies, 152 pages]

CONTENTS

 [I - USSR - E FOUO]

ANNOTATION

The collected papers cover basic ideas about remote sensing of the sea surface from satellites. Data on the determination of temperature, colour, waves and ice-cover of the sea-surface are listed. Also analysed is the relationship between surface radiation variations and internal waves. Theoretical problems and methodology of remote sensing are discussed. Information on automatic buoy systems of subsatellite observational regions and data processing systems are presented.

The collected papers are intended for specialists in ocean physics, students and post-graduates of relevant specialities.

PROBLEMS IN INVESTIGATING THE OCEAN FROM SPACE

Sevastopol' SPUTNIKAYA GIDROFIZIKA in Russian 1980 pp 5-11

[Article by B. A. Nelepo and Yu. V. Terekhin]

[Text]

Abstract: The article examines the fundamental problems involved in remote determination of the informative hydrophysical parameters of the ocean for their use in prognostic models of the ocean. The authors discuss the features of measurement of oceanic characteristics in the IR-SHF and visible ranges of the radiation spectrum. The requirements on the accuracy in measuring hydrophysical parameters and their spatial resolution are formulated. The prospects for the use of space vehicles in investigations of the world ocean are pointed out.

The world ocean, always playing a considerable role in the life of mankind, has now become the sphere of man's economic activity. This has predetermined the ever-increasing attention being given to its investigation, especially since today scientists comprehend the role of the ocean in the formation of weather and climate on the earth, understand that the earth's resources are not unlimited and that the ecosystem is quite brittle relative to the onslaughts of modern civilization.

The eyes of scientists are turning toward the ocean: does it have such a self-regulating system which would enable it to cope with the irreversible effects caused by man's active intervention? In order to answer this question it is necessary to have prognostic models or schemes taking into account the entire complex system of relationships regulating the state of the atmosphere and ocean.

In order to formulate physicomathematical models on the basis of which it is possible to carry out prognostic computations it is necessary to make detailed investigations of the boundary layers of the ocean and atmosphere. It is precisely in these layers that the greatest temperature gradients are formed, these arising as a result of the absorption of solar radiation, contact heat exchange and evaporation. The heat fluxes, directed into the ocean from the atmosphere, or vice versa, create in it a complex circulation of air masses, thus forming the weather. Simultaneously, atmospheric processes (especially wind) exert an extremely important influence on the upper layer of the ocean, leading to a corresponding exchange of thermal energy between the atmosphere and ocean. The diversity of conditions at the boundary between the gaseous and fluid media also leads to a great diversity of circulatory systems in the ocean and atmosphere, forming against the background of macroscale dynamics of the ocean.

In this connection the key problem in modern oceanography is a study of synoptic phenomena in the ocean, among which the most important are oceanic eddies, zones of upwelling and subsidence of abyssal waters, fronts and thermal anomalies. Synoptic eddy movements of water masses affect a thickness of the ocean of several kilometers; their horizontal extent is hundreds of kilometers; the spatial velocity of movement attains several kilometers each day. The energy concentrated in such formations is comparable in quantity to the energy of macroscale ocean currents.

In addition to the development of fundamental concepts concerning ocean dynamics, investigations of ocean eddies are of interest from the point of view of the possibility of formation of productive zones in the open ocean. Sufficiently powerful (with respect to intensity and scale) synoptic eddies of a cyclonic character, existing for two years or more, are capable under definite conditions of maintaining a powerful upwelling of deep waters ensuring the transport of nutrients from the ocean depths to its surface.

Thus, formulation of the problems in prediction essentially involves large-scale (and for the ocean -- at an oceanic scale), operational and regular observations of the transpiring of processes with a periodicity of renewal of information not less than the time scales of synoptic variability (10-15 days). No reasonable number of research ships and buoy stations can ensure such a possibility. Accordingly, the above-mentioned problems can be solved only using instrumentation for the remote sensing of the ocean carried aboard space vehicles, with development of techniques, methods and procedures in space oceanography as a new method for investigating the ocean.

There is a rather great number of theoretical models making it possible to describe the processes transpiring in the ocean. The input parameters of such models are water and air temperature, radiant energy flux, height of waves and wind velocity in the near-water layer of the atmosphere, humidity and atmospheric pressure, extent of cloud cover, depth and intensity of the jump layer, ice characteristics and others. Temperature of the ocean surface is the most informative of these.

The most important tasks of oceanography, whose solution is possible with use of the temperature characteristics of the ocean surface, are: study of mesoscale variability of the ocean, discrimination of frontal zones and zones of strong currents and prediction of structure of the active layer in the ocean.

Data from observations of mesoscale variability in the ocean show that the temperature field of the ocean surface is formed not only under the influence of atmospheric processes, but also to a considerable degree conforms to the character of eddy movement in the main ocean thermocline. The principal features in the distribution of this parameter were caused by eddy advective currents disturbing the principal zonal distribution of temperature. In contrast to the circulatory character of eddy movement in the main ocean thermocline the distribution of temperature at the ocean surface is characterized by an intrusional character of the movement of isotherms.

The characteristic scales of formations in the upper layer of the ocean are 40-400 km; the mean velocity of spatial movement is 5-8 km/day, the temperature drops are 0.2-2.0°C in zones of influence of deep mesoscale eddies and up to 2-3°C in zones of intensive formations of the type of Gulf Stream rings. A not less important role in the general dynamics of the ocean is played by its variability at scales of 15-50 km, which is associated with the high energy level at these scales. The temperature drops in these formations usually fall in the range 0.2-1.0°C. Accordingly, for a study of synoptic variability in the ocean the required accuracy in determining temperature falls in the range 0.1-0.2°C with an in situ resolution not worse than 3-5 km.

Temperature anomalies are traced against the mean climatic background as formations with characteristic spatial scales from hundreds to thousands of kilometers and time intervals from a month to tens of months and a thickness in depth attaining tens of meters. The amplitude (extremal deviation from the climatic norm) of such formations is not more than 2-3°C. As a result of the great thermal inertia of the ocean in comparison with the atmosphere they exert a considerable influence on planetary weather at global scales.

The principal requirements on data from remote sensing, making it possible to trace the evolution of these anomalies, is the breadth of coverage of ocean regions and the frequency of receipt of information. It is best to obtain surface temperature maps at ocean scales with a frequency of once or twice in a 10-day period. In this case the allowable spatial resolution is 20-30 km; the accuracy in determining temperature is not less than 0.5°C.

The position of the principal frontal zones in the world ocean and zones of intensive currents has been determined quite well. Accordingly, the principal task to be solved in this direction is a study of the variability of such factors as the position of the axis of currents and fronts, meandering and stability. The principal indicator for the identification of "images" of ocean fronts and boundaries of intensive currents is a temperature drop at their boundaries which can amount to as much as 2-10°C. This makes possible its reliable detection by instrumentation operating in the IR range. With such great temperature drops the acceptable accuracy of its determination will be 0.5°C (sometimes 1°C) and the principal requirement related to the determination of the boundaries of frontal zones is related to spatial resolution. It appears that the optimum value of such resolution is about 1-2 km. We add that information on the position of the boundaries of frontal zones carries data on the color index of water, the nature of cloud cover over the ocean and other data.

A highly important task of oceanography is prediction of the vertical structure of the active layer of the ocean, which is the principal intermediate link in the processes of interaction between the ocean and the atmosphere. The prediction includes a determination of temperature of the ocean surface, the position of the lower boundary of the homogeneous layer (layers), the position (depth) of the density jump. The temperature and depth of the homogeneous layer determine the intensity of the temperature anomalies (heat content and lifetime), allowance for which is necessary in prediction problems; the position of the jump layer determines the lower boundary of the zone of active photosynthesis in the upper layer of the ocean.

There are now quite a few theoretical models making it possible to compute the mentioned parameters of the vertical structure of the active layer in the ocean. The input parameters of such models are air temperature, radiant energy flux, wind velocity, humidity, pressure, cloud cover, which can be measured by remote methods from artificial earth satellites. Computations with the use of these models make it possible to use the temperature of the ocean surface, measured with an accuracy to 0.1°C, depth of the mixed layer and the position of the jump layer with an accuracy to 1-2 m. It is understandable that the attainment of this same accuracy in measurements by remote methods is a task of the future and therefore the temperature of the ocean surface, measured with the accuracy attained up to now, can serve only as a calibration parameter in choosing the empirical parameters of this type of model. By the time when the necessary accuracy in measuring ocean surface temperature is attained (0.1-0.2°C), the assimilation of this parameter in theoretical models will make it possible to proceed to computation of the heat fluxes at the boundary of the jump layer and thus determine the receipt of heat in the main ocean thermocline.

The attainment of the required accuracy in measuring temperature of the ocean surface from aboard an artificial earth satellite is held back by two principal factors. One of these is related to an increase in the accuracy in determining the atmospheric transfer function. In actuality, investigation of the characteristics of the ocean surface by passive methods in the IR and SHF ranges involves measurements of reflected solar radiation and the characteristic radiation of the ocean. Since the latter are transformed during transmission through the atmosphere, the accuracy in determining the degree of this transformation enters directly into the total error in determining the temperature of the underlying surface. The accuracies in the evaluations of the atmospheric transfer function attained at the present time introduce an error into the measured temperatures at the level ±(0.5-1)°C.

The surface temperature measured with remote sensing instrumentation, which we assign as a characteristic of the mixed upper layer of the ocean, strictly speaking, relates to the uppermost emitting layer, the so-called skin layer of the ocean. However, in this layer the properties of the medium differ substantially from the characteristics of the homogeneous layer, and in particular, the temperature gradients in it attain tenths of a degree per centimeter. The state of this layer, very much dependent on the general hydrometeorological situation, is an important factor, to a considerable degree exerting an influence on the accuracy in determining temperature of the ocean surface. It can be assumed that the existence of a cold surface film is a universal phenomenon and for the most part it is stable with time. In such a case, since IR radiometers measure the brightness temperature of the very thin (micron) water film, whereas the temperature of the underlying homogeneous layer is of practical interest for researchers, the problem of the legitimacy of identifying the temperatures of the quasihomogeneous layer and the surface film or the methods for correction of the measured brightness temperature is of great importance. As long as we do not know the true temperature in the skin layer, and also the pattern of horizontal distribution of the characteristics of this layer, the inaccuracy in determining the temperature of the homogeneous layer will substantially reduce the information content of these data. The reduction in information content will be as follows. First of all, since the characteristic time for the carrying out of IR surveys from a satellite is comparable with the characteristic time of existence of the skin layer, the uncertainty in measurement of the temperature of the homogeneous layer can attain the level of the temperature drop in the skin layer. Second, the temperature of the skin layer exerts a substantial influence on the energy characteristics of the processes of interaction between the ocean and the atmosphere. Since the thickness of the skin layer is very small, its direct role in the energy budget of the upper layer of the ocean is insignificant. For example, the skin layer in a certain sense is "optically transparent" for incident solar radiation. With respect to other heat balance components, such as heat expenditures in evaporation, contact heat exchange and outgoing long-wave radiation, here the skin layer can change these characteristics by 10 or 15%.

Thus, it can be stated that the creation of an adequately correct thermohydrodynamic model of the surface skin layer, together with improvement in methods for taking into account the influence of the atmosphere, opens the way for a substantial increase in the accuracy in determining the temperature of the ocean surface.

Considerable experimental data have now been accumulated from remote sensing of the earth's surface (including the ocean) which have been obtained from Soviet satellites of the "Cosmos" series and also from American meteorological satellites using individual systems operating in the visible, IR and microwave ranges. These data indicated great potentialities for the use of space technology in investigating the ocean and brought to the forefront the task of creating a specialized oceanographic earth satellite supplied with a complex of research apparatus making it possible to obtain evaluations of the informative physical parameters of the ocean and atmosphere.

The artificial earth satellite "Cosmos-1078," launched on 12 February 1979, was our country's first satellite intended for perfecting methods for solving the abovementioned problems.

One of the additional sources of data on the world ocean is measurement in the visible range (wavelengths 0.4-0.7 μm), in which the greatest amount of information is carried by the spectral composition of the ascending light flux. In the open parts of the ocean it carries information on the biological productivity of waters and their hydrooptical characteristics. This is making it possible to discriminate different water masses, determine their boundaries, detect eddies, zones of upwelling of water and other dynamic formations. In coastal regions, on the basis of water color, it is easy to differentiate waters of the continental runoff, their distribution and interaction with waters of the open sea. We note that investigations of the ascending light flux over the ocean in this range have two peculiarities in comparison with measurements over the continents. It is well known that the diversity of colors, hues and contrasts on the continents is incomparably broader than at the ocean surface. For the most part different natural formations have quite distinct and sharp boundaries. In ocean waters all these characteristics are tens of times less clearly expressed and the problems of geographical "tie-in" of the results of observations are more complex to solve. Accordingly, on the one hand, the requirements on the resolution of instrumentation in situ are not so rigorous for oceanological investigations as for the land, but on the other hand, the response of instrumentation for detecting differences in water masses must be higher. A considerably higher spectral resolution is also required. Accordingly, the visible-range instrumentation carried aboard the "Cosmos-1078" oceanographic satellite has transmission bands not exceeding a few nanometers. Instrumentation with such a high spectral resolution was carried on a satellite for the first time.

One of the most important elements in the investigation of the ocean from space is a system of calibration points at which there are direct measurements of the characteristics of the ocean surface layer. In experiments with the "Cosmos-1076" satellite use was made of automatic buoy stations and shipboard data systems for these purposes.

The instrumentation placed on automatic buoy stations and a satellite makes it possible to carry out a regular read-out of the data accumulated on the automatic buoy station and transmit it to the corresponding reception centers for joint processing. In addition to solution of methodological problems and the problems involved in the calibration of remote sensing sensors, the use of a system of automatic buoy stations in the ocean, determining the hydrophysical characteristics with depth, makes it possible to pose the problem of the relationship of surface fields (measured from a satellite) with processes in the deep layers of the ocean, at least within the limits of the active layer.

The launching of the "Seasat-1" and "Cosmos-1078" space vehicles marks a new stage in the study of the ocean. It must be hoped that the processing and analysis of the collected data will enable oceanologists to make considerable progress in comprehending both the methods for organizing observations and the essence of the processes transpiring in the ocean-atmosphere system.

EXPERIMENT FOR INVESTIGATING INTERNAL WAVES IN OCEAN BY REMOTE METHODS

Sevastopol' SPUTNIKOVAYA GEOFIZIKA in Russian 1980 pp 12-18

[Article by Yu. M. Kuftarkov]

[Text]

Abstract: The article gives the results of an experiment for ascertaining the interrelationship of temperature fluctuations in the thermocline and radiation temperature at the free surface of the ocean. It is shown that on the basis of the characteristic thermal radiation of the ocean in the IR spectral range it is possible to reconstruct the scales of internal waves in the ocean.

Studies have appeared recently which have been devoted to the remote sensing of internal waves. Considerable successes in solution of this problem have been attained for the most part due to use of optical methods [1]. However, their use is possible only during the daytime under definite hydrometeorological conditions.

In order to investigate the possibility of the sensing of internal waves in the IR range within the framework of the international program JASIN-78 an experiment was planned which was implemented in September-October 1978 on the expedition on the 18th voyage of the scientific research ship "Akademik Vernadskiy."

We will describe the method for carrying out the experiment.

Variant 1. Observations of the field of internal gravitational waves were made from a drifting ship using an array of three sets of distributed temperature sensors (SRD). Two sets were lowered from the ship's stern and prow and the third was placed on a buoy at a distance of 100 m from the middle of the ship perpendicular to its side. The sets of sensors were made up of links of different scales and occupied the upper quasihomogeneous layer of the ocean and the seasonal thermocline. The distribution of sensors with depth was as follows: the SRD-1 consisted of seven decimeter temperature sensors (RDT) and one sensor 100 m in length. Three SRD-3 sensors, two of which were each 10 m in length and one which was 50 m in length, were lowered from the ship's prow. The SRD-2, placed on the buoy, consisted of six distributed sensors: two of 50 m each, two of 25 m in length, and two with a length of 10 m. A set of current meters was suspended from the stern for determining the ship's drift relative to the water; these occupied the upper 70-m layer of the ocean and consisted of five DISK instruments and three BPV current meters.

This scheme for the placement of RDT made possible a detailed investigation of the vertical structure of the temperature field and made it possible to give an answer to the question as to whether we are dealing with a random group of internal gravitational waves or with mesoscale turbulence.

In order to compute the mean profile of the Väisälä-Brent frequency characterizing the field of internal waves we carried out measurements with ISTOK instruments and a sinking probe to ascertain the fine structure. Directly at the free surface we made observations of the microstructure of the temperature field using a floating-up probe.

The radiation temperature of the ocean surface was measured using an IR radiometer in the range 8-12 μm with a time constant of 3 sec and a response of not less than 0.03°C. The radiometer was mounted on a boom at the ship's prow and was directed vertically downward. The angle of view of 5° ensured averaging of the radiation temperature τ_p in a circle with a radius of 1 m. In the analysis use was made of data for an 8-hour measurement interval in the evening and nighttime hours as being the most favorable for observing the radiation temperature of the ocean surface.

Variant 2. The ship was at anchor (at a depth of 120 m) in the region of Ampere Bank (near Gibraltar). The steep slopes of this bank (the horizontal scale along the isobath 2500 m is 30-40 km) make it a natural generator of internal waves. Observations of the wave field were made using the system of distributed temperature sensors described above with the single difference that it included only two sets of sensors which occupied almost the entire thickness of the water from the surface to the top of Ampere Bank. The distribution of the sensors with depth was as follows: the first RDT-100, lowered from the ship's prow, occupied the water layer from the surface to a depth of 100 m; on this same vertical there were seven other 10-m RDT-10 sensors placed successively one under the other beginning with a depth of 10 m; three sensors (two each 10 m in length and one 50 m in length) were lowered from the ship's prow.

As in variant 1, here we used measurements of the temperature profile obtained with STD instruments, sinking and floating-up probes.

Variant 3. Attention was given to a determination of the interrelationship of the spatial scales of temperature inhomogeneities in the thermocline and at the free ocean surface. The results of observations made while the ship was proceeding on course make it possible to evaluate the influence of the ship's hull on measurements of radiation temperature τ_p obtained in variant 2.

The horizontal structure of the temperature field in the thermocline was investigated using the SRD-1; it was towed by a ship at a speed of 5 knots. Four runs were made of 5 miles each in different directions. At the same time observations were made of the radiation temperature of the ocean surface. The length of the runs does not make it possible to carry out a joint statistical processing of the initial records at the time scales of interest to us but makes it possible to compare the characteristic phase shifts and scales of temperature inhomogeneities in the thermocline and at the free surface*.

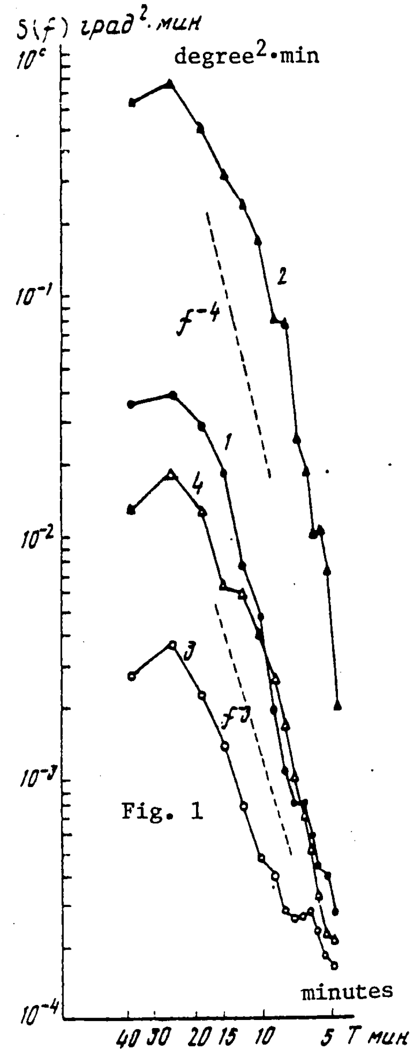

Fig. 1

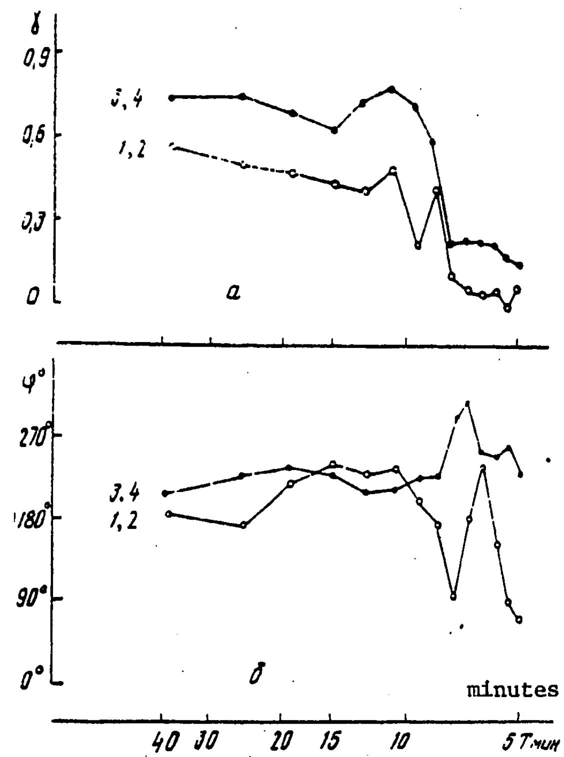

Fig. 2.

Table 1 gives the designations and characteristics of some series of measurements obtained in the experiment in variants 1 and 2. Figure 1 gives the spectral densities of temperature in the thermocline and the radiation temperature of the free surface. All the spectra in the region of time scales 10-20 min are characterized

---

* The observational data obtained at drift, while at anchor and while the ship was proceeding on course are identical with respect to the effect of the interrelationship of temperature fluctuations in the upper thermocline and at the ocean surface and therefore only some results of the experiment will be presented below.

by a rather steep (f^{-3} and f^{-4}) dropoff from the low frequencies to the high frequencies, which gives basis for postulating a wave character of the investigated phenomenon.

Table 1

Variant	Instrument	Number of series	Depth, m	Duration T, hours	Discreteness, min	Number of terms in series
1	IR radiometer	1	0	7.93	0.62	772
	RDT-10	2	40-50	7.93	0.82	772
2	IR radiometer	3	0	7.8	0.82	760
	RDT-10	4	50-60	7.8	0.82	760

The degree of interrelationship of internal waves and radiation temperature of the ocean surface at time scales from 10 to 37 min is illustrated by the coherence spectra (Fig. 2,a) and the phase spectra (Fig. 2,b) of series 1,2 and 3,4. If the series were not correlated, then with a number of degrees of freedom 30 the evaluations of coherence with 95% guaranteed probability would not exceed the level of the random errors 0.36. The stability of the phase shifts in periods from 37 to 10 min also indicates a correlation of the temperature fluctuations in the thermocline and at the free surface of the ocean.

It was found from an analysis of the phase spectrum that the fluctuations of effective temperature in the thermocline with an accuracy to the registry and processing of data are almost in antiphase with the radiation temperature of the free surface of the ocean. Due to the limited nature of the observation series the cited statistical analysis relates to time fluctuations with a period not more than 40 min.

In order to establish the degree of correlation between the radiation temperature of the ocean surface and the field of internal gravitational waves at all the time scales of interest to us (up to 8 hours) we used special processing methods based on the expansion of the initial fields in a system of empirical orthogonal functions [2].

The expansion of the investigated field in empirical orthogonal functions is desirable only when the first two or three eigenvalues in the sum are much greater than the others. In this case there is discrimination of the energy-significant fluctuations; the other nonenergy-carrying disturbances are suppressed or are filtered out.

A special practical advantage of the empirical functions approach is that as a result of expansion of the initial field in these functions on the one hand there is discrimination of the coherent part of the fluctuations from each horizon, and on the other hand, there is information on the distribution of the particular horizon by empirical modes.

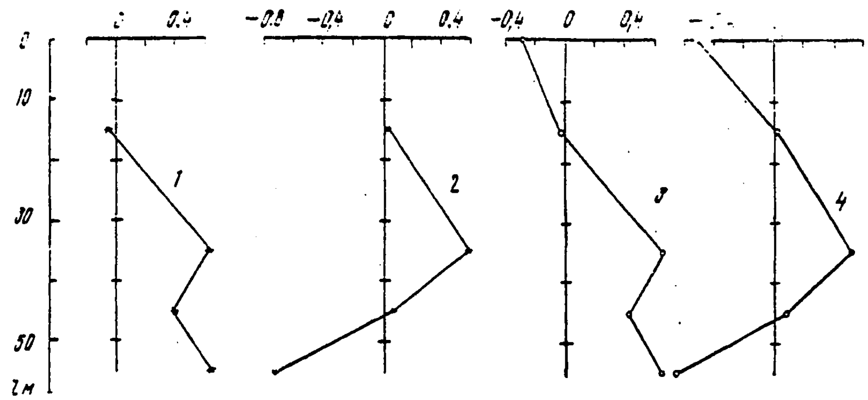

Fig. 3.

Table 2

Percentage Content of Total Energy

Modes	Depths, m				
	0	20-30	30-40	40-50	50-60
1	39	30	79	92	86
2	41	36	20	7	12

Therefore it is possible to propose the following processing procedure. First, on the basis of data for RDT situated on one vertical we obtain the vertical and temporal structure of the significant energy modes of the wave field and then to the initial data we add a τ_p series and again construct empirical orthogonal functions. If in this case a large part of the energy τ_p is distributed in energy-significant modes of a purely wave field, this will mean that fluctuations of the radiation temperature correlate with the field of internal waves.

As the initial mass of data we used data on temperature fluctuations obtained using four RDT and an IR radiometer. Computations were made for these cases: 1) the empirical modes were obtained solely on the basis of data from the distributed sensors; 2) using RDT and IR-radiometer data. An analysis indicated that in both cases the first mode is energy-significant. The two lower modes together contain about 90% of the total energy of pulsation movement. Figure 3 shows curves of the vertical distribution of the empirical functions of the first (curves 1, 3) and second (curves 2, 4) modes characterizing the intensity of temperature fluctuations with depth. Curves 1, 2 describe the vertical structure of temperature fluctuations of the wave field without the "radiation" horizon (z = 0), curves 3, 4 characterize the vertical structure, including the horizon z = 0. It can be seen that the presence of the "radiation" horizon does not impair the vertical structure and the profiles of the corresponding modes with exclusion of this horizon are similar to one another. The temperature fluctuations in the second mode at the ocean surface and in the seasonal thermocline (30 mm$\leqslant z \leqslant$40 m) are in antiphase, that is, the rising of the isotherms in the seasonal thermocline is accompanied by an increase in temperature of the ocean surface.

The first two modes (Table 2) contain more than 90% of the energy at the individual horizons where the RDT are placed, with the exception of the horizon 10-20 m, and 80% of the energy of the radiation series (z = 0). This gives basis for speaking of a high degree of correlation of fluctuations of radiation temperature of the free surface and internal gravitational waves. The energy contribution to the empirical modes from a depth of 10-20 m is determined very inexactly, since less than 1% of the total energy is accounted for by this depth

Thus, the cross-statistical analysis cited above and a special analysis based on an expansion of the initial fields in a system of empirical orthogonal functions indicated that on the basis of IR photographs of the free ocean surface it is in principle possible to "reconstruct" the scales of internal waves and determine the zones of their convergence and divergence.

BIBLIOGRAPHY

1. Apel, J. R., et al., "Observations of Oceanic Internal and Surface Waves From the Earth Resources Technology Satellite," J. GEOPH. RES., Vol 80, No 6, pp 865-881, 1975.

2. Moore, D., "Empirical Orthogonal Functions -- a Nonstatistical View," HOT LINE NEWS, No 67, pp 1-9, 1974.

DETERMINATION OF PARAMETERS OF INTERNAL WAVES BY REMOTE METHODS

Sevastopol' SPUTNIKOVAYA GEOFIZIKA in Russian 1980 pp 19-27

[Article by V. N. Kudryavtsev]

[Text]

Abstract: A study was made of the problems involved in the sensing of internal waves from the characteristic IR radiation of the ocean. The author proposes a very simple model of the appearance of internal waves in the radiation temperature field of the surface based on a redistribution by the field of induced velocity of the concentration of surface active substances having an emissivity differing from sea water. Computations using the formulated model are compared with experimental data. An expression is proposed which makes it possible to reconstruct the energy spectrum of internal waves on the basis of the radiation temperature spectrum.

Introduction. Recently the formulation of the problem of determining the parameters of dynamic processes in the ocean by remote methods has become timely [1]. A solution of such a problem primarily involves an analysis of the effect of the investigated phenomenon on the physical parameters of the ocean surface, whose variations are registered by remote apparatus. For example, the authors of [2] examined the the problem of the appearance of a synoptic eddy formation in the thermal structure of the upper quasihomogeneous layer. The mentioned model can have application to determination of the scales and intensity of an eddy on the basis of data from IR sensing of the ocean surface from aboard flightcraft. Only the first steps have been taken in the investigation of internal waves by remote methods. Using the effects of suppression of ripples in definite zones of a current induced by internal waves the authors of [8] were able to observe internal waves in the Gulf of California from space. However, the use of optical methods is possible only during the daytime under definite hydrometeorological conditions. Source [3] gave the results of an experiment for ascertaining the interrelationship between the field of IR radiation temperature and displacements of the thermocline. An analysis of the experimental data indicated that the radiation temperature field can be a valuable source of information on the scales and energy of internal waves.

The purpose of this article is the formulation of a very simple model for determining the spatial-temporal and energy characteristics of internal waves on the basis of the field of radiation temperature of the ocean surface.

Determination of Radiation Temperature

In the IR range the radiation temperature of the ocean is determined from the energy brightness $\langle e \rangle$, averaged for the surface S_0 viewed by the radiometer,

$$\langle e \rangle = \frac{1}{S_0} \int_{S_0} \varepsilon(\vartheta)\, B(T_s, \nu)\, dS_0 . \quad (1)$$

Here $\varepsilon(\vartheta)$ is the emissivity of the sea surface in the direction ϑ; ϑ is the angle between the normal to an element of the free surface and the direction into the radiometer objective; B is the energy brightness of an ideally black surface. In the near-IR spectral region of thermal radiation for the function B the Wien asymptotic function

$$B(T_s, \nu) = \frac{2h\nu^3}{c^2} e^{-h\nu/kT_s}$$

is correct, where h, k, c are universal constants; T_s is temperature; ν is spectral frequency. With real slopes of the free surface of the sea $\varepsilon(\vartheta)$ is not dependent on the angle ϑ and is determined only by the surface properties, especially the degree and type of its contamination [4].

We will call the radiation temperature of the ocean surface T_p the temperature of an ideally black surface whose energy brightness is $\langle e \rangle$. From this definition it follows that

$$\frac{1}{T_p} = \frac{1}{T_s} - \frac{k}{h\nu} \ln \varepsilon . \quad (2)$$

Taking into account the fact that in the IR range ε is close to unity, we finally obtain an expression for variations of the radiation temperature

$$\tilde{T}_p = \tilde{T}_s + \tau \tilde{\varepsilon} . \quad (3)$$

Here the wavy line at top denotes fluctuation of the parameter; $\tau = kT^2/h\nu$; with a radiation wavelength $\lambda = 10\,\mu m$ $\tau \simeq 60$ K. Since the IR radiation is formed by the surface water layer $\sim 10\,\mu m$, by the term thermodynamic temperature of the surface we understand the mean temperature of this very thin layer -- the so-called skin temperature.

Correlation of Variations of ε and T_p With Field of Internal Waves

We will evaluate the contribution of the terms on the right-hand side of (3) to $\check{T}_p$. The skin temperature of the surface is less than the temperature of the underlying mixed water layer by from several tenths of a degree to a degree; the entire temperature drop ΔT is concentrated in a layer of several millimeters. The thermal structure of the skin layer is essentally dependent on the heat transfer properties of the surface and the degree of development of capillary waves [5].

Accordingly, a change in the intensity of capillary waves and a redistribution of surface active substances (on which the rate of evaporation is dependent) by the field of internal waves leads to the appearance of $\tilde{T}_S$ anomalies which in any case will be a maximum of about ΔT. Emissivity is also dependent on the type and concentration of surface active substances. For example, according to the data in [6], films of petroleum and its products, depending on the concentration, are capable of changing ε by several hundredths. As can be seen from (3), the variation $\tilde{\varepsilon} = 0.01$ leads to $\tilde{T}_p = 0.6$ K. This estimate indicates a potentially high contribution of films of surface active substances to the formation of T_p contrasts. Thus, investigation of problems relating to redistribution of the concentration Γ of surface active substances by the field of internal waves and a knowledge of the functional dependence $\varepsilon = \varepsilon(\Gamma)$ for different really encountered types of surface active substances is the central problem in formulating theoretical models for IR sensing of internal waves.

Now we will examine a very simple model. We will assume that for the field of internal waves the ratio of the induced surface velocity U to the phase velocity C is a small value, that is, $U/C \ll 1$. Under the condition that the surface active substance is a passive admixture, the linearized equation for describing the variability of the concentration $\tilde{\Gamma}$ has the form [7]

$$\frac{\partial \tilde{\Gamma}}{\partial t} + \Gamma_0 \frac{\partial U_\alpha}{\partial x_\alpha} = 0, \tag{4}$$

where Γ_0 is the undisturbed value Γ; U_α are the components of horizontal velocity. We will expand ε into a series in the neighborhood $\varepsilon(\Gamma_0)$

$$\varepsilon(\Gamma) = \varepsilon(\Gamma_0) + \left(\frac{\partial \varepsilon}{\partial \Gamma}\right)_0 \tilde{\Gamma}. \tag{5}$$

In a case when the $(\partial \varepsilon / \partial \Gamma)_0$ is known, the system of equations (4), (5) makes it possible from the known field U_α to determine the field of anomalies of ocean surface emissivity.

Assume that the field of internal waves is statistically stationary and horizontally homogeneous. This makes it possible to represent the components of orbital velocity of the internal wave, displacement of the thermocline and sought-for functions in the form of a Fourier-Stieltjes (F-S) integral

$$Y(x_\alpha, z, t) = \int e^{i(k_\alpha x_\alpha - \omega t)} dY(z), \tag{6}$$

where Y is an arbitrary function; dY is an F-S component; k and ω is the elementary wave number and the frequency of the corresponding component. Substituting (6) into equations (4), (5), we obtain

$$d\tilde{\Gamma} = \Gamma_0 \frac{k_\alpha \, dU_\alpha}{\omega}, \quad d\tilde{\varepsilon} = \varkappa \frac{k_\alpha \, dU_\alpha}{\omega}. \tag{7}$$

Here

$$\varkappa = \Gamma_0 \left(\frac{\partial \varepsilon}{\partial \Gamma_0}\right)$$

is a parameter characterizing the emissivity of the film of surface active substance. It follows from (3) that an expression can be derived for the F-S component of variations of radiation temperature caused by variability of ocean surface emissivity

$$d T_p = \tau \varkappa \frac{k_\alpha \, d U_\alpha}{\omega} . \qquad (8)$$

Within the framework of ordinary approximations of the linear theory of internal gravitational waves the F-S component of induced surface velocity is expressed through the vertical velocity component dW in the following way:

$$d U_\alpha = i \frac{k_\alpha}{k^2} \frac{d}{dz} d W \Big|_{z=0} . \qquad (9)$$

If the thickness of the homogeneous layer $h_0 \ll k^{-1}$, then

Then $$\frac{d}{dz} dw \simeq \frac{i\omega d\xi_{h_0}}{h_0}.$$

$$d\tilde{\Gamma} = -(\Gamma_0/h_0)\, d\xi_{h_0} , \; d\tilde{T}_p = -(\tau\varkappa/h_0)\, d\xi_{h_0} ,$$

that is, the maximum of the concentration of the surface active substance is situated over the bottom of displacements of the thermocline and the position of the T_p maximum is dependent on the sign on $\varkappa$, With $\varkappa < 0$ the crest of thermocline displacements corresponds to the maximum of the surface radiation temperature, and vice versa, with $\varkappa > 0$.

We will give a simple evaluation. For a film of easily spreading petroleum within the range of its thickness 1-10μm $\partial \varepsilon / \partial \Gamma \sim -10^{-2} \mu m^{-1}$ [6].

Assume that $\varkappa = \Gamma_0 \frac{\partial \varepsilon}{\partial \Gamma} = 5 \cdot 10^{-2}$, $d\xi / h_0 = 10^{-1}$. Then with $\tau = 60$ K $d\tilde{T}_p = 0.3$ K, but the T_p maximum is situated above the crests of thermocline displacements.

Interpretation of Experimental Data

With the above taken into account, an attempt will be made at an interpretation of the results of a cross-spectral analysis of series of fluctuations of radiation temperature and the temperature of a distributed sensor situated in the thermocline [3]. The observations were made at nighttime when there was a weak wind ~ 3 m·sec^{-1}. At the time of implementation of the experiment it was impossible to determine the presence of a surface active substance. However, during the daytime the authors of the experiment visually observed "slicks" on the ocean surface (regions with a smoothed short-wave part of the wave spectrum) which were associated with the presence of a surface active substance.

Under the conditions under which the experiment was carried out there can be no significant contrasts of the skin temperature. In actuality, with a wind ~ 3 m·sec^{-1} capillary waves are far from saturation and the dynamic contrasts of capillary-gravitational ripples between the slick and the "unsmoothed" part of the surface are capable of giving a considerable contrast of skin temperature [5]. Moreover, if it is assumed that the variations of the evaporation rate in order of magnitude correspond to variations in the concentration of surface active substance, the expected skin temperature anomalies will be $\tilde{T}_S \sim \Delta TU/C$. With $\Delta T \sim 0.1$-0.5 K we will have $\tilde{T}_S \sim 10^{-2}$-$5 \cdot 10^{-2}$ K. The experimental mean square values of the fluctuations T_p

$$(\overline{\sigma T_p^2})^{1/2} \sim 0.2 \text{ K}.$$

Thus, the observed $\tilde{T}_p$ were caused by variations in ocean surface emissivity.

For comparison of the results of the theoretical analysis and experimental data we will approximate the vertical distribution of temperature in the homogeneous layer and the thermocline by a model in which the temperature in the layer 0-h_0 (40 m) is constant, whereas when $z > h_0$ the mean temperature gradient is constant and equal to $\overline{\partial T/\partial z} = -0.1$ degree·m^{-1}. In a case when the level of placement of the distributed sensor h_* differs little from h_0, the F-S component of fluctuations of temperature of the sensor and the component of displacements of the upper boundary of the thermocline are related by the expression

$$d\tilde{T}_{h_*} = \frac{\overline{\partial T}}{\partial z} \frac{h_*}{h_0} d\xi_{h_0} . \quad (10)$$

It follows from expressions (8)-(10) that there is a correlation between the F-S components of variation of radiation temperature and temperature fluctuations in the thermocline

$$d\tilde{T}_p = -(\tau \varkappa / h_*) \left(\frac{\overline{\partial T}}{\partial z} \right)^{-1} d\tilde{T}_{h_*} . \quad (11)$$

Now we will proceed to the writing of spectral expressions. We will determine the spatial-temporal spectral densities using the formula

$$F_{x,y}(k_\alpha, \omega) = \frac{\overline{dX\, d^*Y}}{dk_1 dk_2 d\omega} , \quad (12)$$

where the line at top denotes theoretical probabilistic averaging, the asterisk denotes a complexly conjugate value. It follows from this definition and from expression (11) that there is a correlation and similarity of the spectra F_{T_p} and $F_{T_{h*}}$

$$F_{T_p} = \left(\tau \varkappa / h_* \frac{\overline{\partial T}}{\partial z} \right)^2 F_{T_{h_*}} . \quad (13)$$

This result corresponds qualitatively with the experimental result. We will evaluate the theoretical similarity coefficient $R^2 = F_{T_p}/F_{T_{h*}}$. Selecting, as before, a surface active substance in the form of a film of spreading petroleum the emission steepness $|\varkappa| \sim 10^{-2}$-$5 \cdot 10^{-2}$, with $h_* = 60$ m we obtain the evaluation $R^2 \sim$ 0.01-0.25. With $h_* = 55$ m the experimental value R^2 is equal to 0.2, and with $h_* =$ 65 m -- equal to 0.04 [3]. The difference in the experimental values one from the other can be attributed to the nonlinearity of the $\overline{\partial T/\partial z}$ profile. But at the same time the agreement of R^2 values in order of magnitude in the experimental and theoretical evaluations is obvious.

It is easy to confirm that in the model Im $F_{T_p,T_{h*}} = 0$ and sign Re $F_{T_p,T_{h*}}$ = sign $\varkappa$. Accordingly, the theoretical phase spectrum $\theta_{T_p,T_{h*}} \equiv \pi$, if sign $\varkappa = -1$ (as for petroleum spreading out freely), and $\theta_{T_p,T_{h*}} \equiv 0$, if sign $\varkappa = +1$. The experimental value $\theta_{T_p,T_{h*}}$ in the range of periods 40-15 minutes on the average has a stable value close to π, that is, displacements of the thermocline and variations of the radiation temperature of the ocean surface are in phase (in antiphase with $\tilde{T}_{h*}$). A comparison of the results of the theoretical analysis with the experimental data gave satisfactory qualitative and quantitative agreement.

Determination of Energy Spectrum of Internal Waves From Radiation Temperature Spectrum

It follows from the results cited above that the radiation temperature field can be a valuable source of information on the scales and energy of internal waves. It is therefore desirable to derive an expression relating the radiation temperature spectrum and the energy spectrum of internal waves, which to a certain degree will be diagnostic with reconstruction of the parameters of internal waves from the T_p field.

It is known that the vertical structure of the field of short-period internal waves in the ocean is determined by solution of the equation

$$\frac{d^2}{dz^2} dW + \frac{N^2-\omega^2}{\omega^2} k^2 dW = 0 \qquad (14)$$

with the boundary conditions dW(0) = dW(H) = 0. Here H is the ocean depth; N is the Väisälä-Brent frequency; ω and k are the elementary frequency and wave number, which are determined from the conditions of existence of a nontrivial solution of equation (14). Without losing universality, we will assume that Im dW = 0. We multiply equation (14) by

$$\frac{d}{dz} dw,$$

and then we integrate it from 0 to H. Then, taking the second integral once by parts and taking the boundary conditions into account, we obtain.

$$[dU(0)]^2 - [dU(H)]^2 = \frac{1}{\omega^2 R_\rho} \int_0^H N^2 (dW)^2 dz. \qquad (15)$$

Here dU is the F-S component of the modulus of horizontal velocity; R_ρ is the mean weighted radius of curvature of the vertical density distribution ρ (z), determined as

$$R_\rho = \int_0^H N^2 (dW)^2 dz / \int_0^H N^2 (dW)^2 (dN^2/dz)/N^2 dz. \qquad (16)$$

Under real ocean conditions $[dU(H)]^2/[dU(0)]^2 \sim (h_0/h_a)^2 \ll 1$, where h_a is the thickness of the abyssal layers. Then, taking into account that dw = $i\omega\, d\xi$, we obtain

$$[dU(0)]^2 \simeq \frac{2}{\rho_0 |R_\rho|} \int_0^H \frac{1}{2} \rho_0 N^2 (d\xi)^2 dz. \qquad (17)$$

The integral in expression (17) represents the doubled potential energy of the elementary harmonic component of internal waves, which within the framework of the linear theory of internal waves is equal to the total energy dE. Taking into account expressions (8), (12), (17), we obtain a final expression for the correlation of the spatial-temporal spectra of the energy of internal waves $E = dE/dk_1 dk_2 d\omega$ and the radiation temperature of the ocean surface

$$E = \frac{1}{2} |R_\rho| \rho_0 \left(\frac{C}{\tau \varkappa}\right)^2 F_{T_p} . \qquad (18)$$

Here C is the phase velocity of internal waves. Since ω and k are related by a dispersion relationship, expression (8) is correct both for the spectra of wave numbers and for the frequency spectra.

For a determination of the radius R_ρ it is necessary to know in advance the modal composition of the internal waves. However, with a known $N^2(z)$ profile having a set of dispersion curves of internal waves it is possible from ω and k of the F_{T_p} spectrum to determine the number of the mode, and accordingly, compute R_ρ and reconstruct the level of spectral density of wave energy. For rough diagnostic evaluations the vertical stratification can be approximated by a two-layer model with a density drop $\Delta\rho$. Then, if $kh_0 \ll 1$, $kH \gg 1$, then

$$C^2 = g \frac{\Delta\rho}{\Delta\rho_0} h_0,$$

$|R_\rho| = h_0/2$ and expression (18) assumes the form

$$E = \frac{g}{4} \Delta\rho \left(h_0 / \tau \varkappa\right)^2 E_{T_p} . \qquad (19)$$

Summary

The results of the cited analyses show the fundamental possibility of determining the dynamic structure of internal waves by the method of remote registry of the characteristic IR radiation of the ocean surface. An important point in the considered theoretical model is the need for the presence of a surface active substance differing with respect to its emission properties from sea water. This circumstance does not reduce the model proposed here to a special case since the ocean surface is virtually always contaminated by surface active substances as a result of vital functions and decomposition of marine organisms, and also as a result of man's activity. The redistribution of the concentration of surface active substances by the field of internal waves leads, on the one hand, to modulation of the coefficient of attenuation of capillary-gravitational ripples and the formation of slicks, and on the other hand, to modulation of ocean surface emissivity. The first effect was used in [8] for sensing of internal waves in the visible range from slicks on the surface; the second lies at the basis of sensing internal waves in the IR range.

In conclusion we note that the possibility of practical use of the method of IR sensing of internal waves is related to an investigation of the capability of the atmospheric layer to transmit the contrasts of characteristic emission of the ocean.

BIBLIOGRAPHY

1. Nelepo, B. A., Khmyrov, B. Ye., Terekhin, Yu. V., et al., PROBLEMY, VOZMOZHNOSTI I PERSPEKTIVY KOSMICHESKOY OKEANOGRAFII (Problems, Possibilities and Prospects of Space Oceanography), Preprint No 4, Sevastopol', Izd-vo MGI AN UkSSR, 1979, 52 pages.

2. Nelepo, B. A., Kuftarkov, Yu. M. and Kosnyrev, V. K., "On the Problem of Determining the Parameters of Synoptic Eddies in the Ocean From Artificial Earth Satellites," DAN SSSR (Reports of the USSR Academy of Sciences), Vol 242, No 6, pp 1289-1292, 1978.

3. Nelepo, B. A. and Kuftarkov, Yu. M., "Experimental Investigation of the Characteristics of Internal Waves in the Ocean by Remote Methods," DAN AN SSSR, Vol 249, No 4, pp 980-983 [year not given].

4. Bramson, M. A., Zel'manovich, I. L. and Kuleshova, G. I., "Emissivity of Water in the Spectral IR Region," TRUDY GGO (Transactions of the Main Geophysical Observatory), No 152, Leningrad, pp 31-67, 1964.

5. Kudryavtsev, V. N., "Evaluation of the Temperature Contrast Between a Slick and the Clean Surface," in press.

6. Bogorodskiy, V. V., Kropotkin, M. A. and Sheveleva, T. Yu., "Investigation of the Influence of Petroleum Contaminations, Salinity and Some Other Factors on the Optical Properties of Water in the IR Spectral Region," METEOROLOGIYA I GIDROLOGIYA (Meteorology and Hydrology), No 12, pp 3-9, 1974.

7. Levich, V. G., FIZIKO-KHIMICHESKAYA GIDRODINAMIKA (Physicochemical Hydrodynamics), Moscow, GIFML, 1959, 699 pages.

8. Apel, J. R., et al., "Observation of Oceanic Internal and Surface Waves From the Earth Resources Technology Satellite," J. GEOPHYS. RES., Vol 80, No 6, pp 865-881, 1975.

REMOTE MEASUREMENT OF OCEAN TEMPERATURE IN IR RANGE USING REFERENCE POINTS

Sevastopol' SPUTNIKOVAYA GEOFIZIKA in Russian 1980 pp 28-32

[Article by V. S. Suyetin]

[Text]

Abstract: A study was made of the possibility of interpreting multichannel remote measurements of IR radiation of the ocean under conditions of cloud cover with gaps having unknown characteristics for the purpose of obtaining the temperature field of the ocean surface. As additional information the author proposes use of data from direct measurements of surface temperature at individual reference points.

Modern oceanology is imposing extremely high requirements on the accuracy and detail of measurements of the temperature field of the ocean surface [1]. These requirements can in principle be satisfied by remote measurement methods in the IR range by means of high-resolution scanning radiometers. One of the principal reasons for the substantial errors in determining ocean temperature on the basis of data from IR measurements is cloud cover, in part covering the radiometer field of view (resolution element) [2] and leading to an apparent temperature decrease.

A rigorous solution of the problem of allowance for clouds is complicated by the fact that their temperature and optical characteristics can vary in a wide range. This leads to an increase in the number of undetermined factors and accordingly requires the use of additional initial information and the adoption of simplifying assumptions.

For example, the authors of [3, 4] proposed a method for the interpretation of simultaneous measurements of the radiation at two wavelengths (λ_1 = 2.7, λ_2 = 11.1 μm) on the assumption that ocean temperature and the characteristics of clouds are constant within the limits of some area considerably greater than the the size of a resolution element. Only the relative error ω of clouds entering into the radiometer field of view is considered variable.

In solving problems in study of variability of the ocean [1] the assumption of a constancy of its temperature is unacceptable. In this article a study is made of the possibility of taking clouds into account under conditions of a substantial spatial variability of the temperature field by use of multichannel remote measurements in the IR range and use of direct measurements of the ocean surface at individual reference points.

In the case of translucent clouds it is proposed that measurements be made at not less than three wavelengths in the windows of atmospheric transparency. In the case of opaque clouds two wavelengths can be adequate. As a simplification we will assume that the directional diagrams for each measurement channel are identical and have a right-angle configuration. Within the limits of a resolution element the temperature T of the ocean surface will be considered constant.

The intensity of the measured radiation of the wavelength λ_i will be represented in the following way:

$$J_i = (1-\omega) J_i^{(1)} + \omega J_i^{(2)},$$

where $J_i^{(1)}$ and $J_i^{(2)}$ is the radiation with $\omega = 0$ and $\omega = 1$ respectively. Assume that $J_i = J_i^{(0)}$ are fixed radiation values measured at the point for which the surface temperature is known and equal to T_0. The corresponding ω value (unknown) will be denoted ω_0. Taking into account that the variations of surface temperature T do not exceed several degrees, for a description of the deviations $\delta J_i = J_i - J_i^{(0)}$ it is possible to use the approximate expression

$$\delta J_i = \varkappa_i P_i \frac{\partial B(\lambda_i, T_0)}{\partial T}\theta + \left[F_i - G_i + \varkappa_i \Gamma_i B(\lambda_i, T_0) - \varkappa_i P_i B(\lambda_i, T_0)\right](\omega - \omega_0) + (\Gamma_i - P_i)\varkappa_i \frac{\partial B(\lambda_i, T_0)}{\partial T}\theta\omega, \tag{1}$$

where $B(\lambda, T)$ is the Planck function;

$$B(\lambda, T) = B(\lambda, T_0) + \frac{\partial B(\lambda, T_0)}{\partial T}\theta;$$

$\theta = T - T_0$; $\varkappa_i$ is the sea surface blackness coefficient; P_i is the transmission coefficient with $\omega = 0$ (cloudless atmosphere); Γ_i is the atmospheric transmission function with $\omega = 1$. Here we used the following expressions:

$$J_i^{(1)} = \varkappa_i P_i B(\lambda_i, T) + G_i, \qquad J_i^{(2)} = \varkappa_i \Gamma_i B(\lambda_i, T) + F_i,$$

where F_i is atmospheric radiation with $\omega = 1$ (including solar radiation reflected or scattered by clouds); G_i is atmospheric radiation with $\omega = 0$.

In vector form model (1) assumes the form

$$\bar{t} = \theta\bar{a}_1 + (\omega - \omega_0)\bar{a}_2 + \theta\omega\bar{a}_3, \tag{2}$$

where

$$t^{(i)} = \delta J_i; \qquad a_1^{(i)} = \varkappa_i P_i \frac{\partial B(\lambda_i, T_0)}{\partial T};$$

$$a_2^{(i)} = F_i - G_i + \varkappa_i \Gamma_i B(\lambda_i, T_0) - \varkappa_i P_i B(\lambda_i, T_0); \quad a_3^{(i)} = (\Gamma_i - P_i)\varkappa_i \frac{\partial B(\lambda_i, T_0)}{\partial T}$$

for $i = 1, \ldots, n$; n is the number of the measurement channels.

We will assume that for the analyzed set of remote measurements at a number of points (scanning elements) only θ and ω are variable factors. The problem essentially involves a search for the θ_k, $k = 1, \ldots, N$ values; N is the full number of analyzed measurement points.

As is well known, the $\varkappa_i$ and P_i values can be stipulated a priori with an accuracy no worse than several percent. In seeking the absolute T values exclusively on the basis of remote measurements such an accuracy is too low, but in an analysis of the values of the deviations δJ_i and θ the solution errors associated with errors in stipulating the $\varkappa_i$ and P_i values will evidently be negligible. We note that for a more precise stipulation of these values it is possible to employ contact measurements at reference points and also remote measurements of microwave radiation. Thus, the vector $\vec{a}_1$ can be considered fully stipulated. With respect to $\vec{a}_2$ and $\vec{a}_3$, they must be considered unknown because the corresponding cloud cover characteristics F_i and Γ_i can be stipulated a priori only extremely approximately.

We will examine the following two characteristic cases.

1. The vectors $\vec{a}_1$, $\vec{a}_2$, $\vec{a}_3$ are linearly independent. In this case $\Gamma_i \neq 0$ (with $\Gamma_i = 0$ the vectors $\vec{a}_1$ and $\vec{a}_3$ are proportional), that is, the cloud cover is translucent. In addition, the number of measurement channels is $n \geqslant 3$.

2. The vector $\vec{a}_3$ is proportional to $\vec{a}_1$, that is, there is some coefficient ε with which $\vec{a}_3 = \varepsilon \vec{a}_1$. In the case of opaque clouds $\Gamma_i = 0$ and $\varepsilon = -1$.

A situation when $\vec{a}_3$ and $\vec{a}_1$ are not proportional and nevertheless the system of vectors $\vec{a}_1$, $\vec{a}_2$, $\vec{a}_3$ is linearly dependent is degenerate and is not examined hereafter.

Case 1. A solution can be obtained directly from (2) in the form $\theta = (\vec{h}, \vec{t})$ if one finds such a $\vec{h}$ vector that $(\vec{h}, \vec{a}_1) = 1$ and $(\vec{h}, \vec{a}_2) = (\vec{h}, \vec{a}_3) = 0$ (the scalar product is denoted by parentheses). Since $n \geqslant 3$ and the vectors $\vec{a}_1$, $\vec{a}_2$, $\vec{a}_3$ are linearly independent, such an $\vec{h}$ evidently exists. In order for it to be determined we will use direct measurements of surface temperature at two other reference points in addition to the point taken as the reckoning level $J_i^{(0)}$. The corresponding θ values are denoted by $\theta_1 = T_1 - T_0$ and $\theta_2 = T_2 - T_0$.

We will rewrite (2) for these points (k = 1, 2) in the form

$$\vec{t}_k - \theta_k \vec{a}_1 = \vec{w}_k = \left(\omega_k - \omega_0\right) \vec{a}_2 + \theta_k \omega_k \vec{a}_3 . \tag{3}$$

The vectors $\vec{w}_1$ and $\vec{w}_2$ are known. If the reference points are representative, it can be assumed that $\vec{w}_1$ and $\vec{w}_2$ are nonproportional; then these vectors generate a plane in n-dimensional space, which according to (3) contains the vectors $\vec{a}_2$ and $\vec{a}_3$. Accordingly, if we take some vector orthogonal to $\vec{w}_1$ and $\vec{w}_2$, with the corresponding normalization it will be the sought-for vector $\vec{h}$.

In this case use is made of reference measurements of temperature at three points: one measurement (T_0) is for establishing the absolute level and two measurements (T_1 and T_2) are for eliminating the uncertainty related to the cloud cover characteristics.

Case 2. In this case the $\vec{h}$ vector does not exist and any vector orthogonal to $\vec{w}_1$ and $\vec{w}_2$ is orthogonal to $\vec{a}_1$ and $\vec{t}$. Accordingly, for seeking θ a different approach is necessary. Model (2) with $\vec{a}_3 = \varepsilon a_1$ undergoes transition into

$$\vec{t} = \left(1 + \varepsilon\omega\right) \theta \vec{a}_1 + \left(\omega - \omega_0\right) \vec{a}_2. \tag{4}$$

We will represent $\vec{a}_2$ in the form of the linear combination $\vec{a}_2 = \alpha \vec{a}_1 + \beta \vec{b}$, where α and β are unknown coefficients; b is a vector of a unit length orthogonal to $\vec{a}$, that is $(\vec{a}, \vec{b}) = 0$; $(\vec{b}, \vec{b}) = \| \vec{b} \|^2 = 1$. With n = 2 the $\vec{b}$ vector is easily stipulated on the basis of known $\vec{a}_1$. In the case $n > 2$ the $\vec{b}$ vector can be found using the formula

$$\vec{b} = \vec{c} \| \vec{c} \|^{-1}, \quad \vec{c} = \vec{t} - \left(\vec{a}_1, \vec{t}\right) \| \vec{a}_1 \|^{-2} \vec{a}_1 .$$

Thereafter, from (4) for k = 1,...,N we obtain

$$\left(\vec{a}_1, \vec{t}_k\right) \| \vec{a}_1 \|^{-2} = \left[1 + \left(\vec{b}, \vec{t}_k\right) \varepsilon \beta^{-1} + \varepsilon \omega_0\right] \theta_k + \left(\vec{b}, \vec{t}_k\right) \alpha \beta^{-1} \tag{5}$$

If the expression in brackets is different from zero and the values $\varphi = \varepsilon\beta^{-1}$, $\psi = \varepsilon\omega_0$ and $\gamma = \alpha\beta^{-1}$ are known, the values θ_k can be determined.

In order to determine the φ, ψ, γ values we will use three reference points for which the θ_1, θ_2, θ_3 are known. We will write (5) for these points in the following way (j = 1, 2, 3):
[β = b]

$$\left(\vec{b}, \vec{t}_j\right) \theta_j \varphi + \theta_j \psi + \left(\vec{b}, \vec{t}_j\right) \gamma = \left(\vec{a}_1, \vec{t}_j\right) \| \vec{a}_1 \|^{-2} - \theta_j .$$

This expression represents a system of three linear algebraic equations relative to the unknown parameters φ, ψ, γ. The matrix of coefficients of this system is known and has the form

$$U = \begin{bmatrix} \left(\vec{b}, \vec{t}_1\right) \theta_1 & \theta_1 & \left(\vec{b}, \vec{t}_1\right) \\ \left(\vec{b}, \vec{t}_2\right) \theta_2 & \theta_2 & \left(\vec{b}, \vec{t}_2\right) \\ \left(\vec{b}, \vec{t}_3\right) \theta_3 & \theta_3 & \left(\vec{b}, \vec{t}_3\right) \end{bmatrix}.$$

In a general case U is nondegenerate and therefore the φ, ψ, γ values can be found at all points at which

$$1 + \left(\vec{b}, \vec{t}_k\right) \varepsilon \beta^{-1} + \varepsilon \omega_0 \neq 0 .$$

For the case of ideally opaque clouds ($\varepsilon = -1$) this means that $\omega \neq 1$, since $(\vec{\beta}_1 \vec{t}_k)\, \beta^{-1} = \omega - \omega_0$.

In this case use is made of reference measurements of temperature at four points: three measurements for determining the φ, ψ, γ parameters, a fourth (T_0) for determining the absolute values $T_k = \theta_k + T_0$.

The described approach to interpretation of remote measurement data can be used in carrying out complex investigations in combination with shipboard and buoy measurements. This approach is also convenient in joint remote observations in the IR and microwave ranges. As is well known, a high response and resolution of a scanning microwave radiometer are difficult to attain. In addition, microwave measurements of ocean temperature can be carried out along the flight path of a carrier in the presence of clouds and have been used with the proposed method as reference and control data in the interpretation of observations with a scanning IR radiometer.

In order to obtain evaluations of the errors in solution which can arise due to deviation from the adopted assumptions and for choice of the optimum measurement channels it is necessary to carry out special investigations taking the specific measurement conditions into account.

BIBLIOGRAPHY

1. Nelepo, B. A., Khmyrov, B. Ye., Terekhin, Yu. V., et al., PROBLEMY, VOZMOZHNOSTI I PERSPEKTIVY KOSMICHESKOY OKEANOGRAFII (Problems, Possibilities and Prospects of Space Oceanography), Preprint No 4, Sevastopol', Izd. MGI AN Ukrainskoy SSR, 1979, 52 pages.

2. Novogrudskiy, B. V., Sklyarov, V. Ye., Fedorov, K. N. and Shifrin, K. S., ISSLEDOVANIYE OKEANA IZ KOSMOSA (Investigations of the Ocean From Space), Leningrad, Gidrometeoizdat, 1978, 54 pages.

3. Kondrat'yev, K. Ya. and Timofeyev, Yu. M., METEOROLOGICHESKOYE ZONDIROVANIYE ATMOSFERY IZ KOSMOSA (Meteorological Sounding of the Atmosphere From Space), Leningrad, Gidrometeoizdat, 1978, 280 pages.

4. Smith, W. L., Hilleary, D. T., Fischer, J. C., Howell, H. B. and Wolf, H. M., "NIMBUS-5 ITPR Experiment," APPLIED OPTICS, Vol 13, No 3, pp 499-506, 1974.

FEATURES OF RADAR DETERMINATION OF SEA WAVE PARAMETERS

Sevastopol' SPUTNIKOVAYA GEOFIZIKA in Russian 1980 pp 33-41

[Article by V. V. Pustovoytenko]

[Text]

Abstract: The features of remote determination of the time parameters of sea waves are determined using radar wave-measurement apparatus operating at small glancing angles ($\psi < 10°$). The author investigates the influence of the characteristics of this apparatus and the conditions for making measurements on the statistical characteristics of the envelope of a radio signal scattered by the sea surface. It is shown that the best results in determining the time parameters of sea waves are attained with angles of incidence $1.5 \leqslant \psi \leqslant 5°$.

On the basis of the results obtained in an investigation of the characteristics of scattering of radio waves by the sea surface, methods are now being intensively developed for the remote determination of the parameters of the sea surface and wind in the near-water layer of the atmosphere. In this connection it is of interest to investigate the possibilities of the radar method for determining the spatial-temporal characteristics of waves.

1. Principal Characteristics of Backscattering of Radio Waves by Sea Surface

Theoretical and experimental investigations carried out on the selective character of the scattering of radio waves by the wave-covered sea surface made it possible to create an electrodynamic model of a scattering surface [8, 9] and within its limits explain the principal patterns of scattering.

The backscattering of radio waves is caused by the presence at the sea surface of "resonance" components of waves with the wave number

$$\varkappa_0 = 2k \cos\psi , \qquad (1)$$

where $k = 2\pi/\lambda$ is the wave number of the radio wave; λ is its length; $\varkappa_0$ is the wave number of the scattering sea wave; $\psi = \arcsin h/R$ is the glancing angle, reckoned from the calm sea surface; h is the height of antenna system placement; R is the slant range to the scattering sector of the sea surface.

It follows from (1) that in the centimeter range of radio waves the scattering element on the sea surface is ripple waves. Since the height of these waves is $h \ll \Lambda_0$, the field scattered by them is computed by the perturbations method.

The specific effective scattering area σ^0 in vertical (BB) and horizontal (ΓΓ) polarizations of the radiation is determined by the expressions

$$\sigma^0_{BB} = 16\pi k^4 \varepsilon\varepsilon^* \sin^4\psi \cdot f(\varepsilon, \psi)\, S(\mathscr{H}_0), \quad (2)$$

$$\sigma^0_{\Gamma\Gamma} = 16\pi k^4 \sin^4\psi \cdot S(\mathscr{H}_0), \quad (3)$$

where ε is the dielectric constant of sea water

$$f(\varepsilon, \psi) = \left[(1 + \eta_1 \sin\psi)^2 + \eta_2^2 \sin^2\psi\right]^{-2}, \quad \eta_1 + i\eta_2 = \sqrt{\varepsilon},$$

ψ. $S(\mathscr{H}_0)$ is the spectral density of sea waves in the region of wave numbers $\mathscr{H}$.

The angular dependences $\delta^0(\psi)$ (2), (3) in the region of small glancing angles $\psi \leqslant 5$–8 have a high steepness, which causes amplitude modulation of the scattered signal.

During the scattering of radio waves by the sea surface there is a Doppler frequency shift of the scattered signal by the value [1]

$$F_{cM} = \sqrt{\frac{gn}{\lambda\pi} + \frac{16\pi\alpha}{n\rho\lambda^3}}, \quad (4)$$

where n is a whole number determining the order of the diffraction spectrum; α is the surface tension coefficient; ρ is the density of sea water.

As demonstrated in [2], the characteristics of the scattered signal are determined for the most part by the first-order (n = 1) diffraction spectrum. It follows from (1) that large sea waves do not directly participate in the scattering of radio waves in the centimeter range but cause amplitude (2), (3) and phase (4) modulation of the signal scattered by ripples.

Figure 1,b shows a part of the record of the envelope of a signal scattered by the sea surface corresponding to the passage of one sea wave through the irradiated area D. The record was obtained during irradiation of the sea surface by a radio wave with λ = 3.2 cm, having vertical polarization of radiation at a glancing angle ψ' = 2° and with a duration of the sounding pulse τ_{pulse} = 0.04 μsec. Here also (Fig. 1,c) we have shown a series of "instantaneous" spectra of the fluctuations $S(\omega)$ of the scattered signal

$$S(\omega) = \frac{1}{2\pi} \int_0^{\tau_{max}} R(\tau) \cos\omega\tau\, d\tau,$$

corresponding to the observation time $\tau_{pulse} < T$. The numbers 1-4 denote segments of the E(t) record for which S(F) was computed.

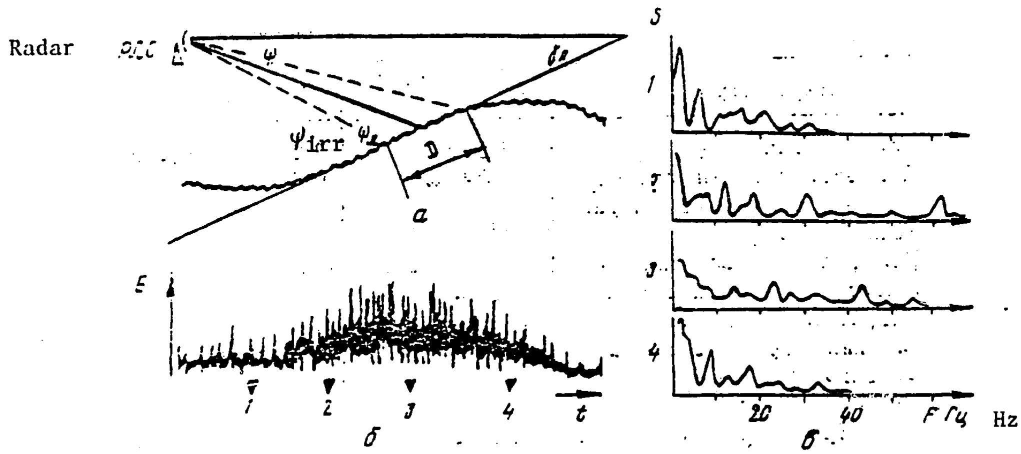

Fig. 1.

The "slow" change in the mean level $\bar{E}$ of the envelope of the scattered signal is attributable to a change in the irradiation angle φ_{irr} (Fig. 1,a) of the irradiated area by a large sea wave. The $\bar{E}$ maximum corresponds to reflection from the frontal slope of a wave for which the angle $\varphi_{irr} = \varphi + \gamma$ is maximum.

"Rapid" high-frequency fluctuations of the envelope are caused by the presence in the "pulse volume" of reflectors (1) moving with different velocities as a result of the modulation of the phase velocity of ripples by the orbital velocity of wave movement. With a high resolution in coordinates the width of the spectrum of fluctuations ΔF also changes in time, attaining its maximum value ΔF_{max} with reflection from the frontal slope of the wave at which the maximum orbital velocity gradients are observed.

2. Apparatus and Methods for Radiooceanographic Measurements

An experimental investigation of the characteristics of radar determination of the spatial-temporal characteristics of sea waves was made using models of a multifrequency radar measurement system [3] and a wave-measuring attachment [4] in the Caspian Sea (Neftyanyye Kamni) and Black Sea (Katsiveli) with sea waves in classes 2-5. The principal characteristics of the apparatus are given in Table 1.

These characteristics made it possible to carry out investigations in the range of glancing angles 0.5-8° in the sector of azimuthal angles $\Delta\varphi = 160°$.

In the measurements a study was made of the influence exerted on the characteristics of the scattered signal by wavelength, resolution and polarization of radar radiation, glancing angle ψ and azimuthal angle φ between the direction of sighting and the direction of sea wave propagation.

Table 1

Parameters	Caspian Sea	Black Sea
Wavelength, λ	3.2 cm	32 and 10.0 cm
Pulse duration τ_{pulse}	0.04 μsec	0.05-1.0 μsec
Width of directional diagram $\theta_{0.5}$	$1^{\circ}.1$	1.1 and $1^{\circ}.8$
Polarization of radiation P	Plane	Plane
Antenna height h	12 m	8 m
Wind velocity W	5-15 m/sec	5-15 m/sec
Sea depth at measurement point H	60 m	20-25 m

The envelope of the signals scattered by the sea surface was registered using high-speed H-700 and H-327-5 automatic recorders.

In the statistical processing of the records we determined: the mean period of fluctuations of the envelope

$$\overline{T} = \frac{1}{N}\sum_i T_i;$$

the dispersion of the periods of fluctuations

$$D_T = \sigma_T^2 = \frac{1}{N}\sum_i (T_i - \overline{T})^2;$$

the variation coefficient $K_T = \sigma_T/\overline{T}$; the asymmetry coefficient

$$A_T = \mu_3/\sigma^3 = \frac{\frac{1}{N}\sum_i (T_i - \overline{T})^3}{\sigma_T^3}.$$

3. Measurement Results

It was noted in [5] that with a high spatial resolution of the radar the time characteristics of the mean level of the envelope of the scattered signal $\overline{E}$ are determined by the change of the "effective" slope of the irradiated sector of the sea surface by large sea waves.

It is obvious that the principal statistical characteristics of the envelope, determined by the magnitude of the resolved sea surface element D, with identical conditions of irradiation and reception at several wavelengths, should be identical.

Figure 2 shows a sector of a synchronous record of the mean level $\overline{E}$ of the envelopes of the scattered signal at wavelengths $\lambda_1 = 3.2$ and $\lambda_2 = 10$ cm during surface irradiation toward large sea waves (Fig. 2,a) and along the crests of sea waves (Fig. 2,b). The upper part of the figure shows the time scale of the record. The period of the marks is 1 sec. In the left part of the figure, by the corresponding "signalograms," we have shown the scale of the record of the scattered signal level in relative units. Similar notations have also been adopted for the subsequent figures. In both signals there is a synchronous low-frequency modulation with a period $T \simeq 4$ sec; the "signalograms" are well correlated. The cross-correlation coefficient varies in the range r = 0.85-0.95. With irradiation of the sea surface along the line of crests the correlation of the fluctuations $\overline{E}$

weakens. In 20-25% of the cases there is no correspondence between the extremal points of the envelopes. This then leads to a noticeable decrease in the cross-correlation coefficient to r = 0.45-0.6 and to a change in the statistical characteristics of the envelopes.

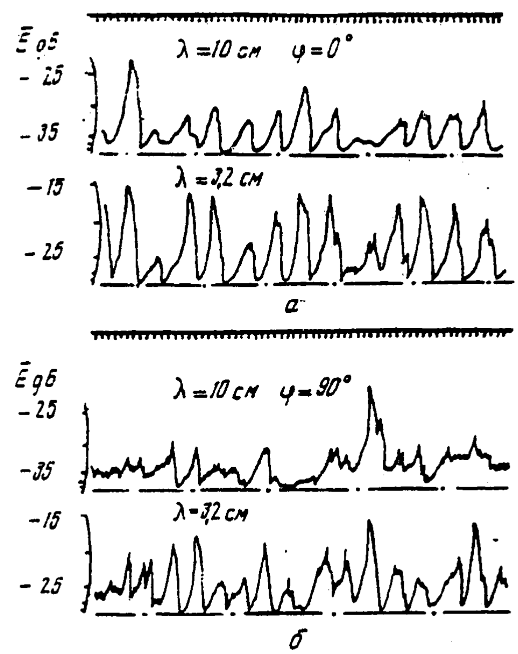

Fig. 2.

Table 2 gives the characteristics of the distribution functions for the periods of fluctuations of the envelope of a signal scattered by the sea surface at radio waves 3.2 and 10 cm.

With the irradiation of the sea surface in the direction toward the wave the characteristics of the envelopes at both radio waves are virtually identical, whereas with irradiation along the wave crests they differ substantially.

By the use of radar wave-measuring apparatus it is possible to determine quite precisely both the mean period and the distribution function of the wave periods [5]. For this procedure it is of considerable importance to make a proper choice of the parameters of the measurement apparatus and measurement conditions.

For example, with irradiation of the sea surface at a glancing angle exceeding the critical value $\psi_{cr} \gtrsim 5$-$6°$ there is a marked decrease in the dependence $\sigma°(\psi)$, which leads to a decrease in the intensity of amplitude modulation of the scattered signal. This effect is manifested particularly strongly in the case of a vertical polarization of the radiation.

Table 2

Parameter	Toward wave		Along crests	
	λ = 3.2 cm	λ = 10 cm	λ = 3.2 cm	λ = 10 cm
Mean period $\overline{T}$, sec	4.14	4.12	3.7	4.25
Standard deviation σ_T sec	1.16	1.14	0.83	1.52
Variation coefficient K_T	0.281	0.278	0.22	0.36

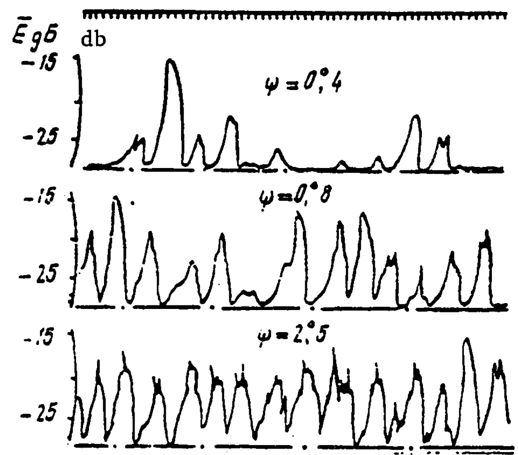

Fig. 3.

With a decrease in the glancing angle there is first an increase in the intensity of modulation of the scattered signal, then a sharp decrease in its absolute value and a shading of lower waves by higher waves, which leads to a difference between the radar and true relief of the sea surface. In this case the radar receives signals scattered only on the steepest of the irradiated sea waves.

Figure 3 shows the transformation of the envelope of a signal in the 3-cm range scattered by the sea surface, caused by a change in the glancing angle ψ. In the region of angles $\psi \simeq 0°.4$ there is a considerable influence of the considered effects, leading to the omission of individual sea waves and accordingly a distortion in the determined characteristics of sea waves. With an increase in ψ the influence of these effects weakens and in the region $\psi \simeq 2°.5$ is virtually not sensed at all.

Table 3 gives a comparison of the parameters of the distribution functions of periods determined from the corresponding "signalograms" (traces) of the scattered signal.

With an increase in the glancing angle ψ there is a decrease in the variation coefficient k_T and, accordingly, an increase in the degree of reliability in determining the mean period of the waves; the distribution curves $\varphi(T)$ acquire a small asymmetry and in their shape approach the curves described by a normal distribution law.

Table 3

Parameter	$\lambda = 0°.4$	$\lambda = 0°.8$	$\lambda = 2°.5$
Mean value $\bar{T}$ sec	5.77	4.64	4.24
Standard deviation δ_T sec	5.03	1.67	0.95
Variation coefficient K_T	0.871	0.36	0.22
Asymmetry coefficient R_T	1.33	1.72	0.94
Excess coefficient E	13.72	3.09	1.52

The determined values σ_T and K_T with glancing angles $\psi \simeq 2°$ agree satisfactorily with the results of direct measurements of similar characteristics of sea waves in the measurement regions [5, 6].

With an increase in the duration of the sounding pulse there is a simultaneous irradiation of several slopes of sea waves. In this case the characteristics of the scattered signal are determined by the totality of the "luminescent points" present in a resolved surface element and the fluctuations of the envelope of the scattered signal are described by a Rayleigh distribution law [7].

The decrease in the intensity of modulation of the mean level of the scattered signal occurring in this case precludes the possibility of determining the statistical characteristics of the waves.

An analysis of the fine structure of the scattered signal in the case of a plane polarization of the radiation indicated the presence of powerful, little-fluctuating bursts of a signal caused by the scattering of radio waves on the crests of sea waves prior to their collapse [10]. Since the bursts are observed both in the region of the peak and in the region of a foot of a wave, and their number varies from 1 to 4 in the period of a large wave, there can be errors in determining the time parameters of such waves. In order to eliminate the influence of bursts envelope filtering was introduced in such a way as to bring about this goal [4]. No differences were observed in the statistical characteristics of the envelopes $\bar{E}$ of the scattered signal in the cases of vertical and horizontal polarizations of radiation in the described experiments.

However, in the radar determination of the parameters of the energy-carrying part of the sea waves in the case of a small glancing angle, due to the energy advantages ($\sigma^o_{BB} \gg \sigma^o_{\Gamma\Gamma}$), it is preferable to use radar systems having a vertical polarization of radiation.

Conclusion

Investigations of features of radar determination of the time parameters of sea waves indicated:

1. With assurance of identical conditions for irradiation of the sea surface the statistical characteristics of the envelope of scattered signals at wavelengths $\lambda_1 = 3.2$ and $\lambda_2 = 10$ cm coincide well with irradiation toward the sea waves;

with irradiation of the surface along the line of crests the statistical characteristics do not coincide.

2. With an increase in the duration of the sounding pulse the dispersion of fluctuations of the mean level of the scattered signal decreases and the fluctuations acquire a random character, which considerably complicates the problem of determining the time characteristics of the waves.

3. The proper choice of the glancing angle exerts a great influence on the accuracy in determining the parameters of sea waves. It is preferable to have it in the range $1.5 \leqslant \psi \leqslant 5°$.

4. The type of polarization of radiation exerts no significant influence on the accuracy in determining the statistical parameters of waves, but due to the energy advantages it is better to use vertical polarization of radiation.

BIBLIOGRAPHY

1. RADIOOKEANOGRAFICHESKIYE ISSLEDOVANIYA MORSKOGO VOLNENIYA (Radiooceanographic Investigations of Sea Waves), edited by S. Ya. Braude, Kiev, Izd-vo AN UkrSSR, 1962, 116 pages.

2. Rozenberg, A. D., Kalmykov, A. I. and Zel'dis, V. I., "Backscattering of Acoustic Waves on Regular Ripples," IZV. VUZov SSSR: RADIOFIZIKA (News of USSR Institutions of Higher Education), 9, No 2, pp 234-240, 1966.

3. Galayev, Yu. M., Kalmykov, A. I., Kurekin, A. S., et al., "Radar Detection of Petroleum Contaminations of the Sea Surface," IZV. AN SSSR: FAO (News of the USSR Academy of Sciences: Physics of the Atmosphere and Ocean), 13, No 4, pp 406-414, 1976.

4. Kalmykov, A. I. and Pustovoytenko, V. V., "Radar Apparatus for Measuring the Spatial-Temporal Characteristics of Sea Waves," NEKONTAKTNYYE METODY IZMERENIYA OKEANOGRAFICHESKIKH PARAMETROV (Noncontact Methods for Measuring Oceanographic Parameters), Moscow, Gidrometeoizdat, pp 27-30, 1977.

5. Zamarayev, B. D., Kalmykov, A. I., Kireyev, I. V., et al., "Methods for Determining the Characteristics of Waves by the Radar Method," NEKONTAKTNYYE METODY IZMERENIYA OKEANOGRAFICHESKIKH PARAMETROV, Moscow, Gidrometeoizdat, pp 7-16, 1975.

6. Kroneva, L. A., "Statistical Characteristics of Wave Elements in the Coastal Zone of an Abyssal Sea," TRUDY MGI AN SSSR (Transactions of the Marine Hydrophysical Institute, USSR Academy of Sciences, Vol 23, Moscow, pp 44-65, 1961.

7. Barton, D. and Vard, G., SPRAVOCHNIK PO RADIOLOKATSIONNYM IZMERENIYAM (Handbook on Radar Measurements), Moscow, "Sov. Radio," 1976, 392 pages.

8. Bass, F. G., Fuks, I. M., Kalmykov, A. I., Ostrovskiy, I. Ye. and Rosenberg, A. D., "Very High Frequency Radio Wave Scattering by a Disturbed Sea Surface," IEEE TRANS. ANTENNAS, PROPAG., AP-16, No 5, pp 554-565, 1968.

9. Wright, J. W., "A New Model for Sea Clutter," IEEE TRANS. ANTENNAS, PROPAG., AP-16, No 2, pp 217-223, 1968.

10. Kalmykov, A. I. and Pustovoytenko, V. V., "On Polarization Features of Radio Signals Scattered From the Sea Surface at Small Grazing Angles," JOURN. OF GEOPHYS. RES., Vol 81, No 12, pp 1960-1964, 1976.

EFFECT OF EXTERNAL ILLUMINATION CONDITIONS ON REMOTE MEASUREMENT OF COLOR INDEX

Sevastopol' SPUTNIKOVAYA GEOFIZIKA in Russian 1980 pp 42-46

[Article by V. Ye. Shemshura and O. V. Martynov]

[Text]

Abstract: A study was made of the effect of external illumination conditions on the results of remote measurement of the color index of the sea. It is shown that the data obtained by contact and noncontact methods correlate well. The color index of the sea is greater in the presence of cloud cover in comparison with clear weather.

Remote optical methods have recently been considerably developed for investigating the natural resources of the world ocean which are based on registry of the spectral brightnesses of radiation emanating from the sea. A knowledge of the corresponding brightnesses makes it possible to determine parameters making it possible to estimate the content of substances dissolved and suspended in water, including those of biological origin. These include the color index of the water layer, by which is meant, in accordance with the adopted terminology [5], the ratio of radiation brightness in the green part of the spectrum to the brightness in the blue part, measured at the nadir under the water-air discontinuity

$$J = \frac{B\uparrow (540\ \text{nm})}{B\uparrow (460\ \text{nm})}.$$

As the color index it is possible to use the ratio of the radiation brightnesses in other parts of the spectrum, so that in a general case

[β = B]

$$J = \frac{\beta^{\uparrow}(\lambda_1)}{\beta^{\uparrow}(\lambda_2)}. \quad (1)$$

In the Optics Section of the Marine Hydrophysical Institute of the Ukrainian Academy of Sciences specialists have recently designed an instrument which now makes it possible to determine the value $J' = k\,J$, where k = const. The operating principle of the instrument and the results of the first investigations were given in [1]. In remote measurements the registered value will be dependent primarily on the external illumination conditions.

For the purpose of clarifying the influence of this factor on the results of non-contact measurements of the color index specialists on the 31st voyage of the scientific research ship "Mikhail Lomonosov" carried out observations with deepening of an instrument similar to [1] by 5-6 m and then at a height of 3-4 m from the water surface. It is evident that in the latter case there will be registry of the value $J'_{sea} = kJ_{sea}$, where

$$J_{sea} = \frac{B^{\uparrow}_{sea}(\lambda_1)}{B^{\uparrow}_{sea}(\lambda_2)}$$

is the color index of the sea, equal to the ratio of the two spectral sea brightnesses. For the direction to the nadir we can write

$$B_{sea}(\lambda) = \frac{t}{n^2} B^{\uparrow}(\lambda) + r\, B^{\downarrow}_{sky}(\lambda), \qquad (2)$$

where $B^{\downarrow}_{sky}(\lambda)$ is the spectral brightness of the sky in the zenith; t and γ are the coefficients of transmission and reflection of light by the water surface respectively (surface free of foam); n is the refractive index. Simultaneously with ' and J'_{sea} there was also registry of the value $J_{sc}' = kJ_{sc}$, where

$$J_{sc} = \frac{B^{\uparrow}_{sc}(\lambda_1)}{B^{\uparrow}_{sc}(\lambda_2)}$$

is the color index of a horizontally placed white screen isotropically reflecting solar radiation and sky radiation ($B_{sc}(\lambda)$ is the spectral brightness of the screen), λ_1 and λ_2 in the index meter are equal to 568 and 448 nm respectively.

In order to compare the data obtained with different instruments it is necessary to normalize the J' and J'_{sea} values to the color index of a standard object, using a white screen for this purpose. It can be seen that the normalized color indices for the water layer and sea, that is, $J^{sky} = J'/J'_{sc}$ and $J^{sky}_{sea} = J'_{sea}/J'_{sc}$ are equal to the ratio of the corresponding spectral brightness coefficients

$$\begin{aligned} J^{sky} &= \rho(\lambda_1)/\rho(\lambda_2), \\ J^{sky}_{sea} &= \rho_{sea}(\lambda_1)/\rho_{sea}(\lambda_2). \end{aligned} \qquad (3)$$

It is known that the spectral brightness coefficients for the water layer, and accordingly, also their ratio, are dependent in this case only on the primary hydrooptical characteristics. Table 1 gives the values of the parameters J', J'_{sea}, J^{sky} and J^{sky}_{sea} obtained at one of the stations during sunny weather and after a half-hour when there was a continuous cloud cover. It can be seen that the normalized color index of the water layer J^{sky} is not dependent on the external illumination conditions.

Figure 1 shows the dependence of J'_{sea} on J^{sky} under different meteorological conditions: from a full sun in a cloudless sky (O) to continuous low cloud cover and a sun in the haze (●). There were 32 series of measurements, of which 10 were in clear weather. The presence of cloud covers of different character lead to a considerable scatter of the experimental points. Table 2 gives the correlation coefficients r_{xy}. The upper lines in Table 2 correspond to the results obtained in sunny weather; the lower lines correspond to cloudy weather. The high value of the correlation coefficient between J'_{sea} and J^{sky} in the case of a clear sun and a relatively low value of the correlation coefficient in the presence of a cloud cover is evidently attributable to the fact that the spectral composition of the radiation incident on the sea surface in the first case (with a not very low sun) changes insignificantly, but in the second case was subject to considerable variations [2], which leads to fluctuations $B^{\uparrow}_{sea}(\lambda)$, and accordingly, fluctuations of the color index of the sea. The value of the J'_{sea} parameter is also dependent on meteorological conditions: as a rule, it is greater when a cloud cover is present than when there is a clear day. This means that the fraction of green light in the radiation of the cloudy sky is greater than in the radiation of a clear sky, since the J'_{sea} measurements were made at the nadir and the direct sunlight reflected from the sea surface did not enter the instrument field of view. Sun flashes arising due to the waves were excluded. In actuality, using the data in Table 11.3 from [2] we find that the ratio $B^{\downarrow}_{sky}$ (568 nm)/$B^{\downarrow}_{sky}$ (446 nm) for the cloudy and clear sky is equal to 0.92 and 0.55 respectively.

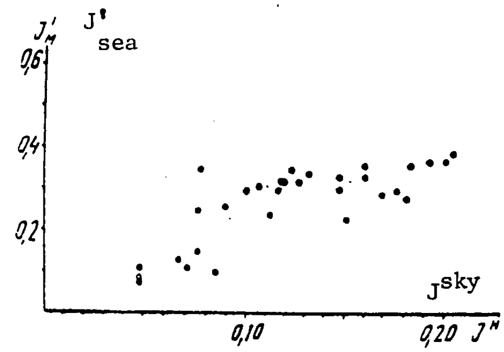

Fig. 1.

Table 1

Type of illumination	Measurement time	J'	J'_{sea}	J^{sky}_{sea}	J_{sky}
Sunny	1400	0.092	0.23	0.38	0.15
Continuous clouds	1430	0.075	0.30	0.59	0.15

The dependence of the normalized color index of the sea on the normalized color index of the water layer as a whole is similar to the functional relationship $J'_{sea} = f(J^{sky})$. The normalization of the J'_{sea} to J'_{sc} leads to some decrease in the scatter of points and an increase in the correlation coefficient in comparison with the data considered earlier. However, the r value for the cloudy sky nevertheless remains low (Table 2).

Accordingly, with the use of an instrument registering radiation of the sea layer some uncertainty is introduced into the color index, making it impossible to make full allowance for the spectral composition of skylight reflected from the sea surface.

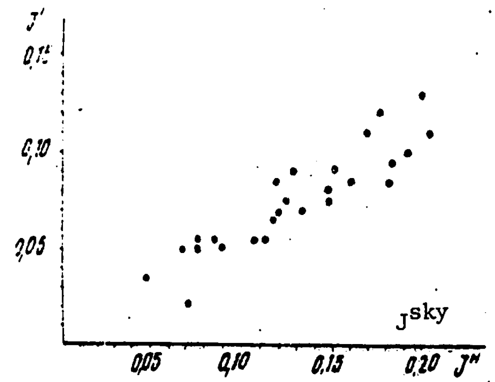

Fig. 2.

Table 2

Type of dependence	r_{xy}
$J'_{sea} = f(J^{sky})$	0.972
	0.611
$J^{sky}_{sea} = f(J^{sky})$	0.982
	0.762
$J' = f(J^{sky})$	0.996
	0.869

It is interesting to clarify the degree of influence of external illumination conditions on the J' value, measured by the contact method. Figure 2 represents the dependence of J' on J^{sky}. Here the r_{xy} values in both cases are quite high. It can be seen that the color index of the water layer is slightly dependent on the changes in the spectral composition of the incident radiation, as was demonstrated earlier in [4].

Conclusions

1. The results of measurements made by contact and noncontact methods correlate with one another. The numerical value of the correlation coefficient is dependent on the conditions of external illumination: it is greater in the case of a cloudless sky.

2. The values of the normalized color index of the sea J^{sky}_{sea} are greater in the presence of a cloud cover than during clear weather.

3. The color index of the water layer J' is slightly dependent on the external illumination conditions.

The results obtained in this study are of a preliminary character since the investigations were made in regions of the Atlantic Ocean characterized by a high transparency [3] and a low biological productivity (the concentration of chlorophyll "a" in the upper layer of the ocean is $\leqslant$ 0.2 mg/m^3). In the future, for a more complete analysis, it is necessary to carry out such measurements in waters with a high level of the light attenuation index and biological productivity.

BIBLIOGRAPHY

1. Li, M. Ye. and Martynov, O. V., "Some Results of Investigations of the Color Index in the Sea," MORSKIYE GIDROFIZICHESKIYE ISSLEDOVANIYA (Marine Hydrophysical Investigations), No 1, Sevastopol', Izd-vo MGI AN UkrSSR, pp 133-138, 1976.

2. Semenchenko, I. V., "Sea Brightness," PRIMENENIYE AEROMETODOV DLYA ISSLEDOVANIYA MORYA (Application of Aerial Methods for Investigating the Sea), Moscow-Leningrad, Izd-vo AN SSSR, p 15, 1963.

3. Voskresenskiy, V. N., Martynov, O. V. and Shempura, V. Ye., "Hydrooptical Investigations During the 31st Voyage of the Scientific Research Ship 'Mikhail Lomonosov'," MORSKIYE GIDROFIZICHESKIYE ISSLEDOVANIYA, No 2, Sevastopol', Izd-vo MGI AN UkrSSR, pp 180-184, 1974.

4. Neuymin, G. G., Solov'yev, M. V. and Martynov, O. V., "Some Results of Measurements of the Color Index of Waters of Different Regions in the World Ocean," OPTICHESKIYE METODY IZUCHENIYA OKEANOV I VNUTRENNIKH VODOYEMOV (Optical Methods for Studying the Oceans and Internal Water Bodies), Novosibirsk, "Nauka," pp 27-33, 1979.

5. Clarke, G. L., Ewing, G. C. and Lorenzen, D. J., "Remote Measurements of Ocean Color as an Index of Biological Productivity," PROC. OF VI SYMPOSIUM ON REMOTE SENSING OF ENVIRONMENT, Univ. of Michigan, Oct 69.

INVESTIGATION OF THE ICE COVER OF SEAS FROM ARTIFICIAL EARTH SATELLITES

Sevastopol' SPUTNIKAYA GIDROFIZIKA in Russian 1980 pp 47-57

[Article by A. V. Bushuyev]

[Text] Abstract: The article describes the characteristics of the ice cover, which can be determined from television photographs of artificial earth satellites, and also methods for finding the boundaries of zones of different compaction and ice drift vectors. The effectiveness of use of the analytical method for studying the ice cover and supporting the navigation of ships developed at the Arctic and Antarctic Scientific Research Institute is demonstrated. Also considered are the prospects for further improvement of methods for obtaining and processing satellite information from ice cover observations.

From the moment of launching of the first meteorological artificial earth satellites it became obvious that they can be an effective means for studying not only meteorological elements, but also sea ice. Already in 1968 the first satellite maps of ice distribution in Antarctica were compiled and satellite photographs came into regular use for refining and supplementing ice maps compiled on the basis of data from aircraft ice reconnaissance [3].

In the initial stage only frame TV systems which made a survey in the visible range were used for ice observations. Artificial earth satellites are outfitted with scanning systems which are used in a survey in the blue or several spectral ranges and have a higher resolution and constant light distribution over the frame field, as a result of which the photographs have measurement properties.

The collection of information in the visible range (TV information) is possible when the survey region is adequately illuminated by the sun. Such a survey is used for ice observations in arctic seas from March through October, in Antarctica -- from September through April.

With development of remote sensing techniques it was possible to obtain images of the earth's surface in the IR (8-12μm) and microwave or SHF (0.8-3.0 cm) spectral ranges of electromagnetic waves.

Thermal IR radiation is almost not dependent on illumination, but for the detection of sea ice it is necessary that there be an adequate temperature contrast between surface ice fields and open water. Since in summer such a contrast is virtually absent, IR information can be used for ice observations only during winter.

Instruments for the registry of the natural radiation of underlying surfaces in the microwave part of the spectrum (passive SHF sensors) make it possible to carry out observations regardless of meteorological conditions and illumination. This is a substantial advantage of such instruments, but in actual practice extensive use is made of instruments operating in the visible range, since the photographs taken with such instruments most precisely transmit the desired information on the parameters of the ice cover.

The data obtained on ice conditions obtained as a result of the processing of space videoinformation at sea should be represented in the form of maps at a stipulated scale and in a stipulated projection. The principal processes used in the compilation of ice maps are interpretation and geographic tie-in. By the term interpretation of sea ice is meant the recognition of different ice features and determination of the characteristics [4, 8, 11] of the ice cover as a whole.

In order to identify the image peculiarities on a television photograph of a specific sector of the ice cover with its characteristics it is necessary to have data on characteristic "standard" sectors. The observations in such polygons, including radar observations and aerial photographs and other types of remote sensing, as well as a broad complex of on-ice observations, including with the use of diving techniques, are being systematically carried out by the Arctic and Antarctic Scientific Research Institute on the drifting ice in the Arctic Ocean.

The institute has developed a system of interpretation criteria and the possibilities of determination of the characteristics of the ice cover were evaluated on the basis of its image on the television photographs. Using TV photographs with a resolution of 1-2 km on the ground, taken in the absence of a cloud cover, it is possible to determine the compaction of ice in the range of the principal gradations (9-10, 7-8, 4-5, and sometimes also 1-3 scale units), the position of boundaries of zones of different compaction, individual ice fields greater than 4 km across, channels and leads wider than 0.5-1.0 km. As a result of simultaneous scanning of the entire sea area the photographs of artificial earth satellites make it possible to detect a complex pattern of ice distribution, inevitably simplified with the interpolation of conditions between aerial ice reconnaissance flight lines, to register a system of main channels and leads, to determine the position and configuration of gigantic ice fields.

The most valuable data can be obtained on the dynamics of ice. If the distribution of ice has been established by aerial ice reconnaissance, information on drift was limited to data from two or three drifting stations and data from individual runs obtained as a result of repeated aerial photographic surveys in individual straits and in the coastal sectors of the seas.

With the appearance of satellites whose scanning radiometers have the above-mentioned resolution, it became possible to determine the drift field within the limits of the entire sea.

The plotting of the boundaries of zones with different ice compaction in the compilation of ice maps and the investigation of ice dynamics require a high accuracy in geographic tie-in, by which is meant determination of the position on the earth's surface (and accordingly, on any map) of the features interpreted on the photograph. Since space photographs cover extensive sectors of the earth's surface (which leads to a need for taking into account the earth's curvature and the variable scale of the maps) and due to the peculiarities in obtaining images with scanning systems, the transformation of satellite photographs into a stipulated projection requires nonlinear transformations. Such a transformation is accomplished most precisely by the analytical method with use of digital computers.

The geographic tie-in of TV photographs when they are used for ice and meteorological observations was accomplished by a graphic method [5, 7, 10]. Due to the low accuracy, in this case it was possible to compile only small-scale general ice maps (1:10,000,000 or smaller); there was virtually no possibility of determining the ice drift vectors.

During recent years specialists at the Arctic and Antarctic Institute have developed and introduced a method which provides for the analytical transformation of coordinates not for all photograph elements, but only for individual points (the turning points of ice boundaries, individual ice fields). The process of geographic tie-in in such cases includes three principal stages: measurement of the coordinates of points on the photograph and the input of data into a computer, analytical transformation of the measured coordinates and output in digital or graphic form. In the processing scheme the input units were photogrammetric instruments for measuring the rectangular coordinates of the photographs; the data output units are curve plotters and a printout unit. In the future this will make it possible to introduce the analytical method at most autonomous data reception stations.

It is desirable that the processing system be developed on the basis of a minicomputer (an "Iskra-125" keyboard electronic computer is used at the Arctic and Antarctic Scientific Research Institute [9]), but it is also possible to employ large universal computers ("Minsk-22," "Minsk-32" and others).

Among the most important features of the algorithm for solution of this problem is that it can be solved using the formulas of spherical trigonometry without the introduction of an intermediate geodetic coordinate system; the coordinates of the control points are computed after simultaneous measurement (on a stereophotogrammetric instrument) of the coordinates of photograph points and the corresponding points on the map diapositive; the correction equation along each coordinate axis is a first-degree polynomial.

The data obtained as a result of the processing of a single photograph are ready for output to a curve plotter (Fig. 1) and for transmission to users in the form of telegrams (the geographic coordinates of the turning points of ice boundaries). The developed method provides for the possibility of joint processing of a pair of photographs for determining the drift vectors during the period between photographic surveys (Fig. 2,a).

The results of the calculations, in addition to output to the digital printout unit, are simultaneously registered on the magnetic tape in a cassette, which makes it possible to carry out further processing (Fig. 2,b).

The analytic geographic tie-in method was developed in 1975 and was used for the first time on an expedition aboard the scientific research ship "Mikhail Somov" in May-June 1976. Experience has shown that for the direct support of ship navigation, in addition to the maximum possible accuracy, there must also be a maximum detail of map representation of individual fields, channels, leads, ice accumulations and spots.

Due to the impossibility of an analytical determination of coordinates of the necessary number of points a detailed representation of ice conditions to a considerable degree is impossible. Taking this into account, a method for combined analytical and optical-mechanical processing of TV photographs of the "Meteor-2" artificial earth satellite was developed [2]. This method involves essentially the following: some of the photograph, depicting the navigation region, is broken down into a grid of squares of limited area (or rectangular grid units) and the geographical and rectangular (on a map of a given scale) coordinates of their corners are determined analytically. Using these data a grid of quadrilaterals is constructed on a blank map, after which the photograph is projected by elementary areas onto the map. In order to exclude the transformation process within the limits of each quadrilateral there has been a modernization of the "Neva" FPVF phototelegraphic apparatus, ensuring an approximate reduction of the photographs to a near-horizontal form.

It has been established that such a combined method, retaining the accuracy of analytical tie-in, makes it possible to represent far more details of structure of the ice cover. In order to make use of all the information available on the photograph we also developed a method for determining the position of the ship directly on a satellite photograph, which is accomplished using the main program for a geographic tie-in by the successive approximations method.

The relatively high resolution of the new Soviet artificial earth satellites of the "Meteor-2" type, their operation in a direct transmission regime, and the practical introduction of the methods for interpreting and processing of satellite videoinformation developed at the Arctic and Antarctic Scientific Research Institute have substantially increased the possibility and effectiveness of use of the latter both for the study of the ice regime of the seas and for routine support of the navigation of ships.

Under favorable meteorological conditions, using satellite photographs it is possible to compile maps of the distribution of ice by degree of compactness, which with respect to detail and accuracy are not inferior to maps prepared on the basis of aerial ice reconnaissance. There are great possibilities for using these photographs for investigating the parameters characterizing ice dynamics (displacement of the boundaries and edges, drift of individual components of the ice cover, formation of polynias, channels and thinnings, breaking off of shore ice, formation and breakup of ice concentrations, spots and bands).

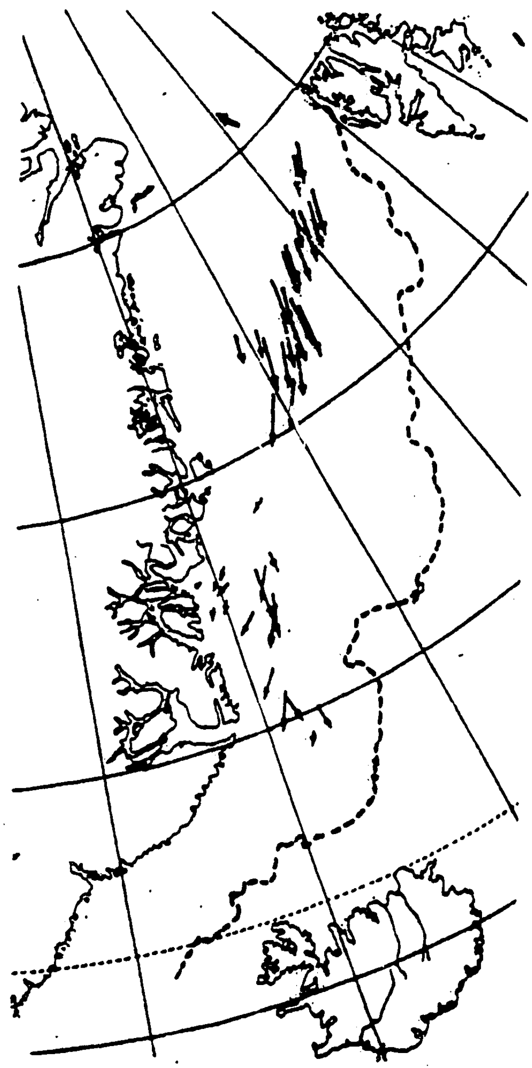

Fig. 2a. Map of ice drift vectors.

A further increase in the role of satellite ice observations involves an improvement of instrumentation and methods for remote sensing from space, means for the processing and interpretation of data.

The principal direction in improvement of instrumentation is an increase in the accuracy of the measured parameters of electromagnetic fields and the spatial-temporal resolution of multispectral measurements in the visible, IR and microwave spectral regions. Emphasis must be on the microwave range, observations in

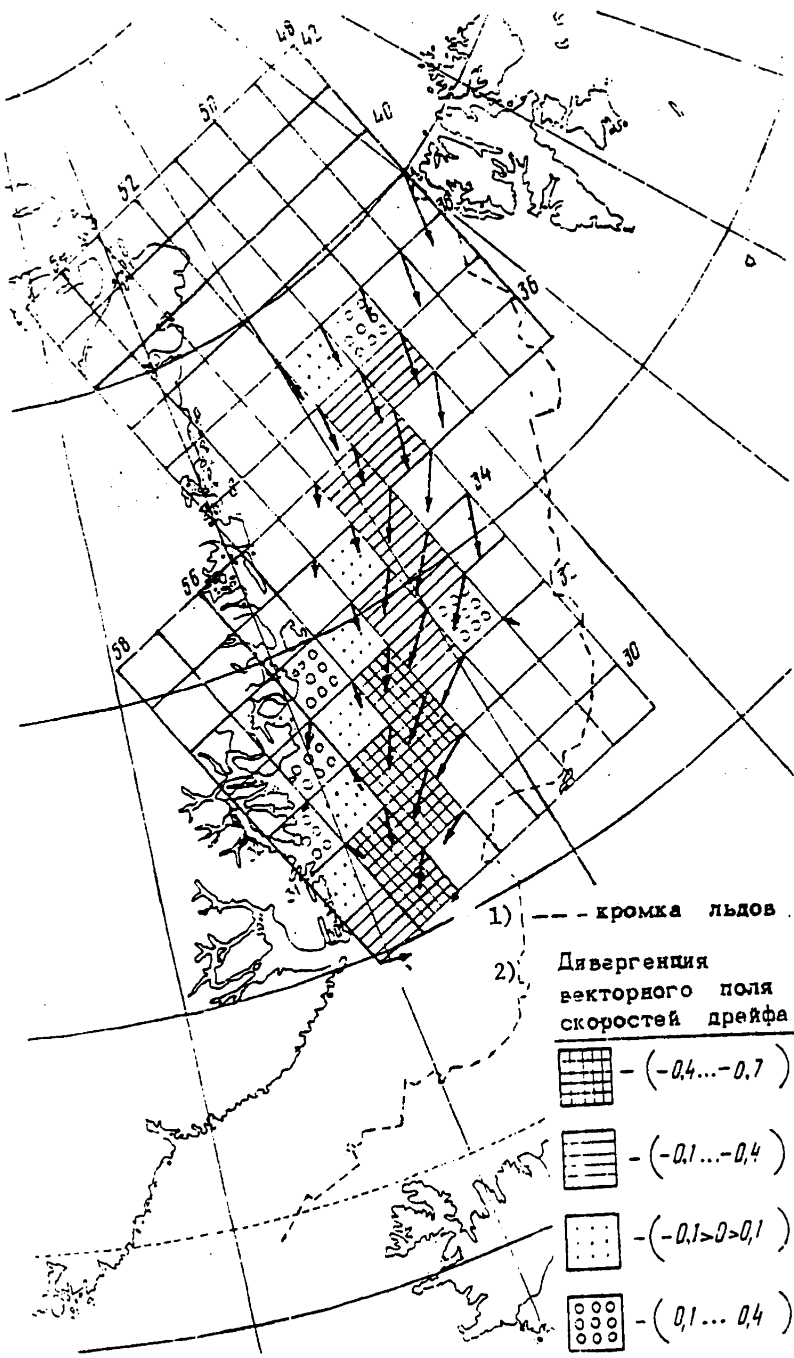

Fig. 2,b. Field of drift at points of intersection of a regular grid and map of divergence of current velocities.

KEY:

1) Ice edge
2) Divergence of vector field of drift velocity

which are virtually not dependent on illumination and cloud cover and can actually become regular. At the present time the limited use of this range is associated only with the low resolution of videoinformation. Thus, on the basis of photographs from the SHF scanning radiometer on the American "Nimbus-5" artificial earth satellite [13], operating in the range of wavelengths 1.55 cm and having a resolution at the nadir of about 30 km, for practical purposes it is possible to make a reliable determination only of the ice edges, that is, the boundaries between the drifting ice and the open water. This is attributable to the fact that the radiobrightness temperature is dependent on the thermodynamic temperature and emissivity of matter. It has been established [12] that the emissivity in the wavelength range 1.55 cm is: for sea water -- 0.40, for one-year sea ice -- 0.95, for perennial ice -- 0.80. Such a difference ensures an adequate contrast of radiobrightness temperatures of all three underlying surfaces. However, in order to determine the age composition of ice and its degree of compactness on the basis of data from the SHF radiometer the resolution area must be less than the dimensions of uniform ice fields (2-5 km). Otherwise the change in compactness may be interpreted as a change in the age composition of the ice and vice versa.

The variability of ice conditions leads to a rapid "aging" of ice information, after which it loses operational significance and can be employed only for research purposes. According to established practice, ice information must be sent to the direct user -- the director of sea operations or ship's captain -- several hours after a survey has been made. Accordingly, in the future everything possible must be done to develop a system for direct radio transmissions from satellites to autonomous simplified data reception stations servicing individual users [6].

All remote methods for collecting ice information are indirect. When carrying out aerial and satellite instrumental ice observations the evaluation of ice cover characteristics is possible only as a result of use of a complex of sensors operating in different parts of the spectrum of electromagnetic waves. As a rule, the measured parameters of the field of electromagnetic radiation are dependent on a whole series of factors.

The necessity for correlation of the signals registered from remote sensors with ice characteristics and solution of the problem of collating and correction of data collected at different times and data of different kinds requires the automation of the primary processing and analysis of data from remote sounding of the ice cover.

The investigations carried out at the Arctic and Antarctic Scientific Research Institute indicated the fundamental possibility of automating the determination of ice compactness and forms (horizontal dimensions of floes) from television photographs. The processing process will probably be of a semiautomatic character: the observer will discriminate the part of the photograph free of cloud cover and the boundaries of the zones. The subsequent determination of ice compactness within the limits of the zones and construction of histograms of distribution of ice fields by extent will be accomplished automatically.

Particular attention must be devoted to the creation of a standardized instrument complex adequately simple for introduction in the entire network of data reception points and at the same time making it possible, to the maximum degree possible, to automate the data processing process.

However, in the future satellite ice observations cannot replace all the remaining types of observations. In satellite observations it is impossible to determine the age of hummocking, form and destruction of the ice cover. It is evident that for investigation of macro-, meso- and microprocesses in the ice cover observations must be carried out in all spectral ranges of electromagnetic waves and at all levels, including satellites, aircraft, ships and direct observations on the ice.

Taking this into account, specialists at the Arctic and Antarctic Scientific Research Institute have developed a structural scheme and have initiated studies for the creation of a complex system of an automated type whose subsystems ensure the collection of ice information, input, storage and subsequent processing, tie-in of different kinds of flows of data, output in a form suitable for computer analysis and routine use, preparation of numerical short-range and long-range ice forecasts, archival storage of data, search and output [1].

In this system satellite ice observations will be used for mapping the distribution and dynamic state of the ice within the limits of individual seas and the hemisphere as a whole. Data from aerial and shipboard observations will then be plotted on these very same maps, which makes it possible to combine the breadth of scanning of satellite photographs with the completeness and detail of ice characteristics on ice aerial reconnaissance maps. The determination of drift vectors from artificial earth satellite photographs will make it possible to accumulate data on the age composition, form, hummocking and degree of destruction of the ice cover.

Even adequately modern measurement complexes cannot provide all the necessary information concerning the state of the ice cover with the spatial and temporal detail required for practical work. Accordingly, the computation and forecasting subsystem is of great importance in the created automated ice-information system for the Arctic (ALISA). The task of this subsystem is as follows:

1) daily computation of the spatial distribution of highly important characteristics of the ice cover: thickness, compactness, hummocking, degree of destruction, intensity of compression, etc.;

2) correction of the results of computations by data received from the subsystem for the collection of ice-hydrological information;

3) formulation of ice forecasts for different times in advance.

Since the matching of the results of computations with observational data will occupy an important place in the ALISA system, the problem of developing an effective correction method must be devoted great attention. It is assumed that the basis for this method will be the principles of modeling of deformations of surfaces developed at the Institute of Data Transmission Problems (IPPI, AN SSSR).

The ALISA is being created on the basis of and with the use of the experience with the existing system for scientific-operational support of navigation. Here satellite observations have been assigned an extremely great and very definite place.

With the development and improvement of technology and methods for remote sensing from space the role and importance of observations from artificial earth satellites will be increased still more.

BIBLIOGRAPHY

1. Nushuyev, A. V., Volkov, N. A., Gudkovich, Z. M., et al., "Automated Ice-Information System for the Arctic (ALISA)," TRUDY AANII (Transactions of the Arctic and Antarctic Scientific Research Institute), Vol 343, Leningrad, pp 8-18, 1977.

2. Bushuyev, A. V., "Use of Satellite Information in Studying the Ice Regime of Seas and Support of Ship Navigation," I S"YEZD SOVETSKIKH OKEANOLOGOV. TEZISY DOKLADOV (First Congress of Soviet Oceanologists. Summaries of Reports), No 1, Moscow, "Nauka," 1977, 181 pages.

3. Bushuyev, A. V. and Volkov, N. A., "Meteorological Artificial Earth Satellites as a Means for Observing Ice," PROBLEMY ARKTIKI I ANTARKTIKI (Problems of the Arctic and Antarctic), No 33, pp 5-12, 1970.

4. Bushuyev, A. V., Volkov, N. A. and Loshilov, V. O., ATLAS LEDOVYKH OBRAZOVANIY (Atlas of Ice Formations), Leningrad, Gidrometeoizdat, 1974, 140 pages.

5. Bushuyev, A. V. and Novikov, Yu. R., METODICHESKIYE UKAZANIYA PO VOPROSAM OBRABOTKI I ISPOL'ZOVANIYA SPUTNIKOVOY LEDOVOY INFORMATSII (Methodological Instructions on the Problems of Processing and Use of Satellite Ice Information), Leningrad, AANII, 1974, 84 pages.

6. Vetlov, I. P., "Results of Investigations in the Field of Satellite Meteorology," PROBLEMY SOVREMENNOY GIDROMETEOROLOGII (Problems in Modern Hydrometeorology), Leningrad, Gidrometeoizdat, pp 145-164, 1977.

7. German, M. A., SPUTNIKOVAYA METEOROLOGIYA (Satellite Meteorology), Leningrad, Gidrometeoizdat, 1975, 367 pages.

8. Yegorov, N. I., FIZICHESKAYA OKEANOGRAFIYA (Physical Oceanography), Leningrad, Gidrometeoizdat, 1974, 455 pages.

9. Butrin, V. P., Nakul'tsev, G. S., Bogatyr', B. N. and Novikov, Yu. R., "Complex of Technical Instrumentation for the Collection and Processing of Hydrometeorological Information (KTS ASOGI)," AVTOMATIZATSIYA SBORA I OBRABOTKI GIDROMETEOROL. INFORM. (Automation of Collection and Processing of Hydrometeorological Information), 8, Obninsk, VNIGMI MTsD, pp 3-8.

10. Leont'yeva, A. V. and Nayshuller, M. G., ISPOL'ZOVANIYE TELEVIZIONNYKH I INFRAKRASNYKH SNIMKOV V PROGNOSTICHESKIKH ORGANAKH SLUZHBY POGODY (Use of Television and Infrared Photographs in Prognostic Agencies of the Weather Service), Moscow, GMTs, 1969, 39 pages.

11. NOMENKLATURA MORSKIKH L'DOV. USLOVNYYE OBOZNACHENIYA DLYA LEDOVYKH KART (Nomenclature of Sea Ice. Symbols for Ice Charts), Leningrad, Gidrometeoizdat, 1974, 140 pages.

12. Gloerson, P., Campbell, W. J., Ramsier, R., et al., "Beaufort Sea Ice Zones by Means of Microwave Imagery," X-910-80, Goddard Space Flight Center, Greenbelt, Maryland, April 1975, p 17.

13. Gloerson, P., et al., "Microwave Maps of the Polar Ice of the Earth," BULLETIN OF THE AMERICAN METEOROLOGICAL SOCIETY, Vol 55, No 12, pp 1442-1448, 1974.

ASSIMILATION OF SATELLITE DATA IN NUMERICAL MODELS OF OCEAN DYNAMICS

Sevastopol' SPUTNIKOVAYA GIDROFIZIKA in Russian 1980 pp 58-66

[Article by I. Ye. Timchenko, V. D. Yarin and I. G. Protsenko]

[Text]

Abstract: A method is proposed for the adjustment of remote measurements of ocean level and contact measurements of the density field. It is based on use of a dynamic-stochastic model of state of the ocean. The article gives the results of use of this method for the "POLYMODE" polygon in simulating measurements of the level surface from space. The method of assimilation of satellite data is promising for organizing monitoring of state of the ocean.

Remote observation methods make it possible to obtain virtually simultaneous data on the state of the ocean surface over great areas. Together with contact measurements made from aboard scientific research ships or on autonomous stations, satellite measurements make it possible to trace the evolution of the principal ocean parameters. Accordingly, it is necessary to develop methods for the assimilation of satellite observations in theoretical models of the ocean, which, applying data relating to the upper layer, make it possible to compute the characteristics of deep layers in the ocean.

One of the possible approaches here is dynamic-stochastic modeling based on the theory of optimum filtering of systems with distributed parameters [1] and successfully developed at the present time both in meteorology [2] and in oceanology [3]. The basis for such an approach is a description of the physical processes transpiring in the ocean using variable states. The problem is an optimum evaluation of the vector of state at an arbitrary moment in time, taking into account ongoing measurements of some components of the vector of state. The method has been described in adequate detail, for example, in [3, 4]. Here we will cite only a summary of the formulas necessary for further exposition.

Assume that the evolution of the vector of state $\vec{\alpha}(\vec{x},t)$ is described by the equation

$$\frac{\partial \vec{\alpha}(\vec{x},t)}{\partial t}=L_{\vec{x}}\,\vec{\alpha}(\vec{x},t)+\vec{f}(\vec{x},t), \tag{1}$$

where $L_{\vec{x}}$ is a linearized integrodifferential operator; $f(\vec{x},t)$ is a random term of the "white" noise type -- a probabilistic model of microscale phenomena, not taken into account in explicit form by the operator $L_{\vec{x}}$. With respect to $\vec{f}(\vec{x},t)$ we will assume that

$$E\{\vec{f}(\vec{x},t)\}=0, \qquad E\{\vec{f}(\vec{x},t)\vec{f}(\vec{y},\tau)\}=Q(\vec{x},\vec{y},t)\,\delta(t-\tau).$$

Applying the operation of taking the mathematical expectation conditional relative to all past observations to expression (1), we obtain an equation for the optimum evaluation

$$\frac{\partial E\{\vec{\alpha}(\vec{x},t)\}}{\partial t}=L_{\vec{x}}\,E\{\vec{\alpha}(\vec{x},t)\}. \tag{2}$$

Henceforth the conditional mathematical expectation (optimum evaluation) with respect to past data will be denoted $\vec{\alpha}_{t0}(\vec{x}, t)$, and with respect to ongoing observations -- $\vec{\alpha}_t(\vec{x}, t)$.

The covariation matrix of the error in the evaluation $P_{t0}(x,y,t)$ satisfies the equation

$$\frac{\partial P_{t_0}(\vec{x},\vec{y},t)}{\partial t}=L_{\vec{x}}\,P_{t_0}(\vec{x},\vec{y},t)+L_{\vec{y}}\,P_{t_0}(\vec{x},\vec{y},t)+Q(\vec{x},\vec{y},t). \tag{3}$$

The optimum evaluation of the vector of state is computed using the formula

$$\vec{\alpha}_t(\vec{x},t)=\vec{\alpha}_{t_0}(\vec{x},t)+\sum_{k=1}^{N_0}\vec{\Delta}_k(\vec{x},t)\left[\vec{\beta}_k(\vec{x}_k,t)-\vec{\alpha}_{t_0}(\vec{x}_k,t)\right], \tag{4}$$

where $\vec{\beta}_k$ is the vector of measurements at the point $\vec{x}_k$; $\vec{\Delta}_k(\vec{x},t)$ is a weighting function; N_0 is the number of points at which there are observations. In a general case

$$\vec{\beta}_k(\vec{x}_k,t)=\int_{\vec{x}}\vec{\alpha}(\vec{y},t)\,\vec{g}_k(\vec{y},t)\,d\vec{y}+\vec{n}_k(t), \tag{5}$$

where $\vec{g}_k$ is the kernel of spatial averaging; $\vec{n}_k$ is measurement noise. The weighting function $\vec{\Delta}_k(\vec{x},t)$ is determined from the expression

$$\vec{\Delta}_k(\vec{x},t)=\sum_{l=1}^{N}\left[K^{-1}\right]_{lk}\int_{\vec{x}}\vec{g}_l(\vec{y},t)\,P_{t_0}(\vec{x},\vec{y},t)\,d\vec{y}, \tag{6}$$

where k is a matrix formed from the elements

$$K_{kl}=\iint_{\vec{z}\,\vec{w}}\vec{g}_k(\vec{z},t)\,\vec{g}_l(\vec{w},t)\,P_{t_0}(\vec{z},\vec{w})\,dz\,dw+R_{kl}, \tag{7}$$

K^{-1} is the inverse matrix.

After assimilation of ongoing measurements the covariation matrix of the error in evaluation is corrected in accordance with the formula

$$\rho_t(\bar{x},\bar{y},t)=\rho_{t_0}(\bar{x},\bar{y},t)-\sum_{k=1}^{N_0}\bar{\Delta}_k(\bar{x},t)\int_{\bar{y}}\bar{g}_k(\bar{y},t)\rho_{t_0}(\bar{x},\bar{y})\,d\bar{y}. \quad (8)$$

In an investigation of physical processes on a synoptic scale we use as a point of departure the following system of equations in thermohydrodynamics of the ocean [5]:

continuity equation for an incompressible fluid

$$\frac{\partial u}{\partial x}+\frac{\partial v}{\partial y}+\frac{\partial w}{\partial z}=0, \quad (9)$$

equations of motion

$$\frac{\partial u}{\partial t}+u\frac{\partial u}{\partial x}+v\frac{\partial u}{\partial y}+w\frac{\partial u}{\partial z}-\ell u=-\frac{1}{\rho_0}\frac{\partial p}{\partial x}+\frac{\partial}{\partial z}\nu_z\frac{\partial u}{\partial z}+\nu_x\Delta u, \quad (10)$$

$$\frac{\partial v}{\partial t}+u\frac{\partial v}{\partial x}+v\frac{\partial v}{\partial y}+w\frac{\partial v}{\partial z}-\ell v=-\frac{1}{\rho_0}\frac{\partial p}{\partial y}+\frac{\partial}{\partial z}\nu_z\frac{\partial v}{\partial z}+\nu_x\Delta v, \quad (11)$$

equation of statics

$$\frac{\partial p}{\partial z}=\rho g, \quad (12)$$

density diffusion equation

$$\frac{\partial \rho}{\partial z}-u\frac{\partial \rho}{\partial x}+v\frac{\partial \rho}{\partial y}+w\frac{\partial \rho}{\partial z}=\frac{\partial}{\partial z}\varkappa_z\frac{\partial \rho}{\partial z}+\varkappa_x\Delta\rho. \quad (13)$$

We will use the following boundary conditions:

at the ocean surface with $z=-\zeta_1(x,y,t)$

$$\rho_0\nu_z\frac{\partial u}{\partial z}=-\tau_x,\ \rho_0\nu_z\frac{\partial v}{\partial z}=-\tau_y,\ w=-\left(\frac{\partial \zeta_1}{\partial t}+u\frac{\partial \zeta_1}{\partial x}-v\frac{\partial \zeta_1}{\partial y}\right),$$
$$p_1=p_a,\ \frac{\partial \rho}{\partial z}=Q_\rho, \quad (14)$$

at the ocean floor with $z=H(x,y)$

$$u=v=w=0,\qquad \rho=\rho_H, \quad (15)$$

at the fluid lateral boundaries

[Γ = bound] $$u,v\big|_\Gamma=u_\Gamma,v_\Gamma,\quad \rho\big|_\Gamma=\rho_\Gamma. \quad (16)$$

In equations (9)-(13) and the boundary conditions (14)-(16) u, v, w are the projections of the velocity vector onto Cartesian coordinates -- the x-, y-, z- coordinates in the direction to the east, north and center of the earth respectively, ν_z, ν_x, $\varkappa_z$, $\varkappa_x$ are the coefficients of turbulent exchange and diffusion; p_1 is pressure; g is the acceleration of gravity; ρ, ρ_0 are the anomaly and mean density of water; ℓ is the Coriolis parameter; p_a is atmospheric pressure; τ_x, τ_y are wind shearing stresses.

At the initial moment in time the desired functions z, u, v, ν_2, $\varkappa_2$, ρ are known. After integration of the equation of statics (12) with the boundary condition (14) the expression for the pressure anomaly has the form

$$p^* = \rho_0 g z^* - g \int_z^H \rho\, dz,$$

where z^* is the adynamic increment to the level surface of the ocean. Adhering to the method presented in [8], for the integral function z^* we write a second-degree equation with the boundary conditions of the oblique derivatives type. In determining the coefficients of vertical exchange and diffusion use is made of the formula [7]

$$\nu_z = (ch)^2 \left(\left(\frac{\partial u}{\partial z}\right)^2 + \left(\frac{\partial v}{\partial z}\right)^2 - \frac{1}{\rho_0}\frac{\partial \rho}{\partial z}\right)^{1/2},$$

where c is a proportionality constant; h is the depth of the homogeneous layer.

The system of differential equations closed in this way is solved numerically by the finite differences method with a second order of approximation in space coordinates [4].

The system of equations (9)-(13) is too complex, which leads to great difficulties of a technical nature in attempts to compute the covariation matrix of forecasting errors in accordance with equation (3). Accordingly, we will attempt to simplify the problem. The decisive factor in computing currents is the density field, on the basis of whose known values it is possible to determine other characteristics of state of the ocean. As a first approximation, in equation (3) we leave only one component P_{t0}^{ρ} of the covariation matrix of errors -- the covariation function of the error in predicting the density field.

The corresponding equation has the form

$$\frac{\partial P_{t0}^{\rho}}{\partial t} + u'\frac{\partial P_{t0}^{\rho}}{\partial x'} + v'\frac{\partial P_{t0}^{\rho}}{\partial y'} + w'\frac{\partial P_{t0}^{\rho}}{\partial z'} + u\frac{\partial P_{t0}^{\rho}}{\partial x} + v\frac{\partial P_{t0}^{\rho}}{\partial y} + w\frac{\partial P_{t0}^{\rho}}{\partial z} + \frac{\partial}{\partial z'}\varkappa_z'\frac{\partial P_{t0}^{\rho}}{\partial z'} + \varkappa_x'\Delta' P_{t0}^{\rho} + \frac{\partial}{\partial z}\varkappa_z\frac{\partial P_{t0}^{\rho}}{\partial z} + \varkappa\Delta P_{t0}^{\rho} + Q, \quad \text{where} \quad (u)' = u(x', y', z')\ldots \tag{17}$$

The covariation of the prediction error is a function of six independent variables. Due to this circumstance in the numerical solution of equation (17) it is necessary to have a large computer memory. In order to avoid this difficulty, the authors of [4, 8] proposed an approximation of the correlation function of errors in predicting the density field taking into account the stratification of the field with depth. Here we will approximate the covariation function by the expression

$$P(x, y, z, x', y', z', t) = F(x, y, z, t)\, F(x', y', z', t)\, e^{-\alpha_1 (z-z')^2} e^{-\alpha_2[(x-x')^2 + (y-y')^2]} \tag{18}$$

where F is the standard deviation of the error in evaluating the density field. Then for $d = F^2(x, y, z, t)$ we obtain the equation

$$\frac{\partial d}{\partial t} + u\frac{\partial d}{\partial x} + v\frac{\partial d}{\partial y} + w\frac{\partial d}{\partial z} + cd = \frac{\partial}{\partial z}\varkappa_z\frac{\partial d}{\partial z} + \varkappa_x\Delta d - 2\varkappa_z\left(\frac{\partial F}{\partial z}\right)^2 - 2\varkappa_x\left[\left(\frac{\partial F}{\partial x}\right)^2 + \left(\frac{\partial F}{\partial y}\right)^2\right] + Q, \tag{19}$$

where c = const, dependent on α_1 and α_2.

In the future the creation of operational systems for remote sounding of the ocean is expected. These will give information on such parameters of the upper layer as temperature of the ocean surface, salinity, air temperature in the near-water layer, wind velocity and direction, level, etc. These characteristics give an evaluation of state of the ocean surface and can be used as boundary conditions in models of interaction between the ocean and atmosphere [7]. By means of use of the corresponding hydrodynamic models of the ocean they can be used for refining its state in the deep layers.

Measurements of the level surface are of particular interest because at each point the level rise carries information on the density field in the entire thickness of the ocean. Remote measurements of level, like measurement of other surface parameters, must be assimilated into the numerical model of dynamics of the ocean simultaneously with contact measurements. In order to organize the input of satellite data into the numerical model it is necessary to solve the problem of statistical adjustment of satellite and contact observations and ensure successive analysis of the data in the real time of the experiment [3]. Taking into account the general requirements on the assimilation of satellite information, we will examine a specific example -- assimilation of the ocean level surface profile, measured from a satellite along its trajectory of motion.

In order to assimilate level measurements in a dynamic-stochastic model of state of the ocean we will make use of the circumstance that with some approximation the level surface can be represented in the form of a simple formula [6]. [Note: formula illegible.] Then the covariation function of the error in evaluation is determined by the expression

$$\rho_{t_0}^{z}(\bar{x},\bar{y})=\frac{1}{\rho_0^2}\int_0^H\int_0^H \rho_{t_0}^{\rho}(\bar{x},\bar{y},z,z')\,dz\,dz', (\bar{x},\bar{y})=(x,y,x',y'). \tag{21}$$

The assimilation of data on the level surface is broken down into two stages. First, using equation (19) and formula (18), we will determine the covariation function of the error in evaluating the density field, from which, using (21) it is possible to compute $\rho_{t_0}{}^{z}(x, x', y, y')$. Then, using the relationships (4) and (8) (in which α is replaceable by ζ), we will assimilate the level at each point of a numerical grid on the surface. The covariation of error after assimilation is determined by formula (8).

In the second stage the refined level values are used for introducing corrections into the prognostic values for the density field. The level surface readings are regarded as weighted density measurements in accordance with expression (5). In this case $n_k(t)$ represents the errors in evaluating the level. Then the weighting function for the nonclosures in computing the level surface assumes the form

$$\Delta(\bar{x},\bar{y},z)=\frac{\int_0^H \rho_{t_0}^{\rho}(\bar{x},\bar{y},z,z')\,dz'}{\int_0^H\int_0^H \rho_{t_0}^{\rho}(\bar{x},\bar{y},z,z')\,dz\,dz'\Big|_{\substack{x=\bar{x}\\ y=\bar{y}\\ z=z'}}+R} \tag{22}$$

or with allowance for representation of the covariation function of the error in predicting density (18)

$$\Delta(\bar{x},\bar{y},z)=\frac{e^{-\alpha_2[(x-x')^2+(y-y')^2]}\int_0^H F(x,y,z)\cdot F(x',y',z')\,e^{-\alpha_2(z-z')^2}dz'}{\int_0^H\int_0^H F(x,y,z)\cdot F(x',y',z')\,e^{-\alpha_2(z-z')^2}dz\,dz'\Big|_{\substack{x=x'\\ y=y'\\ z=z'}}+R} \qquad (23)$$

Model computations were carried out as an illustration of the proposed approach. The initial data were materials from hydrological surveys carried out under the "POLYMODE" program. One of the surveys was used as the initial distribution of the density field. In accordance with the system (9)-(13) we computed the prognostic fields for a time corresponding to the final moment of carrying out the next survey. Due to the absence of remote level measurements over the area of the "POLYMODE" polygon these measurements were modeled on an electronic computer. The "true" data employed were the fields obtained on the basis of the results of the last survey, by means of which we simulated the data from remote observations and evaluated the accuracy of their assimilation.

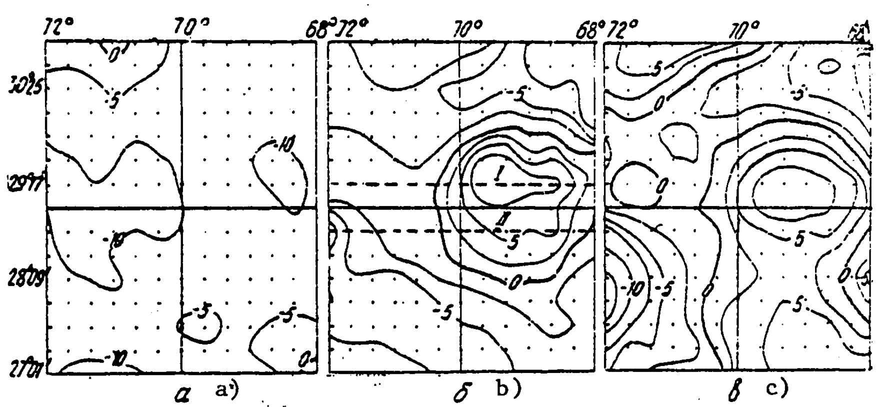

Fig. 1.

The region in which the computations were made is shown as a rectangle between 27 and 30°N and 68 and 72°W. Observations were made at the points of intersection of a square grid with an interval of 34 miles. The interval of the computation grid was 17 miles.

Figure 1,a is a map of the level surface obtained using a purely hydrodynamic prediction; Fig. 1,b is a refined map prepared as a result of assimilation of remote observations of level relief along paths I and II; Fig. 1,c shows the "true" level surface. Similar maps for the density field at the 600-m horizon are shown in Fig. 2.

As indicated in Figures 1,c and 2,c, in the right part of the polygon there was an eddy formation which was traced both in the level surface field and in the density field. It was of interest to determine the influence of remote level measurements on the "resolution" of such field characteristics by the model.

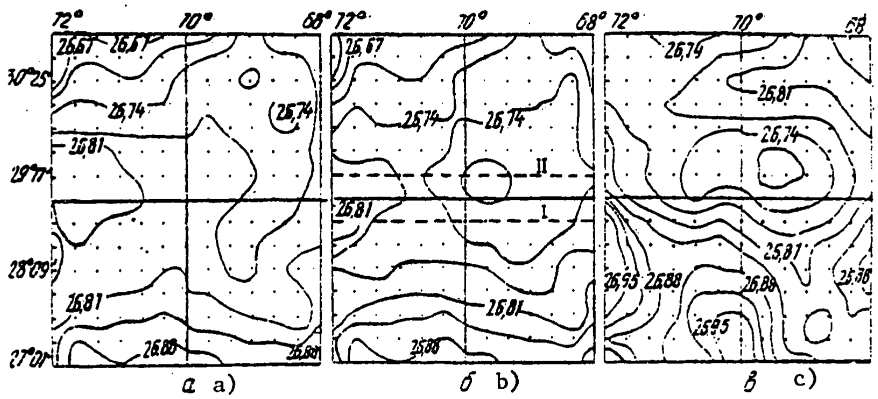

Fig. 2.

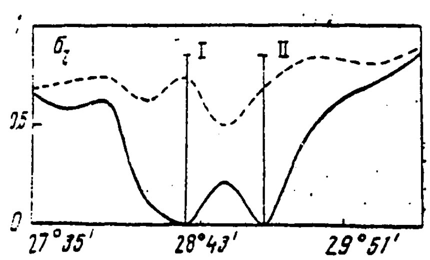

Fig. 3.

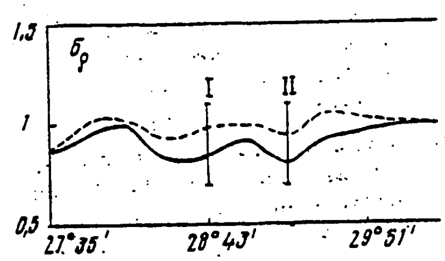

Fig. 4.

A comparison of Fig. 1,a and Fig. 1,c, as well as Fig. 2,a and 2,c, clearly shows that a purely hydrodynamic prediction, by virtue of imperfection of the model, differs considerably from the "true" field pattern. Assimilation of the level measurements along the two paths intersecting the area of the polygon connects the level surface field, and what is especially important, the density field with depth.

Figure 3 shows a curve of the change (along the meridian) of the mean square error in a hydrodynamic prediction (dashed curve) and a corrected field (solid curve), normalized to the standard deviation. The corresponding curve for density is shown in Fig. 4.

It follows from this experiment that satellite data on the level surface of the ocean considerably supplement the information contained in the density surveys in the polygon. This is especially important for creating operational systems for tracking the states of the ocean in the investigated regions. Density surveys carried out from aboard scientific research ships frequently are suspended for technical reasons (replacement of ships in the polygon, bad weather, etc.).

Without employing the additional information arriving from satellites the pattern of evolution of oceanic fields in the polygon during these periods of time will be impaired. Accordingly, the proposed method for the assimilation of satellite data is promising for organizing monitoring of state of the ocean.

BIBLIOGRAPHY

1. Butkovskiy, A. G., METODY UPRAVLENIYA SISTEMAMI S RASPREDELENNYMI PARAMETRAMI (Methods for Control of Systems With Distributed Parameters), Moscow, "Nauka," 1975, 568 pages.

2. Gandin, L. S., CHETYREKHMERNYY ANALIZ METEOROLOGICHESKIKH POLEY (Four-Dimensional Analysis of Meteorological Fields), Leningrad, Gidrometeoizdat, 1976, 61 pages.

3. Nelepo, B. A. and Timchenko, I. Ye., SISTEMNYYE PRINTSIPY ANALIZA NABLYUDENIY V OKEANE (Systemic Principles for Analysis of Observations in the Ocean), Kiev, "Nauka Dumka," 1978, 222 pages.

4. Timchenko, I. Ye., Knysh, V. V., Protsenko, I. G. and Yarin, V. D., "Dynamic-Stochastic Model for Processing Density Surveys in the Ocean," MORSKIYE GIDROFIZICHESKIYE ISSLEDOVANIYA (Sea Hydrophysical Investigations), No 4, Sevastopol', pp 50-64, 1979.

5. Kochergin, V. P., TEORIYA I METODY RASCHETA OKEANICHESKIKH TECHENIY (Theory and Methods for Computing Ocean Currents), Moscow, "Nauka," 1978, 127 pages.

6. Sarkisyan, A. S., CHISLENNYY ANALIZ I PROGNOZ MORSKIKH TECHENIY (Numerical Analysis and Prediction of Sea Currents), Leningrad, Gidrometeoizdat, 1977, 181 pages.

7. Kochergin, V. P., Klimok, V. I. and Sukhorukov, V. A., "Homogeneous Layer of the Ocean Within the Framework of 'Differential Models'," CHISLENNYYE METODY MEKHANIKI SPLOSHNOY SREDY (Numerical Methods of Mechanics of a Continuous Medium), Vol 8, No 5, Novosibirsk, SO AN SSSR, pp 102-114, 1977.

8. Protsenko, I. G., Timchenko, I. Ye. and Yarin, V. D., "Method for Predicting the Statistical Characteristics of the Field of a Passive Impurity," MORSKIYE GIDROFIZICHESKIYE ISSLEDOVANIYA (Marine Hydrophysical Investigations), No 4, Sevastopol', pp 98-106, 1979.

MULTISPECTRAL METHOD FOR DETERMINING OCEAN SURFACE TEMPERATURE

Sevastopol' SPUTNIKOVAYA GEOFIZIKA in Russian 1980 pp 67-74

[Article by V. A. Golovko and L. A. Pakhomov]

[Text]

Abstract: The authors propose a method for choosing an optimum scheme for multichannel IR radiometric measurements making it possible, to a considerable extent, to compensate the error in remote determination of the temperature of a water surface caused by the transformation of IR radiation in the atmosphere. The article gives examples of experimental checking of the proposed schemes.

The remote determination of the temperature of the underlying surface on the basis of measurements of outgoing IR radiation in the atmospheric transparency window 8-14 μm still remains one of the principal types of satellite observations. Data on the thermal regime of the surface of oceans and seas are of the greatest interest because the world ocean for the most part determines climatic conditions.

Despite the great experience in such observations, for the time being the required measurement accuracy has not been attained. The standard (mean square) error in reconstructing the temperature of the water surface is about 3° [1, 2], whereas for most problems in oceanology and investigation of the earth's natural resources there must be an accuracy of about 0.2° [3]. The relatively low accuracy in reconstructing the temperature field is attributable primarily to the transformation of IR radiation in the atmosphere.

The influence of the atmosphere under cloudless conditions is manifested, on the one hand, in an attenuation of radiation of the underlying surface, and on the other hand, in the attenuation of radiation generated by the atmosphere. As a rule, allowance for the influence of the atmosphere is accomplished by introducing the so-called atmospheric transfer function, to whose computation a great number of studies have been devoted, such as [4-7]. However, the considerable variability of the transfer function does not make possible an adequate introduction of corrections for radiation transformation in the atmosphere even by the creation of detailed maps of the geographical distribution of transfer functions for different seasons. Accordingly, when using determined approaches to allowance for the influence of the atmosphere it is scarcely possible to expect a significant increase in the accuracy in determining water surface temperature.

Accordingly, it may be more effective to employ methods at whose basis is the determination of empirical expressions relating the radiation measured on an artificial earth satellite to the actual water temperature. In obtaining these empirical relationships it is proposed that the energy brightnesses (radiances) in a number of spectral intervals, making it possible to take into account the influence of the atmosphere, that is, proceeding from single- to multichannel measurements, be used as independent variables. The effectiveness of such an approach is confirmed by a number of investigations. For example, the authors of [12] proposed a set of spectral intervals in the region 3-14 μm for solution of the problem of remote measurement of ocean temperature. However, this optimum measurement scheme can be realized only in a case when the model of the radiation transfer process is known and a definite state of the atmosphere is stipulated. These conditions introduce an uncertainty into the evaluation of the real possibilities of radiation measurements realizing this sort of scheme.

By virtue of the reasons cited above it is necessary to study the possibility of determining the temperature of the sea surface by a statistical method, using for this purpose, as independent variables, the spectral radiances of outgoing radiation not only in the region of windows of atmospheric transparency, but also in the absorption bands of atmospheric gases. The temperature of the water surface T_s is found using the correlation equation, predetermined on the basis of a set of spatially and temporally matched radiation observations and data from direct measurements of kinetic temperature of the water surface. Below we give the results of checking a statistical method for the interpretation of spectrometric measurements obtained using a spectrometer-interferometer on the 28th and 29th "Meteor" artificial earth satellites. As the ocean surface temperature values use was made of data obtained by the Hydrometeorological Service on the basis of measurements of the kinetic temperature of water by ships of the merchant marine.

We will assume that the temperature of the sea surface T_s is related by means of the vector G and the constants T_s° to the outgoing radiation, stipulated by the vector R, by the linear equation

$$T_s = T_s^\circ + GR. \tag{1}$$

The observed $\tilde{T}_s$ and $\tilde{R}$ values differ from their true values by the magnitude of the measurement error, that is, $\tilde{T}_s = T_s + \varepsilon$, $\tilde{R} = R + \delta$. The statistical evaluation of G and T_s° under the conditions that

$$E[\varepsilon] = \theta,\ E[\delta] = \theta,\ E[T_s \delta^T] = \theta,\ E[R\delta^T] = \theta,\ E = \theta,$$

where θ is the zero matrix, is written in the form

$$\hat{G} = \tilde{S}_{tr}\left(\tilde{S}_{rr} - S_{\delta\delta}\right)^{-1},\quad T_s^\circ = \bar{T}_s - \hat{G}\bar{R}. \tag{2}$$

Evaluation (2) is correct under the condition

$$\tilde{S}_{tt} - \hat{G}\left(S_{rr} - S_{\delta\delta}\right)^{-1} \hat{G}^{T} = \hat{S}_{\varepsilon\varepsilon} \geq 0. \qquad (3)$$

In expressions (2), (3) $\tilde{S}_{tr}$ is the reciprocal covariation matrix of the observed $\tilde{T}_s$ and $\tilde{R}$ values; $\tilde{S}_{rr}$, $S_{\delta\delta}$ are the covariation matrices of radiation measurements and their errors respectively; $\tilde{S}_{tt}$, $\hat{S}_{\varepsilon\varepsilon}$ are the dispersions of kinetic temperature of the water surface and the error in its determination respectively.

We will also assume that in the analysis we selected a spectral region in which the spectral measurements are represented by m spectral radiances, relating to intervals adjacent to one another with the width $\Delta\nu$. Such a set of initial spectrometric information makes it possible to form from each individual spectrum a mass of m = 1/2 m(m + 1) radiometric measurements (potential predictors) $R_1, \ldots, R_m$,

$$R_1, \ldots, R_m, \sum_{i=1}^{2} R_i, \ldots, \sum_{i=1}^{m} R_i.$$

Included in this mass of potential predictors we have the intensities of radiation in intervals of different width and localization. By the choice of an optimum measurement scheme we mean the finding of those mentioned M spectral intervals in which allowance for radiation makes it possible to obtain the best $\hat{S}_{\varepsilon\varepsilon}$ evaluation using equation (1). For solving this problem it is convenient to use the multiple-step regression method. Now we will examine the procedure of step-by-step choice of the optimum predictors.

In the first step, by trial-and-error, from the M potential predictors we select that allowance for which minimizes the $\hat{S}_{\varepsilon\varepsilon}$ evaluation in (3) since $\hat{S}_{\varepsilon\varepsilon}$ directly characterizes the accuracy of the evaluation

$$\hat{T}_s = \hat{T}_s^{\circ} + \hat{G}\tilde{R}. \qquad (4)$$

The determined predictor is fixed, and in the second interval we add to it from the others that which jointly with the first minimizes the $\hat{S}_{\varepsilon\varepsilon}$ value. The process is repeated until the $\hat{S}_{\varepsilon\varepsilon}$ evaluation attains the a priori stipulated $S_{\varepsilon\varepsilon}$ value. With this the choice of the quasioptimum intervals in the first stage is completed. Then it is possible to refine the optimum measurement scheme by means of the following procedure. In the N determined quasioptimum intervals we discard the first and in its place among the N - N + 1 remaining intervals we seek that which minimizes the $\hat{S}_{\varepsilon\varepsilon}$ value. The determined interval is fixed. Then we discard the second, in place of which we seek a new interval, etc. As a result of many repetitions of this procedure we obtain a series of sets of quasioptimum intervals which corresponds to a convergent series of evaluations $\hat{S}_{\varepsilon\varepsilon}$, since with replacement of the next quasioptimum predictor the $\hat{S}_{\varepsilon\varepsilon}$ evaluation does not increase and there is a limit stipulated by condition (3). As the optimum scheme we select that which corresponds to the minimum of the $S_{\varepsilon\varepsilon}$ evaluation.

In the practical realization of the described method, due to limitations of the initial mass of data, as the criterion for choice of the optimum predictors it is necessary to minimize not $\hat{S}_{\varepsilon\varepsilon}$, but the value S_k, taking into account the number of degrees of freedom of the sample, that is

$$S_k = \sqrt{\frac{\hat{S}_{\varepsilon\varepsilon}(n-1)}{n-k}}, \qquad (5)$$

where n is the volume of the sample; k is the number of selected intervals. Important additional information in the step-by-step selection is provided by the so-called F-ratio [13]. For this purpose, in order that the evaluation (4) can be considered justified for the purposes of prediction (in the sense that the amplitude of the predicted sample T_s will be considerably greater than its standard error S_k), the actual F-ratio value must exceed the selected point of the F-distribution by a factor greater than 4-5 [13].

In order to evaluate the $S_{\varepsilon\varepsilon}$ parameter we will examine the possible sources of error in forming a set of direct matched measurements T_s. For the most part the discrepancy between the true temperature of the ocean surface at the time of registry of the spectrum and the temperature, obtained by direct measurement from a ship, is determined by the asynchronicity of shipboard and satellite measurements. A map of the temperature field of the world ocean is issued by the Hydrometeorological Service once each five days. Accordingly, the maximum asynchronicity is five days. According to data from long-term observations, the dispersion of mesoscale variability of ocean temperature during this period for the temperate latitudes is 1.0 K^2 [8]. The presence of a depth gradient also leads to an error in measuring temperature of the water surface. According to data from the "TROPEX-72" experiment [9], the dispersion of this error is evaluated as 0.6 K^2. Waves cause the appearance of a measurement error whose dispersion is about 0.5 K^2 [10]. The ship's hull, as well as the discharge of waste water from the ship, introduces an error whose dispersion can attain 0.3 K^2 [11]. Due to the statistical nondependence of individual components, the $S_{\varepsilon\varepsilon}$ evaluation is equal to the sum of errors of different kinds, that is, $\sigma_\varepsilon = \sqrt{S_{\varepsilon\varepsilon}} = \sqrt{1.8 + 0.6 + 0.5 + 0.3} \approx 1.7$ K.

The experimental data are represented by spectral radiances in the range 400-1400 cm^{-1} with a resolution ~ 10 cm^{-1}. This set included 47 spectra for the summer (July-September) and 15 spectra for the winter (February-March) seasons of 1977 and 1979 respectively. All the spectra were obtained under conditions with few clouds. The totality of the radiation measurements and the temperatures corresponding to them for each season are called the summer and winter samples.

The choice of the optimum scheme was made using a summer sample; the winter sample, due to its smallness, was employed as a control. The summer sample was divided into two parts, one of which was the working part and the other was a control, serving as an evaluation of the universality of the selected scheme. The natural variability of T_s for the working sample was 4.7 K.

The results of choice of the most significant spectral intervals are given in Table 1. At the left side of the table we have given intervals with a width of 10 cm^{-1} (first scheme); at the right side -- different resolutions. In both cases it is sufficient to have two spectral intervals; the nonclosure error is $\delta \approx 1.4$ K, which statistically differs insignificantly from the value $\sigma_\varepsilon = 1.7$ K. The regression equations for evaluating T_s have the form $\hat{T}_s = 283.682 + 0.675 E_1 - 0.307 E_2$ for the first scheme and $\hat{T}_s = 52.656 + 0.2137 E_1 - 0.0780 E_2$ for the second. In these formulas, as below, E_i is the energy in the i-th spectral range (erg/cm^{2}sec·sr); $\hat{T}_s$ is an estimate of ocean temperature on the Kelvin scale.

Table 1

Results of Choice of Spectral Predictors

Type of spectral measurements	Resolution 10 cm^{-1}				Different resolution			
Number of predictors	1	2	3	4	1	2	3	4
Additional spectral interval, cm^{-1}	1078.4-1088.8	400.5-410.9	1140.8-1151.2	650.8-661.2	1057.5-1088.8	567.4-702.2	400.5-410.9	1026.2-1172.2
Evaluation of regression error, K	2.38	1.39	1.24	1.21	2.38	1.37	1.32	1.26
Multiple correlation coefficient	0.87	0.96	0.97	0.97	0.87	0.96	0.96	0.97
F-ratio	71.6	127.9	109.4	86.7	71.8	138.7	102.7	88.4

The derived regression equations were checked using a control sample. It was found that the mean square errors in the evaluated temperatures differ little from the data of direct measurements for both schemes (2.2° with a shift of the mean of 0.7° and 1.9° with a shift of the mean 0.3° for the first and second schemes respectively). It can be seen that allowance for a great number of predictors does not lead to a substantial decrease in S_k; moreover, the value of the F-ratio decreases (Table 1).

The application of the procedure described above for refining the two selected quasioptimum spectral intervals of different resolution indicated their absolute stability. Due to the limitations of the initial set of data the derived correlation equations can reflect only the partial characteristics of the processes of formation and transfer of IR radiation. Accordingly, we checked the stability of the established relationships using the winter sample. It was found that S_k was equal to 1.9° with a shift of the mean by 3.4°.

In addition to a direct evaluation of sea surface temperature on the basis of an equation of type (1) it is possible to employ a similar statistical approach in validating the optimum determination of the correction to radiation temperature measured on the basis of the radiation in the spectral interval falling in the atmospheric transparency window. The range 10.5-12.5 μm was selected as such an interval; it is used everywhere in the IR radiometers of artificial earth satellites. It was found that for computing the correction it is entirely adequate to take into account radiation in the one channel 14.7-17.9 μm. A determination of sea surface temperature in this case is made using the equation $\hat{T}_S - T_R + 101.28 - 0.1007\ E_2$, where T_R is the radiation temperature measured in the window 10.5-12.5 μm. This equation was used in determining temperature using the control and winter samples. In both cases we obtained the value $S_k = 1.9°$, but with a lesser systematic shift of the winter sample (0.9° versus 3.4°).

Thus, for determining the temperature of the ocean surface on the basis of measurements of outgoing IR radiation it is sufficient to use radiation in two spectral intervals. It is evidently preferable to use a processing algorithm in the form of obtaining (on the basis of measurements in the additional channel) a correction to the radiation temperature. However, in order to obtain an entirely reliable result for validating standardized additional channels for radiometric measurements it is necessary to have a more complete set of spectral and matched direct measurements differentiated by latitude zones and seasons.

Appendix

An evaluation was made of the effectiveness of use of the optimum Kozlov scheme [12] by means of the already described sample of spectroradiometric information. First we used the equation cited in [12] for evaluating T_S. As a result it was found that the mean square error in deviation of the T_S evaluation from the real data was 2.7° with a shift of the mean by 17.6°. Then, using the optimum scheme as the point of departure, we computed the coefficients of the regression equation (1) which were then used in determining T_S within the framework of the independent sample. The results of the regression analysis for this case are cited in Table 2. It can be seen that the minimum of the regression error is attained when using two predictors, but it is greater in value than the corresponding minimum error in Table 1. By means of the step-by-step regression method with the first of these predictors we selected the radiance in the intervals which in the Kozlov scheme corresponded to the first channel. The use of the measurement results in the first channel of this scheme leads to a deterioration in the accuracy of the evaluation.

Table 2

Evaluation of Effectiveness of Optimum Scheme [12]

Number of predictors	1	2	3
Spectral interval	8.4 - 10.8	8.0 - 10.8	8.0 - 12.8
Evaluation of regression error, K	2.80	1.93	2.02
Multiple correlation coefficient	0.82	0.92	0.92
F-ratio	45.6	63.9	41.0

BIBLIOGRAPHY

1. Gorodetskiy, A. K., Klimchuk, Ye. F. and Malkevich, M. S., "Method and Some Results of Determination of Temperature of the Underlying Surface From the 'Cosmos-149' Satellite," IZV. AN SSSR: FAO (News of the USSR Academy of Sciences: Physics of the Atmosphere and Ocean), 5, No 4, pp 355-368, 1969.

2. Gorodetskiy, A. K., Malkevich, M. S., Orlov, A. P., et al., "Some Results of Measurements of the Earth's Radiation in the Spectral Interval 10-12 μm From the 'Cosmos-242' Satellite," IZV. AN SSSR: FAO, 6, No 5, pp 477-489, 1970.

3. PROGRAMMA GLOBAL'NYKH ATMOSFERNYKH ISSLEDOVANIY. VSEMIRNAYA METEOROLOGICHESKAYA ORGANIZATSIYA. KOMITET PO ATMOSFERNYM NAUKAM I KOSPAR (Program of Global Atmospheric Research. World Meteorological Organization. Committee on Atmospheric Sciences and COSPAR. Report of the Scientific Conference), Stockholm, June-July, 1967, 269 pages.

4. Galkin, A. N. and Maksimikhin, D. I., "Use of Satellite Information for Determining the Temperature Field at the Ocean Surface From IR Radiation," SPUTNIKOVAYA OKEANOLOGIYA (Satellite Oceanology), Issue 24, No 379, UCHENYYE ZAPISKI LGU (Scientific Notes of Leningrad State University), pp 326-331.

5. Malkevich, M. S., Georgiyevskiy, Yu. S., et al., "Atmospheric Transparency in the IR Spectral Region," IZV. AN SSSR: FAO, Vol 9, No 12, pp 1257-1269, 1973.

6. Malkevich, M. S. and Potrenko, B. Z., "Influence of Aerosol Attenuation on Accuracy in Determining Temperature of the Ocean and Atmosphere by Remote Methods," IZV. AN SSSR: FAO, Vol 14, No 7, pp 723-733, 1978.

7. Boldyrev, V. G., "Computation of Atmospheric Transfer Functions in the Range 8-12 μm for the Territory of the Northern Hemisphere," IZV. AN SSSR: FAO, Vol 1, No 7, pp 686-703, 1965.

8. Glagoleva, M. G. and Skriptunova, L. I., PROGNOZ TEMPERATURY VODY V OKEANE (Prediction of Ocean Water Temperature), Leningrad, Gidrometeoizdat, 1979, 138 pages.

9. Vinogradov, V. V., "Results of Measurements of Water Surface Temperature by an IR Radiometer in the Tropical Zone of the Atlantic," TROPEKS-72 (TROPEX-72), Leningrad, Gidrometeoizdat, 1974, 216 pages.

10. Shifrin, K. S., "Wind Effect on Effective Sea Radiation," IZV. AN SSSR: FAO, Vol 10, No 7, pp 803-805, 1974.

11. Vinogradov, V. V. and Mironov, L. V., "Temporal Variability of Water Temperature at the Surface in the Tropical Zone of the Atlantic Ocean," TROPEKS-74 (TROPEX-74), Leningrad, Gidrometeoizdat, 1976, 162 pages.

12. Kozlov, V. P., "Exclusion of the Atmospheric Effect in Remote Measurement of Radiation Temperature of a Water Surface," IZV. AN SSSR: FAO, Vol 14, No 9, pp 974-982, 1978.

13. Dreyner, N., Smit, R., PRIKLADNOY REGRESSIONNYY ANALIZ (Applied Regression Analysis), Moscow, "Statistika," 1973, 329 pages.

SPATIAL RESOLUTION OF INSTRUMENTS WITH STIPULATED FIELD MEASUREMENT ERROR

Sevastopol' SPUTNIKOVAYA GIDROFIZIKA in Russian 1980 pp 75-85

[Article by S. V. Dotsenko and M. G. Poplavskaya]

[Text]

Abstract: The authors have derived expressions making it possible with a stipulated accuracy to compute the intervals between readings for a scanning apparatus and the number of detectors in a line in the reconstruction of a field smoothed by the measurement instrument. The measurement of fields with bell-shaped and exponential correlation functions typical in oceanological investigations is considered.

An important stage in investigation of the ocean by remote instruments carried aboard satellites is the plotting of maps of the distribution of its physical fields. This is possible using systems registering the values of the sought-for parameters not only along the satellite flight trajectory, but also perpendicular to it. This is accomplished by spatial scanning of the sensors (receiving antennas or objectives) of remote instruments perpendicularly to the trajectory of satellite motion, that is, by means of creating systems for the successive scanning of the surface. However, in constructing such systems definite contradictions arise between the requirements of a high response and a high resolution of the instruments [1]. The time required for inspection of one resolution element is considerably reduced during scanning and may be much less than the time ensuring a fluctuation response of the infrared and microwave instruments necessary for measuring the studied field in this element.

One of the possible ways to overcome such an incompatibility is the creation of a parallel scanning system, that is, a multichannel system consisting of a set of simple standard elements forming a line of sensors or detectors and making simultaneous measurements (Fig. 1). Accordingly, for the promising systems planned for use in the 1980's mosaic photodetectors are being developed. These consist of several thousand or tens of thousands of sensors of photosensitive elements, the totality of which takes in the entire field of view [1, 2]. According to the data in [2], specialists in the United States and France are planning the development of nonscanning radiometers supplied with multielement detectors. For example, specialists in France are developing the HVR (Haute Visible Resolution) radiometer on the basis of 3000 detectors forming a line with a scanning width of 30 km and a resolution of 10 m.

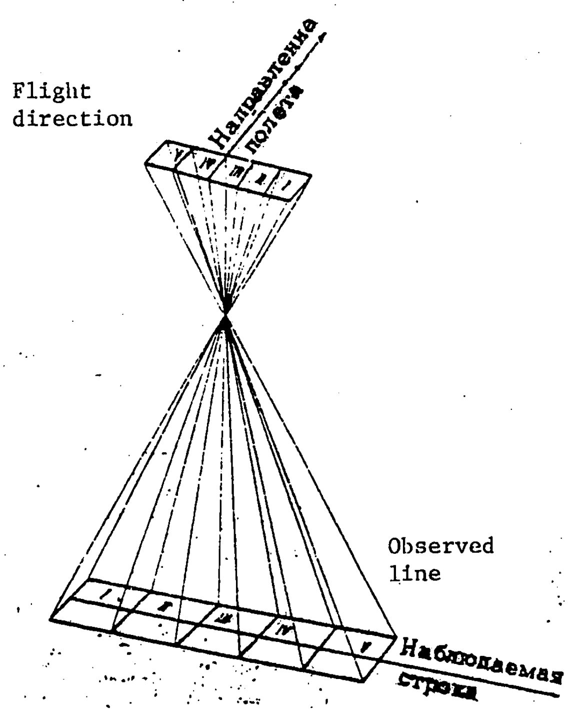

Fig. 1. Line of detectors.

The use of such mosaic photodetectors with a number of elements exceeding 1000 makes possible a considerable improvement in the discrimination of inhomogeneities of the investigated fields. A line of detector sensors mounted perpendicularly to the trajectory of satellite motion makes simultaneous measurement of the field along the entired observed line. During motion of the satellite there is inspection of the entire field in the scanning zone. The complexity, weight and cost of multichannel systems will evidently increase with an increase in the number of detectors in the line. Accordingly, the problem arises of constructing such systems as will ensure stipulated meteorological indices with a minimum number of detectors in the line. The authors of [2] propose that the number of detector sensors necessary for field measurement be determined from the condition

$$n_{det} = \mathfrak{R}/a_{view}, \quad (1)$$

where $\mathfrak{R}$ is the extent of the field of view; a_{view} is the instantaneous angle of the field of view of one instrument sensor; n_{det} is the number of detectors in the line. Formula (1) does not take into account the spatial structure of the field and the form of the instrument function of the sensor; the number

n_{det} is dependent only on the width of the latter. However, as indicated by the investigations presented below, these characteristics play an important role in the designing of instruments intended for measurement of physical fields in the ocean. The purpose of this study is a determination of the dependence of the number of sensors in the line and the distance between the centers of their resolution elements on the form of the instrument function and the structure of the measured field with a stipulated accuracy of its measurement. The conclusions drawn are correct for both parallel and successive scanning of the sea surface.

We will investigate the resolution of remote instruments with their measurement of fields distributed in space. We will assume that a line of detectors with point sensors is used in measuring the field along the observed line. Since these sensors do not perform spatial averaging, the result of such a measurement will be the precise values of the process at the points where the line sensors are situated. The sought-for record of the process along the line can be reconstructed with any degree of accuracy with corresponding intervals between the sensors; the values of the latter will be dependent on the method for interpolation of the process in the intervals between its readings [3, 4].

We will examine step-by-step interpolation which has a simplicity in reconstructing the record and does not require the use of adjacent readings. Since the maximum density of field reading points is necessary in order to achieve the stipulated accuracy, the determined values of the spatial intervals between point instrument sensors will be less than for other interpolation methods.

The dispersion of the error ε_d^2 in step-by-step interpolation of the process, measured at discrete points, is given by the expression [5]

$$\left(\frac{\varepsilon_d}{\sigma}\right)^2 = 2\left[1 - \frac{2}{x_d}\int_0^{x_d/2} R(x)\,dx\right], \qquad (2)$$

where σ^2 and R(x) are the dispersion and the normalized correlation function of the measured process (or field); x_d is the distance between the points of its measurement (interval of field readings). The mean square relative error is determined both by the interval of the readings and by the spatial structure of the measured process. By stipulating the error in reconstructing the process it is thereby possible to find the reading interval corresponding to it.

The spatial interval of resolution of instruments with point sensors necessary for their measurement of physical fields of the ocean surface with a stipulated reconstruction error ε_0 is called the reading interval r_p with which

[p = resolution] $$\varepsilon_d = \varepsilon_0. \qquad (3)$$

The ratio of the necessary spatial interval of resolution and the characteristic scale of the measured field $k_r = r_p/r_x$ is called the coefficient of spatial resolution of such instruments. In order to ensure the stipulated accuracy in reconstructing the field on the basis of the results of its measurement with point instruments it is necessary that the distance between them be not greater than r_p. Inhomogeneities of a scale less than r_0 evidently cannot be resolved by such a system of sensors.

We will determine the spatial resolution of instruments with point sensors when they are used in measuring fields with a one-dimensional spectrum having a bell shape,

$$G_1(\alpha) = \frac{\sigma^2 r_x}{\pi} \exp\left(-\frac{\alpha^2 r_x^2}{\pi}\right), \tag{4}$$

where r_x and σ^2 are the characteristic scale and dispersion of this field. Such a model is used in approximating the real spectra of physical fields in the ocean [6, 7]. We will ascertain the error in reconstructing this field along the line of detector point sensors. Taking into account that the correlation function of this field has the form

$$R(x) = \exp\left[-\frac{\pi}{4}\left(\frac{x}{r_x}\right)^2\right],$$

and using formula (2), we obtain [8]

$$\left(\frac{\varepsilon_d}{\sigma}\right)^2 = 2\left[1 - \frac{2r_x}{x_d}\,\Phi\left(\frac{\sqrt{\pi}}{4}\,\frac{x_d}{r_x}\right)\right] \approx \frac{\pi}{24}\left(\frac{x_d}{r_x}\right)^2,$$

where $\Phi(x)$ is the probability integral. Hence, also from condition (3) we find the resolution coefficient for the instruments

$$k_T = 2\sqrt{\frac{6}{\pi}}\,\frac{\varepsilon_0}{\sigma} = 2.764\,\frac{\varepsilon_0}{\sigma}. \tag{5}$$

We will compute the k_T value for the square of the relative error $(\varepsilon_0/\sigma)^2 = 0.1$ (or $\varepsilon_0/\sigma = 0.316$), which in practice is considered the maximum admissible. From formula (5) for this case we have $k_T = 0.874$. Accordingly, with $(\varepsilon_0/\sigma)^2 = 0.1$ it is possible to resolve inhomogeneities of the scale $r_p \geqslant 0.874\ r_x$.

With a decrease in the measurement error the magnitude of the inhomogeneities which can be resolved also decreases.

We will find the spatial resolution of point instruments when they are used in measuring fields whose one-dimensional spectrum has the form [6]

$$G_1(\alpha) = \frac{\sigma^2 r_x}{\pi}\left[1 + (\alpha r_x)^2\right]^{-1}. \tag{6}$$

In contrast to the fields considered earlier, differentiable an infinite number of times, these fields are not differentiable. They have a more clearly expressed high-frequency component. Substituting the expression for the correlation function of this field $R(x) = \exp(-x/r_x)$ into formula (2), after computing the integral under condition (3) and with sufficiently small measurement errors we obtain

$$k_T = 2\left(\frac{\varepsilon_0}{\sigma}\right)^2. \tag{7}$$

It can be seen from a comparison of expressions (5) and (7) that for less smooth fields (6) the resolution coefficient with an increase in ε_0/σ increases more slowly than for the fields (4). For example, with $(\varepsilon_0/\sigma)^2 = 0.1$ for the fields (6) $k_T = 0.20$. This means that when measuring fields having a more clearly expressed high-frequency component inhomogeneities with smaller scales must be resolved in order to attain a stipulated accuracy.

With the measurement of physical fields of the ocean surface by remote instruments with nonpoint sensors there is a smoothing of these fields with the weight set by the instrument function of the sensor. We will assume that the measurement line consists of such sensors and the purpose of the measurement is a determination of the field smoothed in space by these sensors. The pattern of such a field would be obtained directly if the smoothing instrument scanned it continuously in space. But in the considered case the field is measured in a discrete set of spatially separated points. Accordingly, here it is necessary to solve the problem of reconstructing fields smoothed by measurement instruments forming the line with the stipulated accuracy. For this purpose we will find the distance between the centers of the resolution elements for the detectors in the line that will ensure a stipulated accuracy in reconstructing the smoothed field. Measurement of the true field with an instrument with a spatially averaging sensor is equivalent to measurement of the output signal of this instrument by some hypothetical instrument with a point sensor. Accordingly, we will use the concept, introduced above, of the necessary spatial resolution, but applied to the output signal of a remote instrument.

If the measured $X(\vec{\rho})$ field is homogeneous, isotropic, stationary and "frozen-in," and the instrument sensor is linear and inertialess, the instrument output signal $Y(\vec{x})$ is related to this field by the expression [9]

$$Y(\bar{x}) = \int X(\bar{x}-\bar{\rho})\,\tilde{h}(\bar{\rho})\,d\bar{\rho} \ ,$$

where $h(\vec{\rho})$ is the instrument function of the instrument sensor. Denoting the normalized correlation function of the instrument output signal by $R_y(x)$, its dispersion by σ_y^2, we obtain, in accordance with expression (2) a formula for the dispersion of error in reconstructing the smoothed field in the case of step-by-step interpolation

$$\left(\frac{\varepsilon_d}{\sigma_y}\right)^2 = 2\left[1-\frac{2}{x_d}\int_0^{x_d/2} R_y(x)\,dx\right]. \tag{8}$$

The field smoothed by the remote instrument can be restored with the stipulated error if the interval between its readings does not exceed the X_d value determined using formula (8).

The spatial interval of resolution of the averaging instruments necessary for their measurement of physical fields of the ocean surface with the stipulated accuracy in reconstructing ε_0 of the latter is the value of the reading interval r_p with which $\varepsilon_d = \varepsilon_0$. The ratio of the spatial resolution interval to the characteristic radius of the instrument resolution element $k_p = r_p/R_x$ is called the relative resolution interval of these instruments. In order to ensure the stipulated accuracy in reconstructing the smoothed field on the basis of the results of its measurement by an averaging instrument it is necessary that the distance between the centers of their resolution elements not exceed the value r_p. Inhomogeneities with a scale less than r_p cannot be resolved by these instruments.

We will find an expression for the square of the error in reconstructing smoothed fields on the basis of the results of their measurement in a discrete set of equally distant points. For this purpose we derive a formula for the correlation function of the output signal and its dispersion. According to [10], the $S_y(x)$ spectrum of the output signal of measurements with an axisymmetric sensor when they are used in measuring an isotropic field is expressed through the two-dimensional field spectrum and the $\tilde{h}(\alpha)$ spectrum of the instrument function as

$$S_y(\alpha) = 2\int_0^\infty G_2\left(\sqrt{\alpha^2+\alpha_1^2}\right)\tilde{h}^2\left(\sqrt{\alpha^2+\alpha_1^2}\right)d\alpha_1, \tag{9}$$

hence the autocorrelation function of the output signal is

$$B_y(x) = 4\int_0^\infty\int_0^\infty G_2\left(\sqrt{\alpha^2+\alpha_1^2}\right)\tilde{h}^2\left(\sqrt{\alpha^2+\alpha_1^2}\right)\cos(\alpha x)\,d\alpha_1\,d\alpha.$$

Substituting this expression into formula (8), we obtain

$$\left(\frac{\varepsilon_d}{\sigma_y}\right)^2 = 2\left[1-\frac{4}{\sigma_y^2}\int_0^\infty\int_0^\infty G_2\left(\sqrt{\alpha^2+\alpha_1^2}\right)\tilde{h}^2\left(\sqrt{\alpha^2+\alpha_1^2}\right)\frac{\sin\left(\frac{\alpha x_d}{2}\right)}{\frac{\alpha x_d}{2}}d\alpha_1\,d\alpha\right].$$

The resulting expression is analytically difficult to compute even in the most simple cases. Accordingly, we will expand it into a series in powers of X_d

$$\left(\frac{\varepsilon_d}{\sigma_y}\right)^2 = 2\left[1-\frac{4}{\sigma_y^2}\sum_{k=0}^\infty\frac{(-1)^k}{(2k+1)!}\left(\frac{x_d}{2}\right)^{2k}a_k\right], \tag{10}$$

where

$$a_k = \int_0^\infty\int_0^\infty G_2\left(\sqrt{\alpha^2+\alpha_1^2}\right)\tilde{h}^2\left(\sqrt{\alpha^2+\alpha_1^2}\right)\alpha^{2k}\,d\alpha_1\,d\alpha. \tag{11}$$

The dispersion of the instrument output signal is $\sigma_y^2 = 4a_0$. In computing the integral (11) we will replace the variables $\alpha = \beta\cos\varphi$, $\alpha_1 = \beta\sin\varphi$. After the integration of [8] and several transformations expression (11) is reduced to the form

$$a_k = \frac{\pi}{2}\,\frac{(2k-1)!!}{(2k)!!}\int_0^\infty G_2(\beta)\,\tilde{h}^2(\beta)\,\beta^{2k+1}\,d\beta.$$

Then formula (10) is written in the following way:

$$\left(\frac{\varepsilon_d}{\sigma_y}\right)^2 = \frac{2}{B_0}\sum_{k=1}^\infty\frac{(-1)^{k+1}\,x_d^{2k}}{(k!)^2\,(2k+1)\,16^k}\,B_k, \tag{12}$$

where

$$C_r = \int_0^{\infty} G_z(\beta)\, \tilde{h}^2(\beta)\, \beta^{2k+1}\, d\beta .$$

Formula (12) makes it possible with any degree of accuracy to find the interval of spatial resolution by a remote instrument corresponding to a stipulated reconstruction error. This interval is dependent on the form of the measured field and the instrument function.

We will find the spatial resolution of remote instruments whose sensors have a bell-shaped instrument function

$$h(x) = \frac{1}{4R_x^2} \exp\left[-\frac{4}{\pi}\left(\frac{x}{R_x}\right)^2\right] . \tag{13}$$

Formula (13) is used in the approximation of the instrument functions of sensors of IR radiometers and the directional diagrams of the antennas of microwave radiometers which are used extensively at the present time in remote sounding of the ocean surface [11, 12].

We will ascertain the resolution interval of these instruments when they are used in measuring fields with a bell-shaped spectrum (4). The substitution of the instrument function spectrum (13)

$$\tilde{h}(\alpha) = \exp\left[-\frac{1}{\pi}(\alpha R_x)^2\right]$$

and the two-dimensional field spectrum corresponding to its one-dimensional spectrum (4) into formula (12) gives

$$\left(\frac{\varepsilon_d}{\sigma_y}\right)^2 = 2\sum_{k=1}^{\infty}(-1)^{k+1}\left(\frac{x_d}{R_x}\right)^{2k}\frac{(\pi z^2)^k}{k!(2k+1)4^{2k}(2z^2+1)^k} .$$

The approximate value of the relative error with an accuracy to 10^{-3} for $0 \leqslant z \leqslant 1$ is written in the form

$$\frac{\varepsilon_d}{\sigma_y} = \frac{\sqrt{\pi}}{2\sqrt{6}} \frac{z}{\sqrt{1+2z^2}} \frac{x_d}{R_x} = c_1(z)\frac{x_d}{R_x} . \tag{14}$$

where $z = R_x/r_x$. From expression (14) we express the resolution coefficient for the considered instrument through the radius of its resolution element for a reconstruction error $\varepsilon_d = \varepsilon_0$

$$k_p = \frac{r_p}{R_x} = 2\frac{\varepsilon_0}{\sigma_y}\sqrt{\frac{6}{\pi}(1+2z^2)}\,\frac{1}{z} = d_1(z)\frac{\varepsilon_0}{\sigma_y} .$$

The dependence $d_1(z) = 1/c_1(z)$ is represented by curve 1 (Fig. 2). With an increase in z it decreases, most steeply for $0 < z \leqslant 0.2$.

We will find the spatial resolution of an instrument with the instrument function (13) when it is used in measuring a field with an exponential correlation function. For this we will determine the error in reconstructing the smoothed field. By substituting the two-dimensional field spectrum corresponding to the spectrum (6) and the spectrum of the instrument function into formula (12) we find

$$\left(\frac{\varepsilon_d}{\sigma_y}\right)^2 = \sqrt{\pi}\,\frac{e^{2z^2/\pi}}{1 - z\sqrt{2}\,e^{2z^2/\pi}\left[1-\Phi\left(z\sqrt{2/\pi}\right)\right]} \times$$

$$\times \sum_{k=1}^{\infty} \frac{(-1)^{k+1}}{k!(2k+1)}\left(\frac{x_d}{R_x}\right)^{2k}\left(\frac{z}{16}\right)^{k}\left(\frac{\pi}{2}\right)^{k/2} W_{-k/2-3/4,\,k/2-1/4}\left(\frac{2z^2}{\pi}\right),$$

where $W_{\lambda,\mu}(z)$ is the Whittaker function [8]. The approximating expression for the relative reconstruction error has the form

$$\frac{\varepsilon_d}{\sigma_y} = c_2(z)\frac{x_d}{R_x},$$

where

$$c_2(z) = \frac{\sqrt{\pi z}}{4\sqrt{3}\sqrt[4]{2}}\sqrt{\frac{\left[1-\Phi\left(z\sqrt{\frac{2}{\pi}}\right)\right]\left(1-\frac{4z^2}{\pi}\right)+2\frac{\sqrt{2}}{\pi}z e^{-2z^2/\pi}}{\left\{1-z\sqrt{2}\,e^{2z^2/\pi}\left[1-\Phi\left(z\sqrt{\frac{2}{\pi}}\right)\right]\right\}}\,e^{z^2/\pi}}$$

Hence the relative instrument resolution interval for the reconstruction error $\varepsilon_d = \varepsilon_0$ of the smoothed field

$$k_p = d_2(z)\,\frac{\varepsilon_0}{\sigma_y}, \qquad (15)$$

where $d_2(z) = \frac{1}{c_2(z)}$.

A graph of the coefficient $d_2(z)$ is given as Fig. 2 (curve 2). The $d_2(z)$ curve decreases with an increase in z. Thus, for this error in reconstructing the smoothed field the distance between the centers of the resolution elements of the line detectors is dependent on the type of field and on the z value. For example, with z = 0.1 for a field with a bell-shaped correlation function with $(\varepsilon_0/\sigma_y)^2 = 0.1$ the distance between these centers is equal to 8.71 R_x; for a field with an exponential correlation function -- 4.30 R_x. With a decrease in z the difference between these values increases; with an increase it decreases. In actuality, with z = 0.8 for the first field $r_0 = 1.88\ R_x$; for the second -- 1.37 R_x.

We will apply these results to specific instruments. We will determine the resolution intervals of a five-channel radiometer and a descent vehicle (DV) [13, 14].

We will assume that from an altitude of 300 km these instruments measure the field of surface temperature, whose spatial correlation function can be approximated by the expression

$$R(x) = \exp\left(-\frac{|x|}{r_x}\right),$$

where r_x = 130 km [7].

First we will find the spatial resolution of a five-channel radiometer. The characteristic radius of its instrument function R for the indicated altitude is 13.05 km and the value z = 0.1. We find from formula (15) that for the square of the relative reconstruction error $(\varepsilon_0/\sigma_y)^2 = 0.1$ $r_p = 4.36 \cdot R_x =$ 57 km.

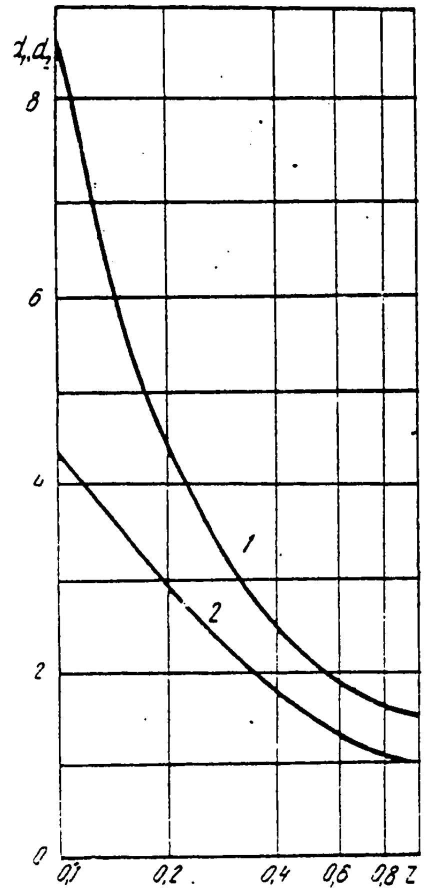

Fig. 2. Dependence of d_1 and d_2 coefficients on value $z = R_x/r_x$.

If the line consists of detectors whose sensors are radiometers of the DV type for which R_x at this same altitude is equal to 6.6 km, then the z value for the considered field is equal to 0.05. Using formula (15) we find that for this error the distance between the centers of the elements of detectors in the line is $r_p = 5.81 \cdot R_x = 38.4$ km.

When measuring a field with a bell-shaped correlation function with the same $r_x = 130$ km for this error the resolution interval for a five-channel radiometer is 113.65 km and for the DV radiometer -- 115.35 km.

If formula (1) is used in computations of the resolution elements, we find that r_p is equal to $2R_x$, regardless of the type of field and variety of instrument. Then the relative error in reconstructing the smoothed field with an exponential correlation function, measured with a five-channel radiometer, is 0.145, with the DV radiometer -- 0.106. In the case of measurement of fields with a bell-shaped correlation function the relative error is much less: for the first radiometer it is 0.072, for the second -- 0.038. However, due to the influence of the atmosphere the striving for such a high accuracy in the measurements is scarcely feasible. With satisfaction of the condition $(\varepsilon_0/\sigma_y)^2 = 0.1$ the distance between the centers of the resolution elements of detectors whose sensors are the antennas of a five-channel radiometer must be 2.18 times greater than follows from formula (1) and three times greater than for detectors with sensors of the type of the antennas of the DV radiometer.

The expressions derived above are applicable not only for designing lines of nonscanning apparatus, but also in computing the intervals between readings of scanning instruments having an adequately high response.

BIBLIOGRAPHY

1. Khodarev, Yu. K., Bespalova, Ye. A., Pashin, Yu. N., et al., VOPROSY PRIMENENIYA RADIOFIZICHESKIKH METODOV DLYA IZUCHENIYA ATMOSFERY I POVERKHNOSTI ZEMLI S POMOSHCH'YU KOSMICHESKIKH APPARATOV (Problems in the Use of Radiophysical Methods for Study of the Earth's Atmosphere and Surface Using Space Vehicles), Preprint 112, Moscow, IKI AN SSSR, 1972, 50 pages.

2. Safronov, Yu. P. and Andrianov, Yu. G., INFRAKRASNAYA TEKHNIKA I KOSMOS (Infrared Technology and Space), Moscow, "Sov. Radio," 1978, 248 pages.

3. Karandeyev, K. B. and Tsanenko, M. P., "Problems in the Theory and Practice of Data Measurement Systems," KIBERNETIKU - NA SLUZHBU KOMMUNIZMU (Cybernetics in the Service of Communism), Vol 5, Moscow, "Energiya," pp 87-118, 1967.

4. Kavalarov, G. I. and Mandel'shtam, S. M., VVEDENIYE V INFORMATSIONNUYU TEORIYU IZMERENIY (Introduction to the Information Theory of Measurements), Moscow, "Energiya," 1974, 376 pages.

5. Dotsenko, S. V. and Khudyakov, Yu. A., "Optimum Discretization and Quantization of a Measured Physical Process," MORSKIYE GIDROFIZICHESKIYE ISSLEDOVANIYA (Marine Hydrophysical Investigations), No 3, Sevastopol', pp 86-99, 1973.

6. Monin, A. S. and Yaglom, A. M., STATISTICHESKAYA GIDROMEKHANIKA (Statistical Hydromechanics), Part 2, Moscow, "Nauka," 1967, 720 pages.

7. Belyayev, V. I., OBRABOTKA I TEORETICHESKIY ANALIZ OKEANOGRAFICHESKIKH NABLYUDENIY (Processing and Theoretical Analysis of Oceanographic Observations), Kiev, "Naukova Dumka," 1973, 296 pages.

8. Gradshteyn, I. S. and Ryzhik, I. M., TABLITSY INTEGRALOV, SUMM, RYADOV I PROIZVEDENIY (Tables of Integrals, Sums, Series and Products), Moscow, "Nauka," 1971, 1108 pages.

9. Dotsenko, S. V., TEORETICHESKIYE OSNOVY IZMERENIYA FIZICHESKIKH POLEY OKEANA (Theoretical Principles for the Measurement of Physical Fields in the Ocean), Leningrad, Gidrometeoizdat, 1974, 152 pages.

10. Dotsenko, S. V., et al., "Spatial-Spectral Characteristics of Remote Sensors," MORSKIYE GIDROFIZICHESKIYE ISSLEDOVANIYA, No 2, Sevastopol', pp 162-173, 1974.

11. Korzun, V. A., "Apparatus for Surveying the Ocean From Great Altitudes," PROMYSLOVAYA OKEANOLOGIYA (Commercial Oceanology), Series 9, No 4, Moscow, TsNIITEIRKh, pp 1-22, 1974.

12. Zubkovich, S. G., STATISTICHESKIYE KHARAKTERISTIKI RADIOSIGNALOV, OTRAZHENNYKH OT ZEMNOY POVERKHNOSTI (Statistical Characteristics of Radio Signals Reflected From the Earth's Surface), Moscow, "Sov. Radio," 1968, 224 pages.

13. Astkheymer, R., de Vaard, R. and Dzhekson, Ye., "Infrared Radiometers of the 'TIROS-P' Satellite," RAKETY I ISKUSSTVENNYYE SPUTNIKI V METEOROLOGII (Rockets and Artificial Satellites in Meteorology), Moscow, IL, pp 158-170, 1963.

14. Gorodetskiy, A. K., et al., "Methods and Some Results of Determination of Temperature of the Underlying Surface From the 'Cosmos-149' Satellite," IZV. AN SSSR: FAO (News of the USSR Academy of Sciences: Physics of the Atmosphere and Ocean), Vol 5, No 4, pp 358-381, 1969.

CALIBRATION OF REMOTE INSTRUMENTS ON THE BASIS OF POLYGON MEASUREMENTS

Sevastopol' SPUTNIKOVAYA GIDROFIZIKA in Russian 1980 pp 86-96

[Article by S. V. Dotsenko]

[Text]

Abstract: A study was made of the possibility of calibrating remote instruments on the basis of the results of measurement of a physical field in a sea polygon by a direct contact measurement instrument. The author has determined the configuration and extent of a polygon ensuring a stipulated calibration accuracy. It is shown that for large resolution elements a substantial improvement in accuracy is obtained by optimum calibration.

The use of remote instruments carried in flight vehicles is affording great possibilities for study of physical fields in the ocean. However, at the present time investigators have met with difficulties in using remote sounding data because in the study of one and the same physical field the results of measurements may be different in dependence on the operating regime of the vehicle, state of the atmosphere, sighting angles, etc. Accordingly, there must be a regular comparison (in time) of the readings of a remote instrument and the values of the measured parameter in the ocean, whose absolute value is found using direct-measurement instruments in sea polygons. In the future such a procedure will be called calibration.

Any contact instrument used under marine conditions has a much lesser field averaging scale than a remote instrument. For this reason on the basis of signals of contact instruments containing a very broad spectrum of high-frequency fluctuations it is impossible, with the necessary accuracy, to evaluate the variation of a low-frequency signal at the output of the remote instrument, considerably smoothed by its resolution element. In order to increase the evaluation accuracy it is necessary to average the output signals of contact instruments.

The authors of [1] proposed and investigated optimum time averaging of signals of a contact instrument for direct measurement work for obtaining the best evaluation of the field value measured by the remote instrument. The measurement scheme was as follows. The center of a resolution element of the remote instrument moves along a linear trajectory which includes the point O, the place where the direct contact measurement instrument was situated. By means of optimum averaging of the signal of a contact instrument it is possible to find the best evaluation of the field measured by the remote instrument at the time when the center of its resolution element coincides with the point 0 [1].

However, due to different factors, the flight trajectory of the flight vehicle, and this means, the trajectory of the center of a resolution element of the remote instrument, may not pass directly through the site of the contact measurement instrument. Evidently, in this case as well the data from field measurements with a contact instrument can be used in calibration work, but the accuracy of the latter will be the worse the farther the centers of these instruments are from one another. By stipulating a definite accuracy it is possible to compute the configuration and extent of the polygon within whose limits calibration on the basis of one contact instrument can be carried out.

Assume that there is a direct contact measurement instrument at the point 0 (Fig. 1), adopted as the origin of coordinates. This instrument registers values of the field $\vec{X}(\vec{r};t)$ whose changes at the fixed point 0 are related both to the movement of the field relative to its mean velocity $\vec{V}_0$ and to its temporal evolution, determined by the "non-frozen-in" character of this field.

The point 0', at which it is necessary that the instrument be calibrated, lies on the trajectory of motion of the remote instrument. The vector $\vec{\rho}_0$ connects the points 0 and 0'. The angle between the vectors $\vec{\rho}_0$ and $\vec{v}_0$ is equal to φ; the angle between the vector $\vec{v}_0$ and the x-axis $0\xi_1$ is equal to θ.

[g = remote]

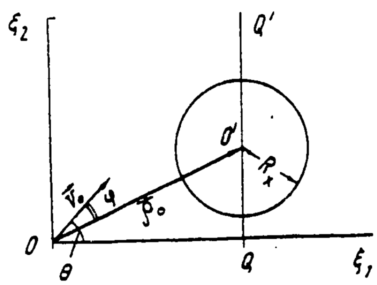

Fig. 1. Diagram representing field measurements during calibration. The center of a resolution element of the remote instrument (point 0') does not coincide with the contact instrument (point 0).

The sensor of the remote instrument performs spatial averaging of the measured field. Assuming that this instrument is inertialess, the signal at its output can be registered as [2]

$$y_g(\vec{\rho}_0;t')=\int X(\vec{\rho}_0-\vec{\rho};t')h(\vec{\rho})d\vec{\rho},$$

where $h(\vec{\rho})$ is the instrument function of the remote instrument characterizing this averaging; $\vec{\rho}_0$ is the radius-vector of the center of a resolution element for this instrument; t' is the time of field measurement by this instrument. Integration is carried out in all of two-dimensional space, including a surface resolution element of the remote instrument. Assume that the center of the resolution element of the remote instrument is situated at the calibration point with the radius-vector $\vec{\rho}_0$

at the time t' = 0. In this case the signal at its output is

$$y_{remote} = y_g(\bar{\rho}_0; 0) = \int X(\bar{\rho}_0 - \bar{\rho}; 0)\, h(\bar{\rho})\, d\bar{\rho}. \quad (1)$$

At the point 0 the field changes with time as $x_0(t) = x(\vec{v}_0 t;\, t)$; the first argument of the expression on the right-hand side determines the field transfer with the constant velocity v_0 and the second determines its temporal evolution, unrelated to this transfer. Since the sensors of the direct measurement instruments are much smaller than the extent of the resolution elements for the remote sensors, we will assume that the first are points. In addition, the contact instruments will be regarded as inertialess. In this case the $x_0(t)$ value is a signal at the output of the contact instrument.

Using some temporal weighting function $u(\tau)$, at each moment in time t it is possible to obtain the time-averaged signal at the output of the direct measurement instrument. At the calibration time t = 0 this value is equal to

$$y_{inst}(0) = \int_{-\infty}^{\infty} X(-\bar{v}_0\tau; -\tau)\, u(\tau)\, d\tau. \quad (2)$$

Optimum calibration of a remote instrument essentially involves obtaining (by use of procedure (2)) the $y_{inst}(0)$ values differing least from the y_{remote} value determined by formula (1) and its use for comparison with the real signal value at the output of the remote instrument at the time t = 0.

We will find the weighting function $u(\tau)$ ensuring the minimum mean difference $y_{inst}(0)$ from y_{remote}, that is, the minimum calibration error. The mean square of this error is

[пр = inst] (3)

Assuming that the measured field is also centered uniformly and applying formulas (1), (2), we obtain

$$\overline{y^2_{np}(0)} = \iint_{-\infty}^{\infty} B[\bar{v}_0(\tau_1 - \tau_2);\, \tau_1 - \tau_2]\, u(\tau_1)\, u(\tau_2)\, d\tau_1\, d\tau_2, \quad (4)$$

[п p = inst; g = remote]

$$\overline{y^2_g} = \iint B(\bar{\rho}_1 - \bar{\rho}_2; 0)\, h(\bar{\rho}_1)\, h(\bar{\rho}_2)\, d\bar{\rho}_1\, d\bar{\rho}_2, \quad (5)$$

$$\overline{y_{np}(0)\, y_g} = \int B(\bar{\rho} - \bar{\rho}_0 - \bar{v}_0\tau; -\tau)\, h(\bar{\rho})\, u(\tau)\, d\bar{\rho}\, d\tau, \quad (6)$$

where $B(\vec{\rho};\tau)$ is the generalized autocorrelation function for the x(r;t) field.

We will find the averaging function $u(\tau)$ minimizing the ε^2 value. For this we will equate the variation of the functional $\varepsilon^2[u(\tau)]$ to zero. We obtain an integral equation for determining the optimum weighting function

[опт = optimum]

$$\int_{-\infty}^{\infty} B[\bar{v}_0(\tau - \tau_1);\, \tau - \tau_1]\, u_{onr}(\tau_1)\, d\tau_1 = \int B(\bar{\rho} - \bar{\rho}_0 - \bar{v}_0\tau; -\tau)\, h(\bar{\rho})\, d\bar{\rho}. \quad (7)$$

The generalized autocorrelation functions present in formula (7) are dependent on two spatial shifts and one temporal shift. We will assume that the measured field is anisotropic and not "frozen-in" and that its surfaces of equal correlation are ellipsoids in the coordinates of the spatial-temporal shifts [4]. The generalized correlation function for such a field can be written as $B(\sqrt{\vec{s}^T A \vec{s}})$, where A is a matrix of quadratic form of its argument; $\vec{s}^T = \| x_1, x_2, v_c\tau \|$ is the matrix-row of the shifts. The "relaxation rate" for the field entering into the last element of this row is $v_c = \rho_c/\tau_c$, where the ρ_c and τ_c values are the characteristic spatial and temporal field scales respectively. The generalized autocorrelation function can be expressed through the three-dimensional field spectrum $G_3(\vec{\gamma})$ in the following way [5]:

$$B(\sqrt{\vec{s}^T A \vec{s}}) = \frac{1}{v_c}\iiint_{-\infty}^{\infty} G_3(\sqrt{\vec{\gamma}^T A^{-1}\vec{\gamma}})\, e^{j(\alpha_1 x_1 + \alpha_2 x_2 + \omega\tau)} d\alpha_1 d\alpha_2 d\omega, \tag{8}$$

where the matrix-row of wave numbers is

$$\vec{\gamma}^T = \left\| \alpha_1, \alpha_2, \frac{\omega}{v_c} \right\| .$$

We will assume that the measured field is spatially isotropic but is not "frozen-in." In this case the A matrix is transformed into a unit matrix [4] and the autocorrelation function has the structure

$$B(\vec{r};\tau) = B\left[\sqrt{|\vec{r}|^2 + (v_c\tau)^2}\right],$$

and its representation (8) through the three-dimensional spectrum assumes the form

$$B(\vec{r};\tau) = \frac{1}{v_c}\int G_3(\sqrt{\vec{\gamma}^T\vec{\gamma}})\, e^{j(\vec{\alpha}\vec{r} + \omega\tau)} d\vec{\alpha}\, d\omega. \tag{9}$$

We will substitute this expression into equation (7) and we will express the instrument function of the instrument entering here and the weighting function of averaging through their spectra $\tilde{h}(\vec{\alpha})$ and $\tilde{u}_{opt}(\omega)$. Then multiplying both sides of the derived equation by $\exp(-j\,\omega_1\tau)$, integrating for τ in infinite limits and carrying out simple transforms, we find the spectrum of the optimum weighting function

$$\tilde{u}_{opt}(\omega) = \frac{\sqrt{1+\eta^2}}{G_1\left(\frac{1}{\sqrt{1+\eta^2}}\frac{\omega}{v_c}\right)}\int G_3\left[\sqrt{|\vec{\alpha}|^2 + \left(\frac{\omega + \vec{\alpha}\vec{v}_0}{v_c}\right)^2}\right]\tilde{h}^*(\vec{\alpha})\, e^{-j\vec{\alpha}\vec{\rho}_0} d\vec{\alpha}, \tag{10}$$

where $\eta = v_0/v_c$ is the parameter corresponding to the "non-frozen-in" character of the field; $G_1(\alpha)$ is a one-dimensional field spectrum. Hence the optimum weighting function is found by use of the inverse Fourier transform

[опт = opt]

$$u_{opt}(\tau) = \frac{1}{2\pi}\int_{-\infty}^{\infty} \tilde{u}_{opt}(\omega)\, e^{j\omega\tau} d\omega. \tag{11}$$

Through the field spectra of the instrument and weighting (not necessarily optimum) functions we will express the mean square of the calibration error. This value is found by the substitution of expression (9) into formulas (4)-(6) and by the use of the derived expressions in formula (3)

$$\epsilon^2 = \frac{1}{v_c}\int G_3\left[\sqrt{|\vec{\alpha}|^2 + \left(\frac{\omega}{v_c}\right)^2}\right]\left[|\tilde{u}(\omega + \vec{\alpha}\vec{v}_0)|^2 - 2\tilde{h}^*(\vec{\alpha})\,\tilde{u}(\omega + \vec{\alpha}\vec{v}_0)\, e^{-j\vec{\alpha}\vec{\rho}_0} + |\tilde{h}(\vec{\alpha})|^2\right] d\vec{\alpha}\, d\omega. \tag{12}$$

Two cases of the latter expression are of interest. Their comparison makes it possible to clarify the effectiveness of use of optimum averaging in time for calibration when employing the considered scheme. First we will find the calibration error on the basis of one instantaneous reading of the output signal of a direct measurement instrument obtained some time t after the remote measurement. In this case the calibration weighting function is a delta function of time $u(\tau) = \delta(t - \tau)$. With $t > 0$ the calibration is carried out using the reading of a contact instrument obtained later than the reading of the remote instrument. In this case the spectrum of the weighting function of averaging $\tilde{u}(\omega) = \exp(-j\omega t)$ and expression (12) assumes the form

$$\varepsilon_1^2(t) = \frac{1}{V_c}\int G_3\left[\sqrt{|\vec{\varkappa}|^2 + \left(\frac{\omega}{V_c}\right)^2}\right]\Big\{1 - 2\tilde{h}^*(\vec{\varkappa})\, e^{-j[(\omega + \vec{\varkappa}\vec{V}_0)t + \vec{\varkappa}\vec{\rho}_0]} + |\tilde{h}(\vec{\varkappa})|^2\Big\}\, d\vec{\varkappa}\, d\omega. \tag{13}$$

Then we find the error in optimum calibration which by definition is the minimum possible. For this purpose we substitute the spectrum $\tilde{u}_{opt}(\omega)$ into (12)

[ОПТ = opt]

$$\varepsilon_{min}^2 = \frac{1}{V_c}\int G_3\left[\sqrt{|\vec{\varkappa}|^2 + \left(\frac{\omega}{V_c}\right)^2}\right]\Big[|\tilde{u}_{опт}(\omega + \vec{\varkappa}\vec{V}_0)|^2 - 2\tilde{h}^*(\vec{\varkappa})\,\tilde{u}_{опт}(\omega + \vec{\varkappa}\vec{V}_0)\, e^{-j\vec{\varkappa}\vec{\rho}_0} + |\tilde{h}(\vec{\varkappa})|^2\Big]\, d\vec{\varkappa}\, d\omega. \tag{14}$$

We will analyze the determined values in the example of calibration of a remote instrument with an axisymmetric bell-shaped field instrument function whose energy spectrum also has a bell-shaped form. In this case

$$G_n(\vec{\varkappa}) = G_n(\varkappa) = \frac{\sigma^2 r_x^n}{\pi^n}\exp\left[-\frac{(r_x\varkappa)^2}{\pi}\right], \tag{15}$$

where r_x is the characteristic spatial field scale ($r_x = \rho_c$), σ^2 is field dispersion. In this case the instrument function spectrum is also axisymmetric and has a bell-shaped form

$$\tilde{h}(\vec{\varkappa}) = \tilde{h}(\varkappa) = \exp\left[-\frac{(R_x\varkappa)^2}{\pi}\right], \tag{16}$$

where R_x is the characteristic radius of the instrument function. The substitution of expressions (15) and (16) into formula (13) gives

$$\frac{\varepsilon_1^2(t)}{\sigma^2} = 2\left\{\frac{1+z^2}{1+2z^2} - \frac{1}{1+z^2}\exp\left[-\frac{\pi}{4r_x^2}\left(V_c^2t^2 + \frac{V_0^2t^2 + \rho_0^2 + 2\rho_0 V_0 t\cos\varphi}{1+z^2}\right)\right]\right\}, \tag{17}$$

where φ is the angle between the vectors $\vec{v}_0$ and $\vec{\rho}_0$; $z = R_x/r_x$ is the ratio of the characteristic radius of a resolution element for the remote instrument to the characteristic field scale (Fig. 1).

If the calibration is carried out using a reading of a contact instrument obtained at the time of remote measurement, that is, with $t = 0$, we obtain

$$\frac{\varepsilon_1^2(0)}{\sigma^2} = 2\left[\frac{1+z^2}{1+2z^2} - \frac{1}{1+z^2}\exp\left(-\frac{\pi}{4}\,\frac{\rho^2}{1+z^2}\right)\right], \tag{18}$$

where $q = \rho_0/r_x$ is a value characterizing the relative distance between the centers of the instrument sensors whose signals are compared. If for a particular instrument (z = const) the stipulated relative measurement error is $\varepsilon_1^2(0)/\sigma^2$ = const, we also have $q = q_0$ = const. This means that in the case of synchronous calibration in an isotropic field on the basis of one signal reading of a contact instrument an equal calibration accuracy for a remote instrument is realized at points in the polygon situated at equal distances from the contact instrument. Accordingly, here a polygon ensuring a stipulated calibration accuracy has the form of a circle (curve 1, Fig. 2).

According to formula (17), the magnitude of the error in very simple calibration is dependent on the interval between field readings by remote and contact instruments. It is minimum if this interval is equal to

$$t_0 = -\frac{\rho_0 z}{V_c} \frac{\cos\varphi}{1+z^2+\eta^2}. \tag{19}$$

The mean square error in such calibration is given by the expression

$$\frac{\varepsilon_1^2(t_0)}{\sigma^2} = 2\left[\frac{1+z^2}{1+2z^2} - \frac{1}{1+z^2}\exp\left(-\frac{\pi}{4}\frac{q^2}{1+z^2}\frac{1+z^2+\eta^2\sin^2\varphi}{1+z^2+\eta^2}\right)\right]. \tag{20}$$

Comparison with formula (18) shows that $\varepsilon_1^2(t_0)$ differs from $\varepsilon_1^2(0)$ to the greatest degree when the φ angle between the $\vec{v}_0$ and $\vec{\rho}_0$ vectors is equal to 0 or 180° since field inhomogeneities, measured at the time $t = -t_0$ by a contact instrument, with $\varphi = 0°$ due to field transfer at the time t = 0 will be situated at the center of a resolution element of the remote instrument. Since the field is not "frozen in," the form of these inhomogeneities will to some degree be distorted, which in expression (20) is taken into account by the η parameter. However, if $\varphi = \pm 90°$, then $t_0 = 0$ and formula (20) undergoes transition into (18). The results of computations of the calibration error with use of the last formula are given in Fig. 3a. With $z > 0.5$ the accuracy of such calibration may be inadequate even in the case of coincidence of the center of a resolution element of the remote instrument with the position of the contact instrument sensor.

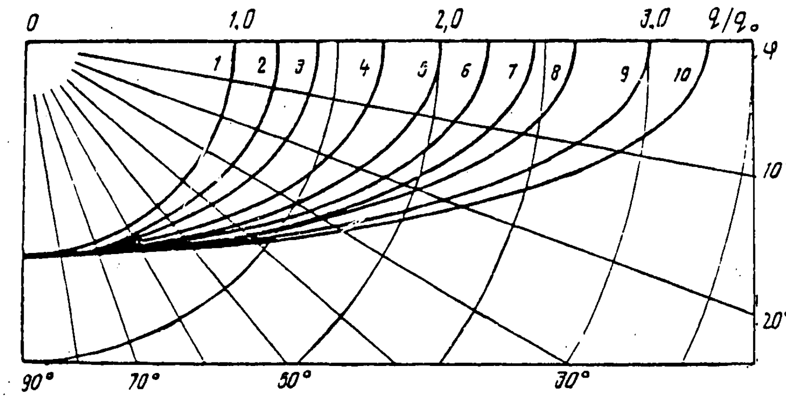

Fig. 2. Form of calibration polygon: 1) $\mathcal{H}$ = 0; 2) $\mathcal{H}$ = 0.5; 3) $\mathcal{H}$ = 1.0; 4) $\mathcal{H}$ = 2.0; 5) $\mathcal{H}$ = 3.0; 6) $\mathcal{H}$ = 4.0; 7) $\mathcal{H}$ = 5.0; 8) $\mathcal{H}$ = 6.0; 9) $\mathcal{H}$ = 8.0; 10) $\mathcal{H}$ = 10.0.

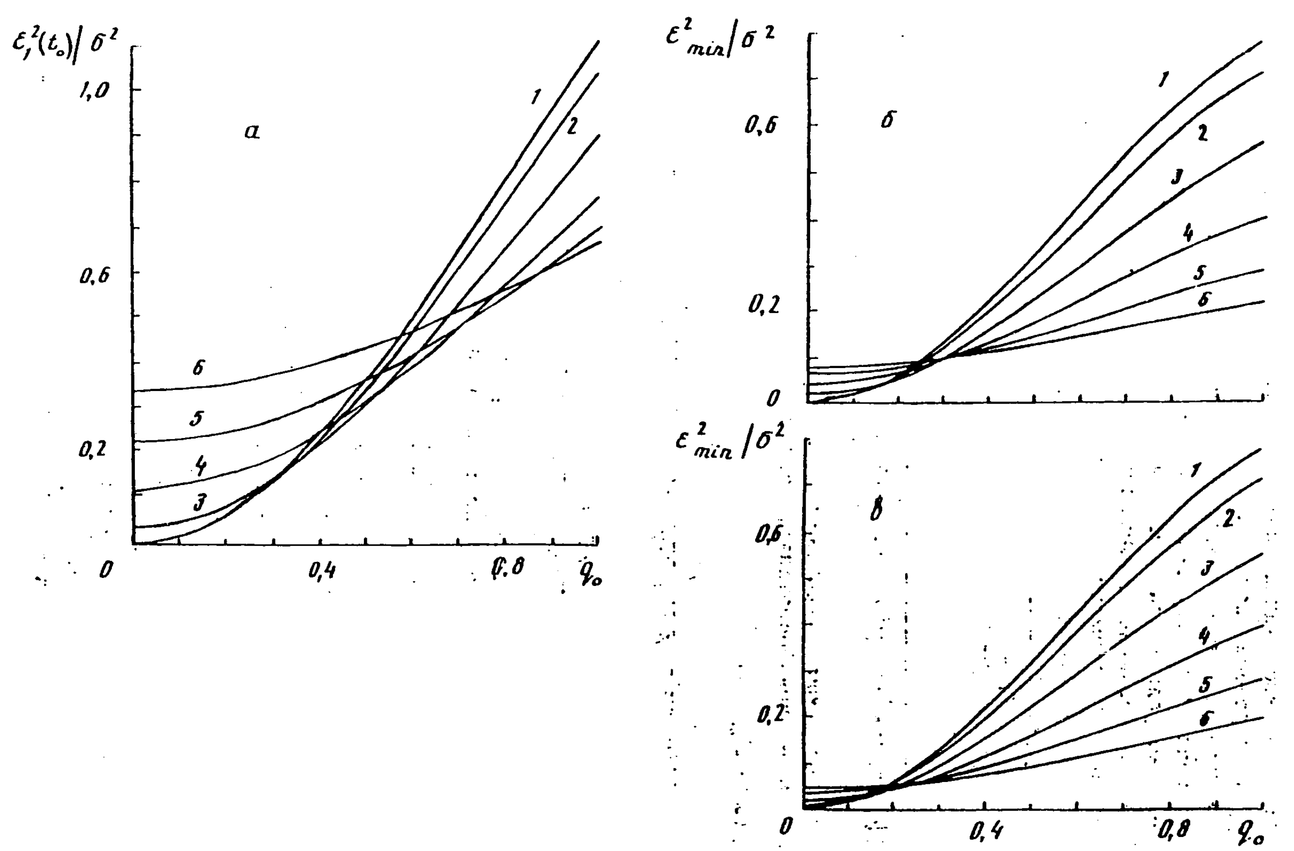

Fig. 3. Calibration error: a) on the basis of one reading obtained at optimum moment in time t_0; b) optimum with q = 0; c) optimum with q = 10. 1) z = 0; 2) z = 0.2; 3) z = 0.4; 4) z = 0.6; 5) z = 0.8; 6) z = 1.0.

The equations for the boundaries of the polygons $q(\varphi)$, corresponding to the condition of a constancy of the calibration error $\varepsilon_1^2(t_0)/\sigma^2$ = const, have the form

$$q = q_0 \sqrt{\frac{1+\varkappa}{1+\varkappa \sin^2\varphi}}, \qquad (21)$$

where $\varkappa = \eta^2/(1 + Z^2)$; q_0 is the radius of a polygon ensuring the same calibration accuracy with t = 0. In Cartesian coordinates they are written as

$$x^2 + (1+\varkappa)\, y^2 = (1+\varkappa)\, q_0^2.$$

Accordingly, the curves (21) have the shape of ellipses with a center at the point 0 (Fig. 1). Their large axes are directed along the $\vec{v}_0$ vector. The ratio of the longer axis of each ellipse to the shorter axis is $\sqrt{1+\varkappa}$. The shorter axis coincides with the radius of the circle limiting the polygon during synchronous calibration (Fig. 2).

The area $S = \sqrt{1+\varkappa}\, S_0$ occupied by such a polygon is greater than the area $S_0 = \pi(q_0 r_x)^2$ of the polygon used in synchronous calibration. The $\varkappa$ parameter is greater in value the larger the "frozen-in" field. The area of the polygon suitable for the calibration of remote instruments increases with an increase in the "frozen-in" character of the measured physical field. This increase is attributable to an elongation of the polygon along the direction of the velocity of field transfer both in the direction of transfer and in the opposite direction with retention of a constant width of the polygon.

Now we will proceed to study of optimum calibration. We will select such a coordinate system that the direction of the x-axis will coincide with the direction of velocity $\vec{v}_0$. In accordance with Fig. 1 formula (10) can be written in the form

[ОПТ = opt]

$$\tilde{u}_{\text{опт}}(\omega) = \frac{\sqrt{1+\eta^2}}{G_1\left(\frac{1}{\sqrt{1+\eta^2}}\,\frac{\omega}{v_c}\right)} \times$$

$$\times \iint\limits_{-\infty}^{\infty} G_3\left[\sqrt{\left(\frac{\omega}{v_c}\right)^2 + \alpha_2^2 + (1+\eta^2)\alpha_1^2 + 2\frac{\omega}{v_c}\eta\alpha_1}\right] \tilde{h}^*(\alpha_1,\alpha_2)\, e^{-j\rho_0(\alpha_1\cos\varphi - \alpha_2\sin\varphi)}\, d\alpha_1 d\alpha_2$$

Substituting here the expressions (15), (16) and carrying out the corresponding transforms, we obtain

$$\tilde{u}_{\text{opt}}(\omega) = \tilde{u}_{\text{opt}}(0) \times \exp\left[-\frac{r_x^2}{\pi}\,\frac{\eta^2 Z^2}{(1+\eta^2)(1+\eta^2+Z^2)}\left(\frac{\omega}{v_c}\right)^2 + j\,\frac{\eta\rho_0}{1+\eta^2+Z^2}\left(\frac{\omega}{v_c}\right)\cos\varphi\right], \qquad (22)$$

where

$$\tilde{u}_{\text{опт}}(0) = \sqrt{\frac{1+\eta^2}{(1+Z^2)(1+\eta^2+Z^2)}}\, \exp\left[-\frac{\pi}{4}\,\frac{1+Z^2+\eta^2\sin^2\varphi}{(1+Z^2)(1+Z^2+\eta^2)}\, q^2\right].$$

Carrying out the transform (11), we find that the optimum weighting function also has a bell-like shape

$$u_{\text{opt}}(\tau) = u_{max} \exp\left[-\frac{\pi(1+\eta^2)(1+\eta^2+Z^2)\, v_c^2}{4 r_x^2\, \eta^2 Z^2}(\tau - t_0)^2\right], \qquad (23)$$

the position of its maximum t_0 is given by formula (19). Its maximum value is

$$u_{max} = \frac{V_c(1+\eta^2)}{2\eta^2\sqrt{1+z^2}\,r_1} \exp\left[-\frac{\pi}{4}\,\frac{1+z^2+\eta^2\sin^2\varphi}{(1+z^2)(1+z^2+\eta^2)}\,q^2\right].$$

Accordingly, in the considered case in the case of optimum calibration the averaging of the signal (2) at the output of the contact instrument must be accomplished with the weighting function (23).

We will find the magnitude of the error in optimum calibration. Substituting expressions (15), (16) and (22) into (14), we obtain

$$\frac{\varepsilon^2_{min}}{\sigma^2} = \frac{1}{1+2z^2} - \frac{1+\eta^2}{1+z^2}\left[(1+z^2)^2(1+\eta^2)^2-\eta^4 z^4\right]^{-1/2} \times \exp\left[-\frac{\pi q^2}{2(1+z^2)}\cdot\frac{1+z^2+\eta^2\sin^2\varphi}{1+z^2+\eta^2}\right]. \quad (24)$$

A comparison of this expression with formula (20) shows that the curves $q(\varphi)$ corresponding to the condition of a constancy of the calibration error $\varepsilon^2_{min}/\sigma^2$ = const are given by the same equation (21) as for very simple calibration at the optimum moment in time t_0. Accordingly, in these cases the form of the polygon has an identical form. However, with a stipulated ε^2 value the absolute dimensions of these polygons will be different, since the dependences of $\varepsilon_1^2(t_0)$ and ε^2_{min} on q, found in formulas (20) and (24), are different. The families of $\varepsilon^2_{min}(q_0)/\sigma^2$ curves for different η and z values are given in Fig. 3,b,c, from which it follows that the ε^2_{min} value with finite z and identical q_0 is substantially less than the $\varepsilon_1^2(t_0)$ value, especially for more "frozen-in" fields.

Optimum calibration is desirable in the case of large flight altitudes. In this case calibration on the basis of one reading in general cannot ensure the required accuracy. In this case it is necessary to select for the polygons those ocean areas for which the investigated field to the highest degree satisfies the "frozen-in" condition. Since the polygons are elongated along the mean direction of field transfer, their position in the ocean must be selected in such a way that the probability of intersection of the trajectories of motion of the remote instrument with the polygon will be maximum. It follows from the preceding computations that the velocity of transfer of the physical field in the polygon must be orthogonal to the velocity of instrument movement.

BIBLIOGRAPHY

1. Dotsenko, S. V. and Salivon, L. G., "Optimum Calibration of Remote Instruments Using Time Averaging," MORSKIYE GIDROFIZICHESKIYE ISSLEDOVANIYA (Sea Hydrophysical Investigations), No 4, Sevastopol', pp 92-99, 1978.

2. Dotsenko, S. V., TEORETICHESKIYE OSNOVY IZMERENIYA FIZICHESKIKH POLEY OKEANA (Theoretical Principles of Measurement of Physical Fields in the Ocean), Leningrad, Gidrometeoizdat, 1974, 152 pages.

3. El'sgol'ts, L. E., VARIATSIONNOYE ISCHISLENIYE (Variational Calculus), Moscow, GITTL, 1958, 162 pages.

4. Dotsenko, S. V., "Mathematical Description of Random Scalar Anisotropic Fields," MORSKIYE GIDROFIZICHESKIYE ISSLEDOVANIYA, No 1, Sevastopol', pp 100-123, 1971.

5. Dotsenko, S. V., "Spectra of Random Scalar Anisotropic Hydrophysical Fields," MORSKIYE GIDROFIZICHESKIYE ISSLEDOVANIYA, No 3, Sevastopol', pp 65-82, 1971.

CHOICE OF SOME DESIGN PARAMETERS OF A SATELLITE DATA SYSTEM FOR REMOTE SOUNDING OF THE OCEAN

Sevastopol' SPUTNIKOVAYA GIDROFIZIKA in Russian 1980 pp 97-104

[Article by S. S. Kavelin]

[Text]

Abstract: The article discusses some parameters determining the output characteristics of the system: mean information content, readiness factor, efficiency factor and reliability of elements. The correct choice and allowance for the considered parameters in the stage of designing of satellite data systems for remote sounding of the ocean will make it possible to attain a definite efficiency.

The experience of use of experimental space vehicles ("Cosmos-1076," "Seasat," "Meteor," NOAA) has indicated the possibility of use of space vehicles as carriers of special measurement apparatus for remote sounding of the ocean in an adequately wide spectral range. The gradual complication of tasks, with transition from construction of the diagnostic fields of physical parameters to prognostic fields, will make it possible to proceed to solution of major fundamental problems of physics of the ocean and practical problems in oceanography in the interests of the national economy.

The solution of this problem is related primarily to the development of research apparatus of the necessary resolution and measurement accuracy, with the choice of a complex of instruments, with the development of methods for collecting and interpreting information, and a number of others. On the other hand, the successful solution of the formulated problems is unthinkable without improvements in space technology.

As noted in [2], the most important characteristics of space oceanographic information, determining its quality and effectiveness of employment by users, are the makeup of the measured oceanographic parameters and the accuracy in their determination, the accuracy of tie-in of the collected data to the terrain, resolution at the surface, periodicity in revision of information, routineness in the delivery of data to users, possibility of continuous or periodic global scanning of the surface of the world ocean. Assurance of these parameters predetermines the choice of the on-board measurement instruments and corresponding space vehicle service (support) systems and also the choice of the principal system parameters because the solution of different problems in this global remote sensing of the ocean with the necessary time periodicity is unthinkable when making use only of individual space vehicles. A problem of interest in this connection is the choice of the parameters of a space system for the remote sounding of the ocean because its solution predetermines the effectiveness of use of space vehicles for this purpose.

A satellite system for remote sounding of the ocean can be put into the most numerous class of space systems -- satellite data systems (ISS). With complication of the problems to be solved using these systems there will be an increase in the requirements both on individual elements (space vehicles, carrier rockets, etc.) and on the system as a whole. The development of such systems is a multistage process with characteristic technical and organizational measures. Designing as a stage in the development of a space system has a number of substages which include both functional-structural problems and the designing of the elements of the system as physical units, in particular, the designing of one of the most important elements of the system -- the space vehicle. The rapid development and complication of the ISS and the introduction of automation leads to the necessity for a quantitative analysis of their functioning from the point of view of optimum organization of their structure and control processes. This also relates to the choice of the principal design parameters for an oceanographic ISS (ISS -- informatsionnaya sputnikovaya sistema).

The existence of several partially contradictory tasks imposed on the system, the great number of structural components, their diversity, the complexity of their interrelationships in the functioning process and the presence of a whole series of factors of different physical nature which must be taken into account in the designing of the system, to which quite limited times are allocated, all this requires the optimization of the design parameters of the system with respect to definite criteria.

We will call the totality of jointly functioning technical apparatuses intended for solving the tasks of collection and transmission of oceanographic information with the use of several simultaneously functioning space vehicles a "satellite data system."

Such an ISS consists of a large number of diverse, interrelated elements interacting with one another in the functioning process. The overall result of operation of the system is determined by the result of performance of functions by all its elements, including all the space vehicles included in the system.

A block diagram of such a system is shown in Fig. 1. Its elements are the space vehicle system, launching complex, complex for placement in orbit, complex for the reception, processing and distribution of information, network of underwater (surface) data sensors, system control center and measurement complex.

We will examine some parameters determining the system output characteristics.

1. Mean Information Content

In the course of functioning of an ISS for remote sounding of the ocean the system can be in different states determined by the number of working elements of the system and the place in its structure. Each state is characterized by a definite information content (data yield) of the system. We will assume that the set of all possible states of the system is a finite set G:

$$G = \{q_\nu\}_{\nu=1,2,\ldots,N_G}, \tag{1.1}$$

where q_ν is an element of G; N_G is the total number of possible states of the system.

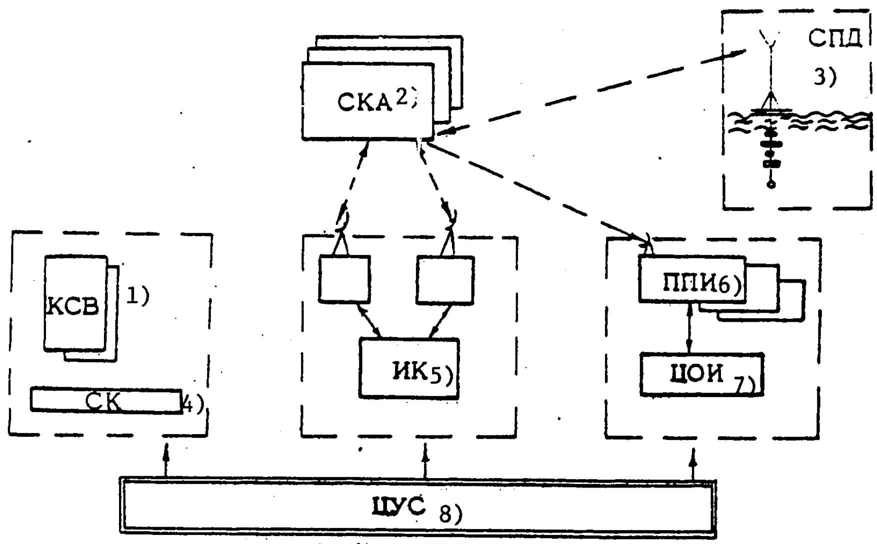

Fig. 1. Block diagram of system.

KEY:
1) complex for placement in orbit
2) space vehicle system
3) network of underwater (surface) data sensors
4) launching complex
5) measurement complex
6) complex for the reception, processing and distribution of information
7) data processing center
8) system control center

Assume that $\beta_\nu(t)$ is a function characterizing the state of the system, where ν is the sequence number of the state.

$$\beta_\nu(t) = \begin{cases} 1, \text{ if the system at a particular moment } t \text{ is} \\ \text{precisely in the } \nu\text{-th state,} \\ 0, \text{ in the opposite case.} \end{cases}$$

Each state of the system unambiguously corresponds to a definite value of the relative information content h_ν of the system.

Under the condition that the system functioning regime is stationary and has an ergodic property, the mean information content is found using the formula

$$J_{mean} = \lim_{T\to\infty} \frac{1}{T} \int_0^T \sum_{\nu=1}^{N_G} h_\nu \cdot \beta_\nu(t)\, dt. \tag{1.2}$$

where $0 \leqslant h_\nu \leqslant 1.0$. The statistical evaluation of this information content is

$$J^*_{mean} = \frac{1}{T} \sum_{\ell=1}^{\alpha(t)} \tau_\ell \sum_{\nu=1}^{N_G} h_\nu \beta_{\nu\ell}, \tag{1.3}$$

where $\beta_{\nu\ell}$ is a criterion characterizing the state of the system in the ℓ-th time interval τ_ℓ; τ_ℓ is the duration of the ℓ-th time interval between two successive changes in the state of the system; $\alpha(t)$ is the number of changes in the state of the system during the time T. For sufficiently large T we obtain

$$J_{mean} = \sum_{\nu=1}^{N_G} h_\nu \rho_\nu, \tag{1.4}$$

where

$$\rho_\nu = \lim_{T\to\infty} \frac{1}{T} \int_0^T \beta_\nu(t)\, dt$$

and has the sense of the probability of presence of the system in the ν-th state at an arbitrary moment in time.

2. System Readiness Factor

This is one of the principal indices of the system, which is defined as the probability that the system at an arbitrary moment in time is in one of the states satisfying the requirements imposed on it and characterizes the reliability of the satellite system. If $G = \{q_\nu\}_{\nu = 1,2,3,\ldots, N_G}$ is the total set of states of the system, $A \subset G$ is the subset of states being in which the system satisfies the requirements imposed on it, then

$$SRF = \text{Prob}\left\{ q_\nu(t) \in A \right\}, \tag{2.1}$$

where $q_\nu(t)$ is the state of the system at the time T. Since each state of the system unambiguously corresponds to a definite information content value J_ν, then

$$SRF = \text{Prob}\left\{ J(t) \geqslant J_0 \right\}, \tag{2.2}$$

where J_0 is the information content level corresponding to the minimum of all the levels of the set of states A. The statistical readiness factor of the system can be determined as

$$SRF^* = \frac{1}{T} \sum_{\nu=1}^{\beta(t)} \tau_\nu,$$

where τ_ν is the duration of the ν-th stage in the process of functioning of the system in which it satisfies the requirements imposed on it; β_ν is the number of intervals τ_ν during the time T of system functioning.

3. System Efficiency Index

In the designing process the need arises for a final evaluation of the correspondence between the selected variant of the system to those problems for whose solution it is intended. The system efficiency index is introduced for evaluating the efficiency of a particular variant. It is a functional of the principal technical (operational) and economic indices of the system. The determination of the efficiency index of a complex system is one of the most difficult tasks in systems analysis, on whose solution is dependent not only the result of the investigations, but also the employed method. Since any system is an element of a higher level, that is, represents an element of a complex hierarchical structure, as the efficiency index based on such an approach it is possible to use the expression

$$W_i = \frac{W_{i+1} - W^*_{i+1}}{W_{i+1}}, \quad 0 \leq W_i \leq 1{,}0, \tag{3.1}$$

where W_i is the efficiency of the considered system $W_i \geq 0$; W_{i+1} is the efficiency of the system for the next level in the hierarchy, which includes the considered system; W^*_{i+1} is the efficiency of the system of the next hierarchical level under the condition of the absence of the considered system in it.

A shortcoming of such an approach, in addition to its complexity, is the difficulty in determining the efficiency of the system of the next $(i+1)$-st hierarchical level and the small response of this index to a change in structure of the system and the technical characteristics of the elements of lower levels. On the other hand, the principal index of an ISS for remote sounding of the ocean is its mean information productivity J_{mean}.

The satellite system will be the more efficient the higher its mean information content and the lesser the expenditures $C_\Sigma(J_{mean}, \Delta T)$ on collecting this information. The value

$$\Delta = \frac{C_\Sigma(J_{mean}, \Delta T)}{J_{mean}},$$

determining the price of a unit of information supplied by the system cannot, however, fully serve as an index of system efficiency because for the user it is important to know both the price of the information and its volume. Since the efficiency of the system is characterized by its information content and the price of a unit of this information, as an index of system efficiency it is possible to use the expression

$$W = \frac{J_{mean}}{\Delta} = \frac{J^2_{mean}}{C_\Sigma(J_{mean}, \Delta T)}, \tag{3.2}$$

where Δ is the price of the information.

4. Reliability of System Elements

One of the principal factors unconditionally determining the operational and economic characteristics of an ISS for remote sounding of the ocean is the reliability of its elements. An increase in the reliability of any element of

ISS structure (space vehicle, data reception stations, etc.) as a rule constitutes a complex scientific and technical problem whose solution involves an expenditure of time and money.

The influence of a low reliability of system elements on its information content and reliability indices can be compensated by the introduction of an excess into its structure at all levels, but this operation results in increased cost and complication of the system. Thus, the problem arises, customary in the investigation of operations, of seeking a compromise between the operational efficiency of a system (in this case its information content) and its cost.

One of the principal elements of an ISS is the space vehicle, whose operational characteristics to a considerable degree determine the appearance of the ISS as a whole.

The most important characteristic of a space vehicle is its reliability. The principal index of reliability of a space vehicle entering into the ISS for remote sounding of the ocean can be assumed to be the mean time of its active existence τ_{ac}, which is determined as the duration of use of the space vehicle for a definite purpose as part of the ISS. As a result of the appearance of different random factors (failure of space vehicle elements in the course of functioning, consumption of supplies of on-board power, etc.) the duration of use of the space vehicle within the system is a random parameter, whose most complete numerical characteristic is its mathematical expectation

$$T_{ac} = M[\tau_{ac}].$$

An ISS is characterized by the fact that as a result of failure of one or even several space vehicles the system does not completely break down, but only experiences a decrease in its information yield.

Since the space vehicle is the principal element of the ISS and its reliability characteristics directly determine system efficiency, at the present time the task of increasing the time of existence is extremely timely.

An increase in space vehicle reliability requires considerable expenditures and these expenditures usually increase more rapidly than reliability increases. Accordingly, an increase in space vehicle reliability above a definite limit without increasing the information yield of the system significantly can sharply increase its cost and accordingly decrease the efficiency of the system as a whole. Accordingly, validation of the requirements on reliability of one of its most impo tant elements, the space vehicle, is an extremely timely important problem.

The value of the mean information content J_{mean} is a function of T_{ac}

$$J_{mean} = J_{mean}\ (T_{ac}).$$

If the mean information content of the system J^{Req}_{mean}, $0 \leqslant J^{Req}_{mean} \leqslant 1.0$ is determined in advance (stipulated), but the cost requirements have not been formulated, the T^{Req}_{ac} value is determined from the expression

$$J_{mean}^{Req} = J_{mean}\ (T_{ac}) \qquad (4.1)$$

The expenditures on the system are determined from the expression

$$C_0 = C_0\ (T_{ac}^{Req}). \qquad (4.2)$$

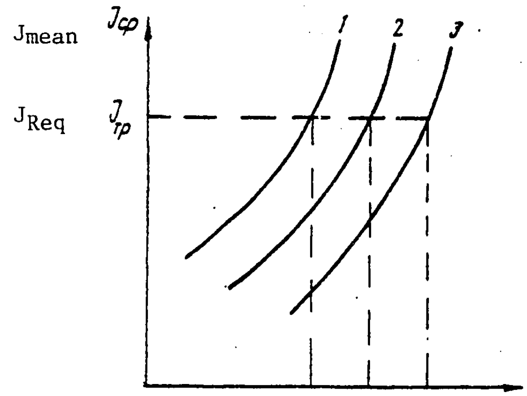

Fig. 2.

In this case the T_{ac} characteristics for different variants of the system and the informational characteristics of the on-board measurement apparatus of a space vehicle can be given in the form of the dependences represented in Fig. 2. In another case, if it is possible to formulate in advance the requirements on the mean information content of the system J_{mean}^{Req} and its cost C_0^{Req}, the requirement on the reliability of the space vehicle in this case is determined as

$$T_{ac}^{Req} = \max \left\{ T_{ac}^{Req'},\ T_{ac}^{Req''} \right\} \qquad (4.3)$$

where $T_{ac}^{Req'}$ was determined from $J_{mean}^{Req} = J_{mean}\ (T_{ac})$, $T_{ac}^{Req''}$ was determined from $C_0^{Req} = C_0^{c}\ (T_{ac}^{Req})$ under the condition that both indices J_{mean}^{Req} and C_0^{Req} are dependent on the very same parameters of the system and are contradictory in the sense that assurance of one of them does not mandatorily ensure the other.

If the requirements on the information content and cost are not stipulated in the stage of designing of a satellite system and the problem involves formulating them, the determination of the most desirable relationship between the mean information productivity of the system J_{mean} and its cost C_0 with stipulated limitations constitutes the problem of optimization of a satellite data system with respect to several (in this case two) indices. The problem is substantially simplified if it is possible to form an index determined as a functional for the J_{mean} and C_0, $W = W(J_{mean}, C_0)$ indices. Since J_{mean} and C_0 are dependent on space vehicle reliability, it is possible to obtain a functional dependence $W = W\ (T_{ac})$.

As the efficiency index $W\ (T_{ac})$ in this case it is desirable to use an index relating the mean information content of the system J_{mean} and the cost of an information unit $\Delta = C_0/J_{mean}$ by the expression

$$W\ (T_{ac}) = J_{mean}\ (T_{ac})/\Delta\ (T_{ac}). \qquad (4.4)$$

The function $J_{mean}\ (T_{ac})$ increases monotonically with an increase in T_{ac}, approaching some J^{max}_{mean} value. If the dependence $C_0(T_{ac})$ decreases monotonically, the $W\ (T_{ac})$ function will increase monotonically with the asymptote W^{max}

$$W^{max} = J_{mean}{}^2\ (max)/C_0\ (T_{ac} \rightarrow \infty\ ) = J_{mean}{}^2/C_0{}^*, \qquad (4.5)$$

where $C_0{}^*$ are the expenditures on a system with an ideal reliability of the space vehicle.

However, due to the fact that an increase in T_{ac} involves an increase in the weight and cost of the space vehicle, the system cost function $C_0\ (T_{ac})$ has an inflection in the region of practical T_{ac} values. As a result, the $W\ (T_{ac})$ function also has a minimum, which means an increase in the reliability of the space vehicle above some T^{Req}_{ac} value without substantially increasing the information content of this system; there is a marked increase in its cost, and accordingly, a decrease in its efficiency.

Thus, the proper choice and allowance for the parameters considered above in the stage of designing of a satellite data system for remote sensing of the ocean will make it possible to achieve a definite level of its efficiency.

BIBLIOGRAPHY

1. Nelepo, B. A. and Timchenko, I. Ye., SISTEMNYYE PRINTSIPY ANALIZA NABLYUDENIY V OKEANE (Systemic Principles for Analysis of Observations in the Ocean), Kiev, "Naukova Dumka," 1978, 222 pages.

2. Nelepo, B. A., Khmyrov, B. Ye., Terekhin, Yu. V., et al., PROBLEMY, VOZMOZHNOSTI I PERSPEKTIVY KOSMICHESKOY OKEANOGRAFII (Problems, Possibilities and Prospects of Space Oceanography), Preprint No 4, Sevastopol', Izd. MGI AN Ukrainskoy SSR, 1979, 52 pages.

PROBLEMS IN THE QUANTITATIVE DISTINGUISHABILITY OF HYDROMETEOROLOGICAL SITUATIONS

Sevastopol' SPUTNIKOVAYA GIDROFIZIKA in Russian 1980 pp 105-112

[Article by B. Ye. Khmyrov]

[Text]

Abstract: Special problems in the development of a theory of quantitative distinguishability of hydrometeorological situations are examined on the basis of a generalization of the existing theory of information. The fundamental principles of the theory of distinguishability are examined applicable to a case when the hydrophysical parameters of the "ocean-atmosphere" system are discrete functions of a denumerable set of states of the modeling physical system.

The modern development of space oceanography already in the not distant future will make it possible to plan the systematic and quite routine operational determination of the hydrophysical characteristics of the world ocean. These data will be used in solution of both fundamental scientific and practical problems in oceanography. However, for the further development of methods for remote sounding it is desirable to create a theory making it possible to evaluate the quantitative characteristics of informational relationships in both the "ocean-atmosphere" system and in the "ocean-observer" system [1]. Among the leading problems requiring development of such a theory we should mention the problems of choosing (planning) the characteristics of systems for remote sensing and identification of hydrometeorological situations in the ocean-atmosphere system as multidimensional images with respect to which existing theories do not give satisfactory results. As the meteorological basis of this theory it is possible to use the presently contemplated approach to the concept of information as the characteristics of the difference in physical phenomena [2].

In this article we examine the possibility of development of such a theory applicable to a case when as a model of the "ocean-atmosphere" system it is possible to use a physical system whose number of states is denumerable and they are not dependent on time and change only under the influence of a complex of external factors. Such a physical system is an idealized model of behavior of the "ocean-atmosphere" system in a limited region of the ocean.

We will assume that the states of the investigated physical system can be characterized both qualitatively and quantitatively either on the basis of individual physical characteristics -- criteria or on the basis of their totality. A knowledge of such a characteristic makes it possible to compare, and accordingly differentiate states only with the introduction of a unit of measurement and the scale of change of this parameter. As such a characteristic it seems desirable to use a limited, normalized measure, henceforth called the significance of state.

We will examine the possible axiomatics of the significance measure. Assuming the set of elementary states of the physical system Ω to be not greater than the denumerable set, we introduce the significance of state measure relative to the selected criterion $\nu(B_i)$ in the algebra of events R and we will require that it satisfy the following conditions:

$$\nu(\Omega) = 1, \quad \nu(\emptyset) = 0, \quad \nu\sum_{1}^{\infty} B_i = \sum_{1}^{\infty} \nu(B_i) \quad \text{with} \quad B_i \cap B_{i+1} = \emptyset. \tag{1}$$

We will establish a correspondence of the number x, the value of the physical criterion j, to each element of the space Ω. This is adequate for constructing a mathematical model of the investigated physical system as a variable parameter -- the function of events introduced in linear space with a measure characterizing the physical system with respect to the selected criterion.

As follows from what has been set forth above, the axiomatics [1] coincides with the axiomatics of the probability measure, which thereafter makes it possible to use probability theory. At the same time, the difference between the significance and probability measures lies in their physical essence. By the term "probability" we mean the normalized limiting value of the frequency of appearance of the investigated phenomenon, being only one of the physical criteria of this phenomenon [3]. The significance measure is introduced as a normalized characteristic of the studied phenomenon relative to any of the quantitative physical criteria. As a result, the probability measure is the significance of this phenomenon with respect to the frequency criterion, if such objectively exists. In a more general case we introduce the concept of significance of states with respect to the totality of its criteria. For this purpose we will divide the possible criteria of state into two classes and it will be required that in each of them the following corresponding conditions be satisfied:

a) the significance of state with respect to the totality of the class of criteria with a reciprocally ambiguous representation of the spaces is determined by the product of the measures of these spaces, taking into account the limitations imposed by the criteria on one another in the sequence of their selection.

$$\nu^{\{j\}}(B_i) = \prod_{j} \nu^{j/1,\dots,j-1}(B_i), \quad j \in m, \tag{2}$$

where $\nu^{j/1,\ldots,j-1}$ is the significance of the j criterion, taking into account the limitations imposed on the space x^j by the existence of the criteria $x^{1,\ldots,j-1}$.

For the independent criteria it follows from (2) that

$$\nu^{\{j\}}(B_i) = \prod_j \nu^j(B_i). \quad j \in m: \tag{3}$$

b) the significance of state with respect to the totality of the class of functionally dependent criteria with reciprocally unambiguous representation of spaces is characterized by the significance of any criterion. In the case of a linear dependence of the criteria their reciprocal representation occurs with retention of the measure, as a result of which the significances of state with respect to these criteria are equal and the criteria are indistinguishable

$$\nu^{\{j\}}(B_i) = \nu^j(B_i). \tag{4}$$

Thus, in a general case, when the physical system is characterized by the totality of the criteria, it is regarded as a multidimensional vector-image whose dimensionality is determined by the number of linearly independent criteria.

Proceeding to the characteristic of distinguishability of states, we will make the space $\Re$ normalized using the measure ν as the norm of its elements and we will introduce the simplest metrics into it

$$G(B_i, B_{i+1}) = \| B_i - B_{i+1} \| = | \nu(B_i) - \nu(B_{i+1}) |, \tag{5}$$

making it possible to differentiate its elements on the basis of the distance between them. For practical purposes it is more convenient to employ a logarithmic scale for reading the significance of states of the physical system. For this it is adequate to proceed from discrimination on the basis of the metrics (5) to discrimination on the basis of the difference in the logarithms of the measures; this leads to a characteristic called information and determined by the expression

$$J^{\{j\}}_{B_i - B_{i+1}} = -\log \frac{\nu^{\{j\}}(B_i)}{\nu^{\{j\}}(B_{i+1})}. \tag{6}$$

In essence this parameter is an element of the space of informational characteristics, obtained with representation of pairs of elements in significance space by means of the operator (6); its norm follows from the metrics of this space for the case of comparison with the zero element $J_0^{\{j\}}$

$$\| J^{\{j\}}_{B_i - B_{i+1}} \| = G\left(J^{\{j\}}_{B_{i+1}, B_i}, J_0^{\{j\}}\right) = \left| -\log \frac{\nu^{\{j\}}_{B_i}}{\nu^{\{j\}}_{B_{i+1}}} \right|. \tag{7}$$

As follows from (6), information is a characteristic of the quantitative distinguishability of the states entering into any paired association, as a result of which in the space of informational characteristics there will be as many norms as desired, following from (6). Among all these norms it is desirable to discriminate some as the most important, or standard, among which it is most important to include the characteristic of the difference of this state from the most distinguishable state.

By the term "maximum distinguishable state" we will mean one whose significance is equal to unity, that is, a physical system with one state; from (6) we obtain

$$H^{\{j\}}(B_i) = -\log \nu_i^{\{j\}} . \qquad (8)$$

Since (8) determines the difference between this state and the maximum distinguishable state, this characteristic henceforth is called the special indistinguishability of the state of the physical system.

The averaging of (8) with the use of the ν measure as a weighting function leads to the mean indistinguishability of state

$$H^{\{j\}}(B) = -\sum_{i \in \mathfrak{R}} \nu_i^{\{j\}} \log \nu_i^{\{j\}} . \qquad (9)$$

This characteristic is a generalization of the mean characteristic of uncertainty of state introduced by Shannon in [4] -- entropy; this, as follows from (9), is an informational characteristic of the difference in state with respect to the probability of a reliable event. As a result of this (8) and (9) have all the properties of Shannon entropy, understood in a broader physical sense. By analogy with the classical theory of information we will consider the unit of measurement of these parameters to be the special and mean indistinguishability of the state of a physical system having two equivalent states, as follows from (8) and (9), with a logarithmic base of 2.

We will introduce the concept of the maximum indistinguishable state as an element of the set $\mathfrak{R}$, the mean and special indistinguishability of which are equal. As a result, the elements of the set are distinguishable only qualitatively, whereas for a finite number of states n their significance is equal to 1/n. Comparing such a state with any i^m, from (8) we obtain

$$R^{\{j\}}(B_i) = \log n - H^{\{j\}}(B_i) . \qquad (10)$$

We will call this characteristic the special information content of the physical system, since due to its physical essence it determines the difference between this state and the maximum indistinguishable state. Similarly it is possible to obtain the mean characteristic of information content in the form

$$R^{\{j\}}(B) = \log n - H^{\{j\}}(B) . \qquad (11)$$

These expressions can be rewritten in the form of a dependence determining the constancy of the properties of standard information characteristics

$$H^{\{j\}}(B_i) + R^{\{j\}}(B_i) = const . \qquad (12)$$

$$H^{\{j\}}(B) + R^{\{j\}}(B) = const. \tag{13}$$

We will introduce the integral quantitative characteristic of uniformity of a physical system as the sum of its information contents in individual states

$$S^{\{j\}}(\mathfrak{P}) = \sum_i R^{\{j\}}(B_i) = n \log n - \sum H^{\{j\}}(B_i) . \tag{14}$$

The second term of expression (14) also has a very definite physical sense and can be interpreted as the diversity of the physical system

$$T^{\{j\}}(\mathfrak{P}) = \sum_i H^{\{j\}}(B_i). \tag{15}$$

As a result, (14) can be rewritten in the form of a law of constancy of the properties of these information characteristics

$$S^{\{j\}}(\mathfrak{P}) + T^{\{j\}}(\mathfrak{P}) = const . \tag{16}$$

The material considered above shows that both the indistinguishability and information content of states of the physical system are equally valid information characteristics, as a result of which an informational description of a physical system can be made using any of them. In this connection we will discuss some properties of the characteristics and the corollaries following from them.

It follows from (3), (8), (10) that with the discrimination of the states of the physical system on the basis of the totality of independent criteria the indistinguishability and information content of the state according to individual criteria are additive

$$H^{\{j\}}(B_i) = \sum_j H^j(B_i) , \tag{17}$$

$$R^{\{j\}}(B_i) = \sum_j R^j(B_i) . \tag{18}$$

By virtue of the positiveness of (8) the special indistinguishability of state always increases, whereas the special information content can change arbitrarily as a result of the sign-variability of (10).

It follows from (4), (8), (10) that with discrimination of the states of a physical system on the basis of the totality of linearly dependent criteria the special indistinguishability and information content of the state remain constant

$$H^{\{j\}}(B_i) = H^j(B_i) , \tag{19}$$

$$R^{\{j\}}(B_i) = R^j(B_i) . \tag{20}$$

The totality of the independent criteria can have the property of asymptotic stability of the special and mean indistinguishability and information content, by which, by analogy with [5], we mean satisfaction of the conditions

$$\frac{H^{\{j\}}(B_i)}{H^{\{j\}}(B)} \to 1 \quad \text{with} \quad m \to \infty , \tag{21}$$

$$R^{\{j\}}(B_i) \to 0, \quad R^{\{j\}}(B) \to 0 \quad \text{with} \quad m \to \infty . \tag{22}$$

A result of this is an asymptotic tendency of the information to zero (6), as a result of which the states of the physical system become the most indistinguishable.

Thus, the use of the measure of both independent and linearly dependent criteria does not lead to an improvement in the discrimination of states in comparison with discrimination on the basis of a single criterion. In a general case the presence of the totality of criteria of state makes it possible to select the most informative in accordance with (6). In the special case of the totality of linearly dependent criteria this possibility does not exist. However, the totalities of criteria are used extensively and successfully in practical work for improving the discrimination and identification of images and this assertion will not contradict the conclusions drawn above if one adopts as axioms the possibility of introducing the functions of totalities of criteria which can be used for the purposes of discriminating images. The set of such functions giving rise to a corresponding set of distinguishability models evidently is limited only by their physical sense and practical feasibility. In this article we limit ourselves to an investigation of only one such case -- a model of the distinguishability of states on the basis of a functional of criteria. In a general case of such distinguishability the significance of the state of a physical system can be introduced as a normalized semilinear functional

$$\nu^{\{j\}}(B_i) = \frac{\prod\limits_j \nu^j(B_i)}{\sum\limits_{i\in\Omega} \prod \nu^j(B_i)} , \tag{23}$$

corresponding to the axiomatics (1) and making it possible to introduce the norm of distinguishability of states (7) in the form

$$\left\| J^{\{j\}}_{B_i, B_{i+1}} \right\| = \left| \log \frac{\prod \nu^j(B_i)}{\prod\limits_j \nu^j(B_{i+1})} \right| = \left| \sum_j J^j_{B_i, B_{i+1}} \right| . \tag{24}$$

It follows from (24) that the distinguishability of states on the basis of the functional of criteria is always equal to the sum of distinguishabilities on the basis of individual criteria. In the case of nondependence or stochastic dependence of criteria, then those special operators standing under the sum sign, in a general case are sign-variable, as a result of which with adherence to (21) the norm (24) asymptotically tends to zero. This confirms the conclusion drawn above that it is desirable to use the totality of such criteria.

In the presence of a functional dependence of the criteria it is possible to choose criteria ensuring satisfaction of the inequality

$$\left\| J^{\{j\}}_{B_i\,,\,B_{i+1}} \right\| > \left| J^{j}_{B_i\,\cdot\,B_{i+1}} \right| , \tag{25}$$

that is, the change in the norms of the space of informational characteristics in the direction of an improvement in distinguishability. In this case it is desirable that the choice be guided by considerations of noncontradiction and specific information content of the criteria. We will consider the criteria to be noncontradictory if in a physical system with indices of state which are ordered and arranged in an increasing sequence with a transition from the state i to the state i + 1 the information (6) has one and the same sign for each of the criteria. The concept of specific information content of the criterion can be introduced as the normalized distinguishability parameter, introduced by the criterion into the general norm (24). As a result, the principles of choice of the functionally dependent criteria, improving the distinguishability of states of the physical system, applicable to the considered model, are reduced to the use for these purposes of the totality of the noncontradictory criteria, the specific information content of which has the same order of magnitude. In the theory of image recognition the problem of the choice of criteria ensuring the best recognition is yet to be solved. This is only natural since such a choice must be made on the basis of the physical essence of the considered phenomenon. The merit of the considered method specifically is that here the decisive role of the physical aspect can be seen more clearly than in the statistical-stochastic approach.

The materials cited above can be considered only as the general principles of the quantitative theory of distinguishability applicable to the investigated model of a physical system. Its application to the specific tasks of space oceanography can be useful not only for the recognition of hydrometeorological situations, but also for a quantitative characteristic of the process of remote measurements because the problem of ensuring reliable measurements is first and foremost the problem of ensuring an admissible difference between the investigated physical phenomenon and the observation result.

BIBLIOGRAPHY

1. Nelepo, B. A., Khmyrov, B. Ye., Terekhin, Yu. V., Kavelin, S. S., Korotayev, G. K., Vdovichenko, I. A., Kosnyrev, V. K., Bushuyev, Ye. I. and Tolkachenko, G. A., PROBLEMY, VOZMOZHNOSTI I PERSPEKTIVY KOSMICHESKOY OKEANOGRAFII (Problems, Possibilities and Prospects of Space Oceanography), Preprint No 4, Sevastopol', Izd. MGI AN Ukrainskoy SSR, 1979, 65 pages.

2. Mazur, M., KACHESTVENNAYA TEORIYA INFORMATSII (Qualitative Theory of Information), Moscow, "Mir," 1974, 125 pages.

3. Mizes, R., VEROYATNOST' I STATISTIKA (Probability and Statistics), Moscow-Leningrad, Gosizdat, 1930, 84 pages.

4. Shannon, C., RABOTY PO TEORII INFORMATSII I KIBERNETIKE (Studies in the Theory of Information and Cybernetics), Moscow, IL, 1963, 141 pages.

5. Stratonovich, R. L., TEORIYA INFORMATSII (Theory of Information), Moscow, "Sov. Radio," 1975, 63 pages.

QUANTITATIVE CHARACTERISTICS OF DISTINGUISHABILITY OF A PHYSICAL SYSTEM WITH CONTINUOUS STATES

Sevastopol' SPUTNIKOVAYA GIDROFIZIKA in Russian 1980 pp 113-119

[Article by B. Ye. Khmyrov]

[Text]

Abstract: The fundamental principles of the theory of quantitative distinguishability of hydrometeorological situations of a physical system with continuous states are examined.

In [1] the author examined the fundamental principles of the theory of quantitative distinguishability of hydrometeorological situations applicable to a very simple case when the hydrophysical parameters of the "ocean-atmosphere" system are discrete functions of some denumerable set of states of a modeling physical system. In a more general case as such a model we use a physical system with continuous states whose number is nondenumerable.

In this connection, by analogy with the axiomatics proposed in [1], we introduce the significance measure (in σ-algebra) of elementary states characterized by a linear space (everywhere by the dense set $\mathfrak{R}$) and the conjugate space of the value of the x criterion). At the same time it is possible to introduce a real, continuous on the left function of the value of the x criterion, called the significance distribution function

$$F(x) = \nu\ (-\infty, x). \tag{1}$$

Since the set $\mathfrak{R}$ is everywhere dense, there is a probability density function of significance which we introduce as the Radon-Nikodym derivative of the Lebesgue measure m

$$f(x) = \frac{dF(x)}{dm}, \tag{2}$$

using the property of absolute continuity of these measures in the form of the condition $\nu(B_i) \ll m\ (B_i)$, if

$$m(B_i) = 0 \to \nu\ (B_i) = 0. \tag{3}$$

From which follows an expression for the linear functional for the significance measure

$$\nu(B_i) = \int_{B_i \in \Omega} f(x)\, dm = \int_{B_i \in \Omega} d\nu, \tag{4}$$

showing that in the considered case the elements of significance space, different from zero, are functions of events whose Lebesgue measure is greater than zero. The simplest metrics of this state can be written in the form

$$G(B_i, B_{i+1}) = \left| \int_{B_i \in \Omega} d\nu - \int_{B_{i+1} \in \Omega} d\nu \right|. \tag{5}$$

Since (5) does not make it possible to differentiate elementary states, the Lesbegue measure of which is equal to zero, by analogy with [1] we will convert to the space of informational characteristics, introducing the concept of information as an absolute characteristic of the difference of events in accordance with the significance measure

$$J_{B_i, B_{i+1}} = -\log \frac{\int_{B_i \in \Omega} d\nu}{\int_{B_{i+1} \in \Omega} d\nu}. \tag{6}$$

The modulus (6) determines the information norm as the distance between the element (6) and the zero element of space, as which we use the distance between two equivalent events.

Among the great number of types of information and their norms we will first examine the absolute indistinguishability and absolute information content [1]. In a comparison of any element with the maximum distinguishable element $\nu(B_i) = 1$, from expression (6) we derive an expression for the vector of special indistinguishability and its norm

$$H(B_i) = -\log \int_{B_i \in \Omega} d\nu \tag{7}$$

and its limiting value

$$\lim_{m(B_i) \to 0} H(B_i) = \infty. \tag{8}$$

A similar situation also arises when determining the mean indistinguishability of an elementary state since for nonintersecting events it is determined by the expression

$$H(B) = -\sum_i \int_{B_i \in \Omega} d\nu \cdot \log \int_{B_i \in \Omega} d\nu \tag{9}$$

and its limiting value with $m(B_i) \to 0$ is equal to infinity. With a uniform division of criterial space into equal semi-intervals $\Delta x_i = (a_i, b_i)$ expression (9) can be rewritten in the form

$$H(B) = -\int_{\Omega} |f(x) \log f(x)| dx - \lim_{\Delta x \to 0} \log \Delta x. \tag{10}$$

A similar expression applicable to the probability measure and its probability density function is used extensively in studies in the classical theory of information. In some studies the authors have used only the first part of (10), having a finite value and called reduced entropy. This characteristic is without independent importance because it is dimensional and is an element of the space of informational characteristics. By analogy with [1] we introduce the concept of special information content of state of the physical system

$$R(B_i) = H(B_i)_{max} - H(B_i) = -\log \frac{d\nu_{max}}{d\nu}, \tag{11}$$

where ν_{max} is the value of the measure maximizing the mean indistinguishability of state. With an absolute continuity of the measures $\nu_{max} \ll \nu$ the expression under the logarithm sign is a Radon-Nikodym derivative and (11) determines the difference of these measures for an elementary state. The mean information content of the state follows from (11) with its priority in conformity to the measure

$$R(B) = -\int_{\Omega} \left| \log \frac{d\nu_{max}}{d\nu} \right| d\nu. \tag{12}$$

As follows from (11), (12) the values of these characteristics are finite, this being their essential advantage in comparison with the special and mean indistinguishability. At the same time, the already considered peculiarities of the absolute informational characteristics make difficult their use and make it desirable to proceed to the relative characteristics, determined by analogy with the proposal of C. Shannon [2] in comparison with some standard. In the most general form, applicable to the probability measure, this problem was examined in [3].

We will introduce into the set Ω the auxiliary dimensionless limited measure μ, for which $\mu(\Omega) \geqslant 1$, and we will use it as such a standard. In this case we will assume that with the exception of the normalization property, the axiomatics of the μ measure corresponds to the axiomatics of the $\nu|1|$ measure (1), and with satisfaction of the absolute continuity condition $\nu \ll \mu$ the property of multiplicativity is correct for the totality of criteria relating to a class with an ambiguous representation. We will determine the informational characteristic of the event B_i from (6) as a result of comparison of two functionally dependent criteria -- the ν and μ measures.

$$J_{B_i} = -\log \frac{\int_{B_i \in \Omega} d\nu}{\int_{B_i \in \Omega} d\mu}. \tag{13}$$

Its limiting value follows from (9) with $m(B_i) \to 0$

$$\lim_{m(B_i) \to 0} J_{B_i} = -\log \frac{d\nu}{d\mu} = H(B_i)^*. \tag{14}$$

The expression under the logarithm sign is the Radon-Nikodym derivative of the ν measure relative to the μ measure, as a result of which the following norms of the set Ω are correct:

$$\int_{\Omega} \frac{d\nu}{d\mu}\, d\mu = 1, \tag{15}$$

$$\int_{\Omega} \frac{d\mu}{d\nu}\, d\nu = \mu(\Omega). \tag{16}$$

Expression (14) can be interpreted as the relative special indistinguishability of state, which makes it possible to introduce the similar mean characteristic -- the measure

$$H(\beta)^* = -\int_{\Omega} \left| \log \frac{d\nu}{d\mu} \right| d\nu. \tag{17}$$

The derived expression can be written in the form of the difference of two infinite measures

$$H(\beta)^* = -\int_{\Omega} \left| \log d\nu \right| d\nu + \int_{\Omega} \left| \log d\mu \right| d\nu, \tag{18}$$

as a result of which (17) is a generalized measure. We will examine the important special case (17). If the measure is stipulated by a probability density function in the form

$$\chi(x) = \frac{1}{\ell_x(x)}, \tag{19}$$

the norm of the set Ω for the μ measure

$$\mu(\Omega) = \int_{\Omega} \frac{dx}{\ell_x(x)} \tag{20}$$

determines some dimensionless number which we will call the number of distinguishable states. This concept is equivalent to the concept known in the classical theory of information as the zero of the $\ell_x(x)$ reading -- the interval within whose limits the states of the physical system can be considered indistinguishable, that is, equivalent. Substituting (19) into (17), we obtain the expression

$$H(\beta)^* = -\int_{\Omega} \left| \log f(x)\, \ell_x(x) \right| d\nu, \tag{21}$$

in particular, with $\ell_x(x)$ = const the dependence

$$H(\beta)^* = -\int_{\Omega} \left| \log f(x) \right| d\nu - \log \ell_x, \tag{22}$$

follows from (21), being a generalization of the classical determination by Shannon [2]. With stipulation of the probability density function of the ν and μ measures in a deltalike form

$$f(x) = \sum_i \nu_i\, \delta(x - x_i), \tag{23}$$

$$\chi(x) = \sum_i \delta(x - x_i) \tag{24}$$

expression (17) will describe the mean indistinguishability of a physical system with a denumerable number of states [1] in the classical Shannon form

$$H(B) = -\sum_i \nu_i \log \nu_i . \tag{25}$$

As a result, (17) is really the most general expression determining the mean relative indistinguishability of the state of the physical system; in particular, from this expression it is possible to obtain a generalized interpretation of the norm (6) in the form

$$\left\| J_{e_i, e_{i+1}} \right\| = \left| \log \frac{f(x_i)}{f(x_{i+1})} \cdot \frac{\ell_x(x_{i+1})}{\ell_x(x_i)} \right|, m(B_i) = m(B_{i+1}) = 0. \tag{26}$$

Thus, in the considered case the elementary states of the physical system differ with respect to the significance of the reading zeroes within which they are situated. The relative indistinguishability of the state (14), (17) has virtually all the properties of absolute indistinguishability introduced in [1]. The difference is that (17) is not mandatorily positive. As a result, from (22) it is possible to determine the origin of the reading with which this characteristic becomes equal to zero

$$\ell_x = 2^{-\int_\Omega |f(x) \log f(x)| dx}. \tag{27}$$

We also note the property of extremality (17), which follows from the limitations (15), (16) with the investigation of (17) by the method of indeterminate Lagrange factors in the form of the maximum condition

$$\frac{d\nu}{d\mu} = \frac{1}{\mu(\Omega)}. \tag{28}$$

Similarly it is possible to investigate the special extrema (21) using the μ and ν measures, which leads to the conditions of special maxima

$$f(x)_{max} = \frac{1}{\ell_x(x) \int_\Omega \frac{dx}{\ell_x(x)}}, \tag{29}$$

$$\ell_x(x)_{max} = \frac{1}{f(x) \int_\Omega \frac{dx}{\ell_x(x)}}. \tag{30}$$

However, for practical purposes it is of considerable importance to choose a reading zero making it possible to minimize (22). Such a conditional minimum can be found with the introduction of additional limitations in the form

$$\int_\Omega \ell_x(x)\, d\nu = B \tag{31}$$

$$\int_\Omega \ell_x(x)\, dx = D. \tag{32}$$

In particular, with the satisfaction of (31) the $H(B)^*$ measure has a minimum with satisfaction of the condition

$$\ell_x(x)_{min} = B, \qquad (33)$$

that is, with a constant reading zero equal to its mean weighted value.

Now we will briefly examine other relative informational characteristics of state of the physical system. For this purpose we introduce the concept of special and mean relative information content as the dependences

$$R(B_i)^* = H(B_i)^*_{max} - H(B_i)^*, \qquad (34)$$

$$R(B)^* = H(B)^*_{max} - H(B)^*. \qquad (35)$$

Using the extremum condition (28) and taking (15), (16) into account, we rewrite (34), (35) in the form

$$R^*(B_i) = \log \frac{d\nu}{d\mu_H}, \qquad (36)$$

$$R^*(B) = \int_\Omega \left|\log \frac{d\nu}{d\mu_H}\right| d\nu, \qquad (37)$$

where μ_n is the normalized measure

$$\mu_H(B_i) = \frac{\mu(B_i)}{\mu(\Omega)}. \qquad (38)$$

The results make it possible to obtain from (34), (35) a law of constancy of the sum of the principal informational characteristics

$$R(B_i)^* + H(B_i)^* = \log \mu(\Omega), \qquad (39)$$

$$R(B)^* + H(B)^* = \log \mu(\Omega), \qquad (40)$$

making it possible to consider the relative information content and indistinguishability to be equivalent characteristics of state. In conclusion we will introduce the relative characteristics of diversity and uniformity of the physical system as Radon integrals of the special relative indistinguishability on the basis of the μ measure

$$T(\Omega)^* = -\int_\Omega \left|\log \frac{d\nu}{d\mu}\right| d\mu, \qquad (41)$$

$$S(\Omega)^* = \int_\Omega \left|\log \frac{d\nu}{d\mu_H}\right| d\mu. \qquad (42)$$

Summing (41) and (42), we obtain the characteristic of the property of the constancy of the sum of these parameters in the form of the dependence

$$T(\Omega)^{*} + S(\Omega)^{*} = \mu(\Omega) \log \mu(\Omega) . \qquad (43)$$

Thus, the introduction of the auxiliary limited measure made possible its use as a standard for determining the relative informational characteristics. As the standard for a system with the maximum indistinguishable states use has been made of a system whose mean and special indistinguishability are equal to log $\mu(\Omega)$, that is, a discrete system the significances of whose states are equal to $1/\mu(\Omega)$.

As the standard for a system with the maximum different state use was made of a system whose mean and special indistinguishability are equal to log $\mu(\Omega)_n$, that is, a system with one state. The introduction of these standards made it possible to make the principal informational characteristics finite, which is equivalent to the replacement of the investigated physical system with continuous states by some discrete equivalent. As a result, the materials in this article constitute a further development and generalization of the fundamental principles of the theory of distinguishability considered in [1] applicable to a physical system with a denumerable set of states.

BIBLIOGRAPHY

1. Khmyrov, B. Ye., "Problems in the Quantitative Distinguishability of Hydrometeorological Situations," in this collection of articles, pp 105-112.

2. Shannon, C., RABOTY PO TEORII INFORMATSII I KIBERNETIKE (Studies in the Theory of Information and Cybernetics), Moscow, IL, 1963, 350 pages.

3. Stratonovich, R. L., TEORIYA INFORMATSII (Theory of Information), Moscow, "Sov. Radio," 1975, 250 pages.

PARAMETRIC INVARIANCE OF MULTICHANNEL EXCESS REMOTE MEASUREMENT SYSTEMS

Sevastopol' SPUTNIKOVAYA GIDROFIZIKA in Russian 1980 pp 120-125

[Article by V. A. Gayskiy]

[Text]

Abstract: A method for the processing of data in a system with remote nonlinear, nonstationary measurement channels is examined. It ensures the nondependence of the measurement result on the parameters of channels with definite limitations.

The problem of excluding the influence of the passive parameters of the medium through which a signal is propagated on the measurement result is timely for remote measurement systems.

If a nonlinear nonstationary inertialess link is used as a model of the channel, in a multichannel excess system under definite conditions it is possible to exclude the parameters of the link from the measurement result and identify them.

We will assume that the object of measurement is characterized by the vector of primary physical parameters

$$\bar{X} = \{x_i\}, \quad i = \overline{1, n},$$

forming electromagnetic radiation in a definite spectral range as the measurable signal in the ξ-th channel in accordance with the expression

$$y_\xi = \varphi_\xi(\bar{X}), \tag{1}$$

where $\varphi_\xi(\vec{X})$ is an a priori known function.

For example, the measurable signal y_ξ can be the electromagnetic radiation of the ocean surface in dependence on temperature, waves and the quantity of foam.

We introduce a time argument into expression (1) and for small time increments we write

$$y_\xi(t + \Delta t) = \varphi_\xi[\bar{X}(t)] + \sum_{i=1}^{n} \alpha_{\xi i}(t) \Delta x_i(t), \tag{2}$$

where

$$\alpha_{\xi i} = \frac{\partial \varphi_\xi}{\partial x_i}\Big|_{\bar{X}(t)} \tag{3}$$

are the coefficients of channel response to the measurable parameters x_i at the point $\vec{X}(t)$.

If the signal propagation channel, including the medium and the instrument channel, has a transfer function (TF) which can be approximated with an adequate accuracy by a power-law polynomial

$$Z_\xi = \sum_{j=0}^{m} a_{\xi j}\, y_\xi^j \; , \tag{4}$$

then for the inverse TF, using an unambiguous inversion of the series [1], we can write [2]

$$y_\xi(t) = \sum_{j=0}^{m} B_{\xi j}(t)\, Z_\xi^j(t) \; , \tag{5}$$

where $B_{\xi j}$ are the channel parameters; Z_ξ is the output signal.

Using expressions (2) and (5), for a multichannel system we obtain

$$\sum_{j=0}^{m} B_{\xi j}(t+\Delta t)\, Z_\xi^j(t+\Delta t) - \varphi_\xi\left[\bar{X}(t)\right] - \sum_{i=1}^{n} \alpha_{\xi i}(t)\,\Delta x_i(t) = 0, \; \xi = \overline{1,k}. \tag{6}$$

For the excess system $k \geqslant n + 1$.

In the regime of system calibration the vector of primary parameters is known, for example, on the basis of data from contact measurements. In this case we write

$$\sum_{j=0}^{m} B_{\xi j}(t)\, Z_\xi^j(t) = \varphi_\xi\left[\bar{X}(t)\right], \quad \xi = \overline{1,k} \; . \tag{7}$$

The system (7) contains k equations and $(m + 1)k$ unknown $B_{\xi j}$ parameters of the channels.

Additional equations can be derived when using τ groups of readings at different moments in time $t = \overline{1,\tau}$ on the assumption that during this time the parameters $B_{\xi j}$ remain unchanged. In this case $\tau \geqslant m + 1$ and expression (7) is transformed to the form

$$\sum_{j=0}^{m} B_{\xi j}\, Z_\xi^j(t) = \varphi_\xi\left[\bar{X}(t)\right], \quad \xi = \overline{1,k}, \; t = \overline{1,\tau}. \tag{8}$$

In order that the system (8) have a solution, all $\vec{X}(t)$ for $t = \overline{1,\tau}$ must be different. Accordingly, for calibration work it is necessary to have not less than $\tau = m + 1$ known vectors $\vec{X}$. The solution of system (8) relative to $B_{\xi j}$ makes it possible to identify the channels for some segment of time in which they can be considered stationary.

On the other hand, for a discrete time the calibration regime ensures a tie-in of the origin of readings and the possibility of using the system of equations (6) in the form

$$\sum_{j=0}^{m} B_{\xi j} Z_{\xi}^{j}(t) - \sum_{i=1}^{n} \alpha_{\xi i} \Delta x_i(t) = \varphi_{\xi}[\bar{X}(0)], \quad \xi = \overline{1, k}, \tag{9}$$

where there are n unknown increments $\Delta x(t)$, $(m + 1)k$ unknown parameters $B_{\xi j}$ of the channels (for nonstationary channels) and k equations. We will take τ groups of readings and with

$$\tau \geq \frac{(m+1)k}{k-n}, \quad t = \overline{1, \tau} \tag{10}$$

we obtain the necessary broadening of system (9). The matrix and the column of free terms of system (9) will have the form

$$\left\| \begin{matrix} |Z_1(t)| & & & |\alpha_1| \\ & \ddots & & \vdots \\ & |Z_\xi(t)| & & |\alpha_\xi| \\ & & \ddots & \vdots \\ & & |Z_k(t)| & |\alpha_k| \end{matrix} \right\| \quad \left\| \begin{matrix} |\bar{\varphi}_1| \\ \vdots \\ |\bar{\varphi}_\xi| \\ \vdots \\ |\bar{\varphi}_k| \end{matrix} \right\|, \tag{11}$$

where

$$|Z_\xi(t)| = \left| \begin{matrix} 1Z_1(1) & \dots & Z_1^m(1) \\ \dots & \dots & \dots \\ 1Z_1(t) & \dots & Z_1^m(t) \\ \dots & \dots & \dots \\ 1Z_1(\tau) & \dots & Z_1^m(\tau) \end{matrix} \right|, \tag{12}$$

$$|\alpha_\xi| = \left| \begin{matrix} -\alpha_{\xi 1} \dots -\alpha_{\xi n} & & \\ & -\alpha_{\xi 1} \dots -\alpha_{\xi n} & \\ & & -\alpha_{\xi 1} \dots -\alpha_{\xi n} \end{matrix} \right|, \tag{13}$$

$$|\bar{\varphi}_\xi| = \left| \begin{matrix} \varphi_\xi[\bar{X}(0)] \\ \vdots \\ \varphi_\xi[\bar{X}(0)] \end{matrix} \right|. \tag{14}$$

The number of working cycles τ determines the speed of the system.

In a system with minimum excess $k = n + 1$ and $\tau = (m + 1)k$. With an increase in the number k of channels the maximum speed of the system will tend to $\tau = m + 2$. Accordingly, with a great excess of the channels the gain in speed will not exceed more than the factor k.

The speed of a system has importance in the sense that the parameters $\{B_{\xi i}\}$ and $\{\alpha_{\xi i}\}$ in system (9) should remain constant during the time τ of the working cycles, which we will call the correction time.

Thus, with allowance for τ groups of readings system (9) will contain τk unknowns and equations and also can be solved relative to the increments of the primary physical parameters $\{\Delta x_i\}$ of the object and also relative to the unknown parameters $\{B_{\varepsilon j}\}$ of the channels for a new moment in time.

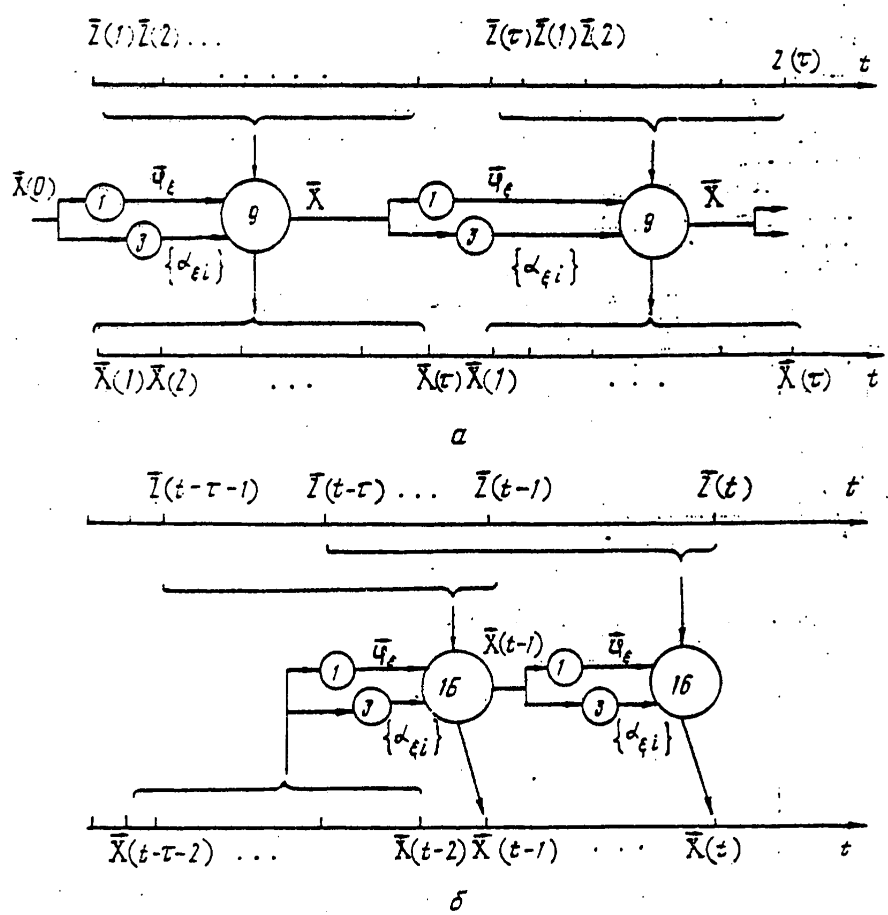

Fig. 1. Diagrams representing data processing in a parametrically invariant system: a) in a regime of accumulation of blocks, b) in a moving regime.

Since the solution of system (9) for $\{\Delta x_i\}$ is not dependent on $\{B_{\varepsilon j}\}$ and vice versa, the system as a whole is parametrically invariant with the above-mentioned limitations.

We will examine the two principal possible operating regimes of the system. The sequence of operations in a regime with accumulation of a block of readings $\overline{Z}$ is shown in the figure (Fig. 1,a). First the values $\{\varphi_\varepsilon[\overrightarrow{X}(0)]\}$ and $\{\alpha_{\varepsilon i}\}$, computed using expressions (1), (8), are introduced in the calibration regime using the known vector $\overrightarrow{X}(0)$. Then in a working regime there is accumulation of a block of τ readings $\overrightarrow{Z}(t)$, $t = \overline{1,\tau}$ of output signals which are used in computing the coefficients Z^j_ε, $j = \overline{0,m}$ of the system (9). Since it is necessary to satisfy the condition

$$Z_\xi(t) \neq Z_\xi(t-1), \quad t = \overline{1,\tau}. \tag{15}$$

so that there will not be identical equations in the system, either the measured parameters $\{x_i\}$ or the parameters of the channels $\{B_{\varepsilon j}\}$ must change in the time correction segment. If these parameters do not change, the values of the measured vector $\vec{X}(t)$ are equal to the values of the calibration vector $\vec{X}(0)$. We will regard as improbable mutually compensating changes $\{x_i\}$ and $\{B_{\varepsilon j}\}$ with which the $\vec{Z}$ vector remains unchanged.

Thus, by virtue of the nonstationarity of the $\{x_i\}$ and $\{B_{\varepsilon j}\}$ parameters the set of τ readings will be a random value.

After obtaining τ groups of readings the system (9) is solved relative to $\{\Delta x_i\}$, using which the value of the vector $\vec{X}(0) \to \vec{X}(\tau)$ is corrected, new values $\varphi_\varepsilon[\bar{X}(\tau)]$, $\varepsilon = \overline{1,k}$ are determined using (1) and the response coefficients $\alpha_{\varepsilon i}$ are determined from (3). Then the correction cycle is multiply repeated.

In the moving correction regime (Fig. 1,b) the block is formed from the current τ readings of the $\vec{Z}(t)$ vector at each discrete moment in time by a shift of one interval to the right.

The system of equations (9) in this case is transformed to the form

$$\left|\sum_{j=0}^{m} b_{\xi j} Z_\xi^j(t-\nu) - \sum_{i=1}^{n} \alpha_{\xi i}(t-\nu-1)\,\Delta x(t) = \varphi_\xi\left[\bar{X}(t-\nu-1)\right],\right. \quad \xi = \overline{1,k}; \quad \nu = \overline{0,\tau}. \tag{16}$$

The matrix and column of free terms in system (16) have the form

$$\left\| \begin{matrix} |Z_1| & & & |\alpha_1(t)| \\ & \ddots & & \vdots \\ & |Z_\xi| & & |\alpha_\xi(t)| \\ & & \ddots & \vdots \\ & & |Z_k| & |\alpha_k(t)| \end{matrix} \right\| \quad \left\| \begin{matrix} |\bar{\varphi}_1(t)| \\ \vdots \\ |\bar{\varphi}_\xi(t)| \\ \vdots \\ |\bar{\varphi}_k(t)| \end{matrix} \right\|, \tag{17}$$

where

$$|Z_\xi| = \left| \begin{matrix} 1 Z_1(t-\tau) \ldots Z_1^m(t-\tau) \\ 1 Z_1(t-\nu) \ldots Z_1^m(t-\nu) \\ 1 Z_1(t) \ldots Z_1^m(t) \end{matrix} \right| \tag{18}$$

$$\left|\alpha_{\xi}(t)\right| = \left|\begin{matrix} -\alpha_{\xi 1}(t-\tau-1) \ldots -\alpha_{\xi n}(t-\tau-1) \\ \vdots \\ -\alpha_{\xi 1}(t-\nu-1) \ldots -\alpha_{\xi n}(t-\nu-1) \\ \vdots \\ -\alpha_{\xi 1}(t-1) \ldots -\alpha_{\xi n}(t-1) \end{matrix}\right| \qquad (19)$$

$$\bar{\varphi}_{\xi}(t-\nu-1) = \left\| \begin{matrix} \left|\varphi_{\xi}(t-\tau-1)\right| \\ \vdots \\ \left|\varphi_{\xi}(t-\nu-1)\right| \\ \vdots \\ \left|\varphi_{\xi}(t-1)\right| \end{matrix} \right\| . \qquad (20)$$

System (16) is solved relative to $\{\Delta x_i\}$ and then the current values $\vec{X}(t)$, $\varphi_{\xi}[\vec{X}(t)]$, $\{\alpha_{\xi i}(t)\}$ are computed.

The moving correction method has a more rapid adaptation to the measurable parameters, but requires a greater number of computations in comparison with the method for accumulation of blocks of readings.

In both cases if at any moment in time the system receives calibration information on the vector $\vec{X}$, the $\varphi_{\xi}(\vec{X})$ and $\{\alpha_{\xi i}\}$ values are computed on its basis, not using correction data.

The $\{B_{\xi j}\}$ parameters can also be determined by solution of systems (9) and (16). If some of the $\{B_{\xi j}\}$ parameters of the channels are known and are constant, the terms containing them in equations (9) and (16) can be shifted to the right part for forming a column of free terms for the purpose of reducing the order of the system.

We note in conclusion that the realization of the considered method for attaining parametric invariance in multichannel excess remote measurement systems provides for the solution of slightly conditional systems of linear inhomogeneous algebraic equations.

BIBLIOGRAPHY

1. Korn, G. and Korn, T., SPRAVOCHNIK PO MATEMATIKE (Handbook on Mathematics), Moscow, "Nauka," 1973, 831 pages.

2. Gayskiy, V. A., "Measurement-Computation Channels With Automatic Correction of the Transfer Function for Hydrophysical Instrumentation," MORSKIYE GIDROFIZICHESKIYE ISSLEDOVANIYA (Marine Hydrophysical Research), No 2, Sevastopol', pp 136-143, 1977.

AUTONOMOUS BUOY COMPLEX FOR USE IN SUBSATELLITE POLYGON

Sevastopol' SPUTNIKOVAYA GIDROFIZIKA in Russian 1980 pp 126-132

[Article by I. B. Pavlovskiy, A. F. Petrukhnov, Ye. M. Epshteyn and G. A. Abramson]

[Text]

Abstract: The technical specifications, block diagram and design principle for an autonomous (self-contained) buoy complex intended for stationary observations of physical processes in a subsatellite polygon in the ocean are examined.

Autonomous buoy complexes (ABC) are used in oceanographic investigations. These complexes are outfitted with modern electronic instrumentation and means for the distant transmission of data, this making it possible to carry out stationary observations of physical processes in the range of temporal and spatial scales [2]. Buoy complexes are used as independent (self-contained) measurement systems collecting the necessary volume of hydrophysical information. The development of satellite oceanography provides for both the development of methods and instrumentation for remote measurements and the development of contact measurements necessary for the calibration and interpretation of data obtained by remote instruments with the use of artificial earth satellites. Accordingly, buoy complexes are being used at the present time in higher-order measurement systems consisting of artificial earth satellites, autonomous buoy complexes and a center for the reception and processing of information. The use of buoy complexes in subsatellite polygons provides a new approach to development of the structure of a measurement system and the organization of work in a polygon and imposes increased requirements on the technical specifications of the complex.

At the Marine Hydrophysical Institute, Ukrainian Academy of Sciences, specialists are carrying out work for creating different measurement facilities for subsatellite polygons, one of which is the "Okean" autonomous buoy complex developed in collaboration with specialists of the institutes of the Ministry of Higher and Specialized Secondary Education of the USSR and the Ukrainian SSR. The experience accumulated in the USSR and United States in the creation of buoy complexes [3-9] determines a new approach to development of the "Okean" autonomous buoy complex.

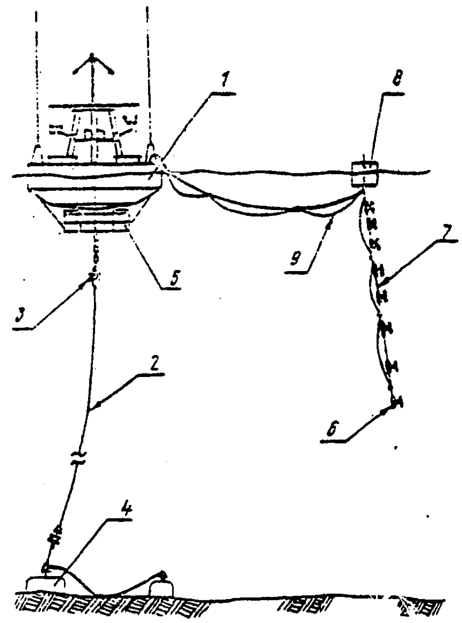

Fig. 1. Diagram of "Okean" autonomous buoy complex.

The buoy complex (Fig. 1) consists of a disk-shaped surface buoy 1 with four hermetically sealed compartments for the placement of on-board electronic instrumentation, anchored in the polygon to be investigated by means of an anchor line 2 formed by a steel cable of variable diameter. The anchor line has two cable pivots 3 and an anchor 4. Beneath the bottom of the buoy there is an assembly with power modules 5. Attached to the buoy is a measurement line consisting of eight hydrological measurement containers 6, connected by a supporting-electrical communication line 7. The line is supported by a float 8. Parallel to the measurement line is a steel cable 9 connected to it by clamps. Mounted on the buoy deck are antennas for short- and ultrashort-wavelength radio lines, a meteorological block with sensors and signaling lamps. The buoy has the following technical specifications: displacement 7.7 m^3; hull diameter 3.5 m; height of hull 1.1 m; height with antennas 8 m; fully outfitted weight 3300 kg; depth of placement up to 5000 m; limit of self-contained operation 30 days.

The structure of a buoy anchor line rated for placement at a depth of 4700 m is given in Table 1.

The deflection of the anchor line corresponds to 5% of the depth of placement. A sixth link of the anchor line runs between anchors with a mass of 300 and 500 kg.

The measurement system of the "Okean" complex (Fig. 2) includes a measurement line, a block for the reception and storage of hydrophysical information, a meteorological measurement container with sensors, apparatus for the storage and transmission of hydrophysical information, unit for signaling the ship, elements of the short-wave command-information radio linkup and an electric power system. This complex ensures the measurement of the following hydrometeorological parameters: hydrostatic pressure in the range 0-2 MPa with an error not greater than 0.8% of the upper measurement limit; water temperature at different depths in the range -2 - +33°C with an error not greater than 0.05°C; specific conductivity of water in the range 17-70 mmho/cm with an error not greater than 0.02 mmho/cm; air temperature in the range -10 - +35°C with an error not greater than 0.05°C; air humidity in the range 30-98% with an error not greater than 7%; wind velocity in the range 1.5-30 m/sec with an error not greater than (0.5+0.05 V) m/sec; wind direction in the range 0-2 π rad with an error not greater than 0.15 rad; buoy listing in the range 0-0.5 rad with an error not greater than 0.08 rad.

Table 1

Number of link	Cable diameter, mm	Mass 100 m, kg	Length, m	Mass of link, kg
1	13.0	55	300	165
2	11.5	43	2000	360
3	9.1	32	1000	320
4	8.5	25	1400	350
5	11.5	43	235	103
6	13.0	55	75	42
Sums			5010	1840

The system provides for outputs of the measured parameters in the form of a successive binary code with a repetition rate of 100 and 600 Hz.

The measurement system of the autonomous buoy complex is a multichannel system for the collection, storage, processing and transmission of hydrometeorological information. It includes sensors with a frequency output in the range 0-120 KHz and sensors with a resistive output in the range 100-2000 ohm. Temperature is measured by a transducer whose operating principle involves the discrimination of the difference frequency of two generators with temperature-dependent and temperature-stable quartz resonators [1]. Hydrostatic pressure is measured by use of vibrating-reed pressure frequency converters of the DDV-A type. The conductivity of sea water is measured by the combined contact-induction method. Meteorological parameters are measured using sensors of an M-49 meteorological station and a PDK-3 sensor-compass. The outputs of these sensors are matched by signals from the measurement system. The apparatus operates on the principle of time separation of signals from the sensors and is designed for the successive interrogation of 64 measurement sensors. In accordance with a prestipulated program, for example, each ten minutes, by means of a quartz programming unit, a device is cut in for the collection of information and this shapes command signals arriving simultaneously at the inputs of decoders distributed in all the measurement containers. After decoding of the address of the corresponding channel each sensor is connected to the input of a converter, and then, with the arrival of the next address, the next sensor is connected.

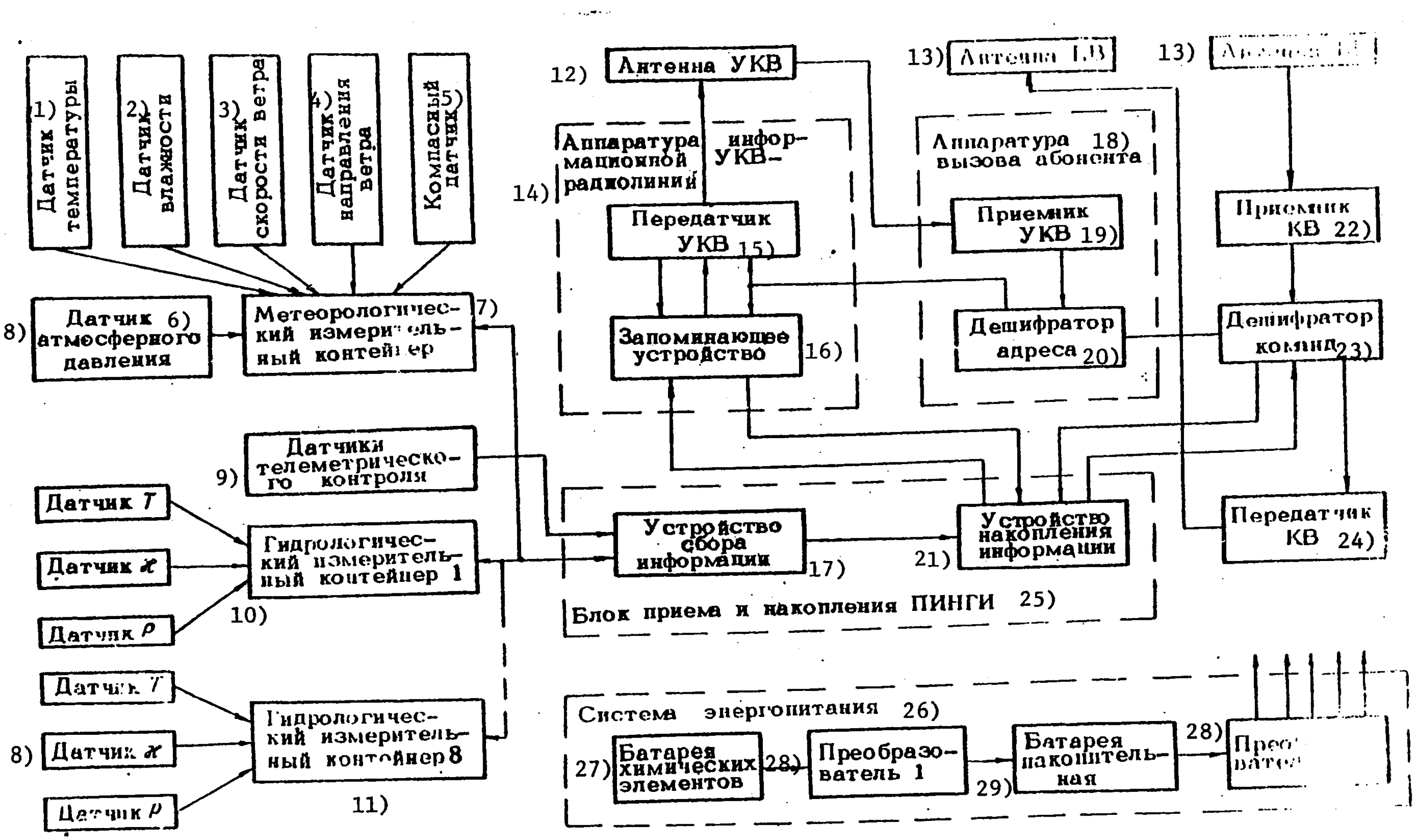

Fig. 2. Block diagram of instrumentation on "Okean" autonomous buoy complex. Annotations on next page.

KEY TO FIG. 2:

1) Temperature sensor
2) Humidity sensor
3) Wind velocity sensor
4) Wind direction sensor
5) Compass sensor
6) Atmospheric pressure sensor
7) Meteorological measurement container
8) Sensor...
9) Telemetric monitoring sensors
10) Hydrological measurement container 1
11) Hydrological measurement container 8
12) Ultrashort-wave antenna
13) Short-wave antenna
14) Apparatus of informational ultrashort-wave radio links
15) Ultrashort-wave transmitter
16) Memory unit
17) Data collection unit
18) Apparatus for signaling ship
19) Ultrashort-wave receiver
20) Address decoder
21) Data storage unit
22) SW receiver
23) Command decoder
24) Short-wave transmitter
25) PINGI unit for data reception and storage
26) Electric power system
27) Battery of chemical elements
28) Converter
29) Storage battery

Thus, there is successive connection of all the sensors to the converters. The interrogation cycle lasts 22 seconds. Information in the form of a frequency or resistance is fed into a unit for the collection of data where it is converted into a digital-pulse form and then into a binary code which is fed into a data storage unit. The latter consists of a summator, operational memory device and transmitter of codes to the buoy memory unit. Using the summator and memory unit there is accumulation of the results of measurements separately for any channel and storage of the averaging results. After a definite number of averaging cycles, set by the program, the result is sent to the buoy memory unit where there is excess coding of information. There data are stored over the course of 24 hours. The interrogation apparatus, after the reception and decoding of the buoy address, cuts in the buoy memory unit for the reproduction of data and transmission through an ultrashort-wave radio link during one communication session to an artificial earth satellite. In necessary cases there can be repeated reproduction of the information, which is transmitted in a 32-digit code. The word must first give the number of the channel and then the measurement result. Each measurement cycle, consisting of 64 words, is separated at the beginning and end by marker words. The number of the particular buoy is transmitted in the zero channel.

In case of necessity, upon command, the information at a real time scale can be transmitted through the short-wave radio link to a shipboard radio center. In addition, the short-wave radio link ensures the reception and decoding of the 12 control commands transmitted from the radio center.

The supplying of power to the buoy instrumentation is ensured by a power system whose primary power source is a battery of chemical elements on the basis of an Mg-CuCl electrochemical system with an electrolyte in sea water. A battery of 24 elements ensures self-contained operation of the autonomous buoy complex for a month. The primary voltage of the battery is transformed into the ratings necessary for supplying of the electronic instrumentation.

In 1979 our country's first specialized oceanographic satellite, the "Cosmos-1076," was launched into orbit. Its purpose was the perfecting of a method for multisided synchronous measurements of hydrophysical parameters of the ocean surface using remote sounding instrumentation. A control-calibration subsatellite polygon was created in the eastern part of the tropical Atlantic Ocean for matching the data from remote measurements with direct measurements of physical parameters. There, using the "Okean" autonomous buoy complex and other technical apparatus, contact measurements were made of atmospheric and oceanic parameters. The buoy complex was used in making around-the-clock measurements of the parameters and storing data in the memory unit. With the appearance of an artificial earth satellite in the zone of radio visibility upon receipt of a call signal data are transmitted from the autonomous buoy complex to the satellite. Then it is communicated to a surface reception station in the general flow of satellite scientific information. A radio center was organized on the scientific research ship carrying out the hydrological survey of the polygon and this center monitored the functioning of the autonomous buoy complex and the satellite command radio line.

The transmitted data are registered on magnetic tape and in analog form are plotted on a paper tape for speedy analysis and evaluation of functioning of the autonomous buoy complex. Data are transmitted on the level of the signals, the numbers of the measurement channels (64) and data proper in a binary code.

The experience of work with the autonomous buoy complex in the ocean, functioning in an active regime for 18 days, during which there were 16 communication sessions, demonstrated that the principles adopted in constructing the complex make its use possible for long-term placement in the ocean and the routine collection of a great volume of scientific information which cannot be obtained with traditionally used measurement apparatus.

BIBLIOGRAPHY

1. Golembo, V. A., Kotlyarov, V. L. and Shchvetskiy, B. I., P'YEZOKVARTSEVYYE ANALOGO-TSIFROVYYE PREOBRAZOVATELI TEMPERATURY (Piezoquartz Analog-Digital Temperature Converters), L'vov, "Vysshaya Shkola," 1970, 170 pages.

2. Monin, A. S., Kamenkovich, V. M. and Kort, V. G., IZMENCHIVOST' MIROVOGO OKEANA (Variability of the World Ocean), Leningrad, Gidrometeoizdat, pp 31-33, 1974.

3. RUKOVODSTVO PO GIDROLOGICHESKIM RABOTAM V OKEANAKH I MORYAKH (Manual on Hydrological Work in the Oceans and Seas), Second Edition, Leningrad, Gidrometeoizdat, pp 505-511, 1977.

4. United States Patent No 3828380, "Fixed Columnar Surface Buoy," Published 13 Aug 74. MKI V63V 21/52, NKI 9/8.

5. United States Patent No 3906565, "Drifting Oceanic Buoy," Published 1974. MKI V63V 35/00, NKI 9/8.

6. Sukhovey, V. F. and Sukhovey, A. G., "Hydrochemical Processes and Problems in the Network of Automatic Buoy Stations in the Ocean," METEOROLOGIYA I GIDROLOGIYA (Meteorology and Hydrology), No 3, pp 106-111, 1974.

7. Winchester, S. W., "Development of Environmental Data Buoys," NAV. ENG. S., 86, No 4, pp 97-106, 1974; Discussion, pp 106-109.

8. Vonbun, F. O., "Earth and Ocean Applications Physics Program (EOPHP). An Overview," IEEE INTERCOM. TECHN. PROGRESS PAP. INT. CONF. AND EXPOSIT., New York City, Sec 34, pp 31/1, 1974.

9. Erochko, A. A. and Koulechoff, S. V., "Group de mesure a commande automatique sur bonee, avec transmission des informations par radio," COLLOQUE INTERNATIONAL SUR L'EXPLOITATION DES OCEANS, Bordeaux (France), Mars, 1971, Theme V, Tome H, Paris, pp 202-203, 1971.

DETERMINATION OF VERTICAL TEMPERATURE PROFILE FROM DRIFTING BUOYS

Sevastopol' SPUTNIKOVAYA GIDROFIZIKA in Russian 1980 pp 133-141

[Article by I. L. Isayev, Yu. P. Lomanov and Yu. V. Terekhin]

[Text]

Abstract: The results of simultaneous measurements of temperature at three horizons and data from measurements with a distributed detector make it possible to derive an analytical expression for temperature distribution at depths 0-150 m. The mean accuracy in determining the depth of isotherms is ~ 3 m. In making measurements it is proposed that use be made of drifting buoy stations. Satellites can be used in tracking the position of drifting stations. It is assumed that information from the stations will be transmitted via satellite.

The use of space technology has afforded new possibilities for determining and monitoring the state of the ocean on a global scale [1]. In addition to improvement of the remote sensing sensors, within the framework of the "artificial earth satellite-subsatellite measurement facilities" complex there has been development of new methods for studying the ocean, among which one of the most promising is the use of drifting buoys, especially surface buoys.

Employing such a complex it is possible to investigate the structure of strong currents in the upper layer of the ocean, advective heat transfer, transformation and movement of temperature anomalies, geography of the seasonal thermocline and position of the jump layer, movement of rings in the Gulf Stream and synoptic eddies, etc.

The launching of drifting buoys into the nucleus of an eddy at different distances from its center makes it possible to determine the volume of the water masses which participates in the translational movement of the eddy and estimate the velocity of the waters present in its nucleus. The parallel use of measurements made on drifting buoys, general scanning data from artificial earth satellites and the results of polygon surveys of eddies from ships will make it possible to estimate the transfer of heat and mass by synoptic eddies.

The principal elements of the buoy are a float, radio equipment for communication with the artificial earth satellite or ship, coordination devices and units for measuring water temperature with depth T(z).

Buoy position can be determined by several methods [2], of which the most acceptable are radio direction finders (passive or active) or coordination by means of a radionavigation system installed on the buoy with the subsequent transmission of data through a radio link to a satellite or ship. The accuracy in radio direction finding is determined to a considerable degree (especially for satellite systems) by the accuracy of information on the position of the direction finder, which over the ocean is not always satisfactory.

For surface buoys it is more effective to use radionavigation systems designed in a simplified variant and performing a minimum volume of operations adequate for subsequent determination of the coordinates of buoys at the data processing point. There are definite possibilities for the use of superdistant radionavigation systems of the "Omega" type and the relaying of data from a buoy via a satellite. The error in determining the position of such a system will be about 1-2 miles with an unlimited effective range. The length of time that it can operate independently is determined exclusively by the supply of electric power aboard the buoy.

We will examine the possibility of estimating the temperature distribution. In order to know the temperature distribution with depth T(Z) it is possible to carry out measurements with a sounding instrument or make a quite detailed hydrological series. The measurements will contain methodological and instrument errors which can be estimated. Such measurements are necessary if there is no a priori information concerning the T(Z) distribution.

If it is known in advance that within the limits of accuracy in measurement by one instrument or another the dependence T(Z) satisfies the relationship

$$T(z)=f\,(z,a_i)\,,\ i=1,\dots,n, \tag{1}$$

containing the empirical coefficients a_i, it is sufficient to carry out only n measurements for determining the a_i parameters and thereby obtain the evaluation $f(Z, a_i)$ of the T(Z) distribution.

Bearing in mind the large-scale use of buoys, the possibility of their loss and the requirement of a high reliability, an effort must be made at maximum simplification and lessening of the cost of the instrumentation installed aboard them. It is also desirable to limit the volume of data transmitted through the communication channels. From this point of view it is desirable to construct the function $f(Z, a_i)$ containing a small number of a_i parameters. The possibility of using a function with a small number of parameters for finding the depth of the upper boundary of the thermocline was demonstrated in [3].

The results of measurements with the ISTOK complex, obtained during the 37th voyage of the scientific research ship "Mikhail Lomonosov," were used in checking the suitability of one of the possible dependences of the type (1) for determining the mean course of T(Z) and in making an evaluation of the necessary measurement accuracy.

We will assume that measurements with the ISTOK complex give true T(Z) profiles. Assume that T_0 is the temperature at one of the points in the layer over the thermocline, Z_{ou} is the position of the upper boundary of the thermocline, T_1 is the temperature at a fixed horizon $Z_2 > Z_0$, T_2 is the temperature at a fixed horizon $Z_2 > Z_1$, $\overline{T}$ is the mean temperature in the layer from the surface to the depth Z_2. As the experimental boundary Z_{ou} we use the depth determined by the intersection of the straight line T = const = T (Z = 0) with the tangent to T(Z) drawn through the "inflection point" closest to the isothermal layer.

As an approximation of the real temperature distribution we will examine the function

$$f(z, a_i) = \begin{cases} T_0, & z \leq z_0 \\ T_0 - (T_0 - T_2)\dfrac{z-a}{bz+c}, & z_0 \leq z \leq z_2, \end{cases} \tag{2}$$

where Z_0 is a still unknown estimate of the depth Z_{ou} of the upper boundary of the thermocline. A dependence of such a type was proposed in [4]. The function (2) contains four parameters: T_0, a, $b/(T_0 - T_2)$, $c/(T_0 - T_2)$, to be determined.

If T_0, T_1, T_2, $\overline{T}$ are measured, which can be done using three point temperature sensors, situated in the subsurface layer and at the known horizons Z_1, Z_2, and one distributed temperature sensor from the surface to Z_2, the conditions for determining the parameters a, b, c, Z_0 have the form

$$T_0 = T_0 - (T_0 - T_2)\frac{z_0 - a}{bz_0 + c}, \tag{3}$$

$$T_1 = T_0 - (T_0 - T_2)\frac{z_1 - a}{bz_1 + c}, \tag{4}$$

$$T_2 = T_0 - (T_0 - T_2)\frac{z_2 - a}{bz_2 + c}, \tag{5}$$

$$\overline{T} = \frac{1}{z_2}\int_0^{z_2} f\,dz = T_0 - (T_0 - T_2)\left(\frac{z_2 - z_0}{bz_2} - \frac{c - z_0 b}{b^2 z_2}\ln\frac{bz_2 + c}{bz_0 + c}\right), \tag{6}$$

hence

$$a = z_0, \tag{7}$$

$$b = \frac{\dfrac{T_0 - T_1}{T_0 - T_2}(z_2 - z_0) - (z_1 - z_0)}{\dfrac{T_0 - T_1}{T_0 - T_2}(z_2 - z_1)}, \tag{8}$$

$$c = (z_2 - z_0) - bz_2 \tag{9}$$

$$\frac{T_0-\bar{T}}{T_0-T_2}=\frac{\frac{T_0-T_1}{T_0-T_2}(z_2-z_0)(z_2-z_1)}{z_2\left\{(z_2-z_1)-\frac{T_1-T_2}{T_0-T_2}(z_2-z_0)\right\}}\times$$

$$\times\left\{1+\frac{\frac{T_1-T_2}{T_0-T_2}(z_1-z_0)}{(z_2-z_1)\frac{T_1-T_2}{T_0-T_1}(z_2-z_0)}\ln\frac{(T_1-T_2)(z_1-z_0)}{(T_0-T_1)(z_2-z_1)}\right\} \tag{10}$$

A numerical solution of (10) gives z_0.

Table 1

j	°C	$\bar{z}_T(T_j)$ м	Δz_j м	σ_z^2 м^2	$\sqrt{\sigma_z^2}$ м	$r\,T_j, f_j$
1	26	30,3	20	19	4,4	0,917
2	24	34	21	10	3,2	0,924
3	22	40,5	24	3	1,7	0,942
4	20	47,5	23	10	3,2	0,948
5	18	57	30	17	4,1	0,938
6	16	69	27	12	3,5	0,907
7	14	92,6	28	18	4,2	0,868

In order to check the possibility of approximating $T(Z)$ by means of $f(Z,a,b,c)$ from the experimental values $T(Z_i)$ obtained during sounding with the ISTOK complex and cited in the table for $Z_i = i\ 5$ m, $0 \leq i \leq 30$, we took T_0 ($Z = 10$ m), T_1 ($Z = 80$ m), T_2 ($Z = 150$ m) and

$$\bar{T}=\frac{1}{30}\left\{-\frac{1}{2}\left[T(z_0)+T(z_{30})\right]+\sum_{i=0}^{30}(z_i)\right\}. \tag{11}$$

Processing in accordance with (7)-(10) and construction of $T(Z)$ and $f(Z)$ curves was carried out for 30 soundings in the region $\lambda \approx 23°$W and $\varphi \approx 8°$N.

Figure 1 shows experimental $T(Z)$ dependences with the maximum Z_{0u} (solid curve), minimum Z_{0u} (long dashes) and computed (short dash-dot curve) approximations of these curves. Using the criterion

$$\int_0^{z_2}|T-f|\,dz$$

the quality of the approximation in the first case is lower, and in the second case is higher than the mean for all 30 soundings. The depth of the upper boundary of the thermocline varies from 20 to 38 m.

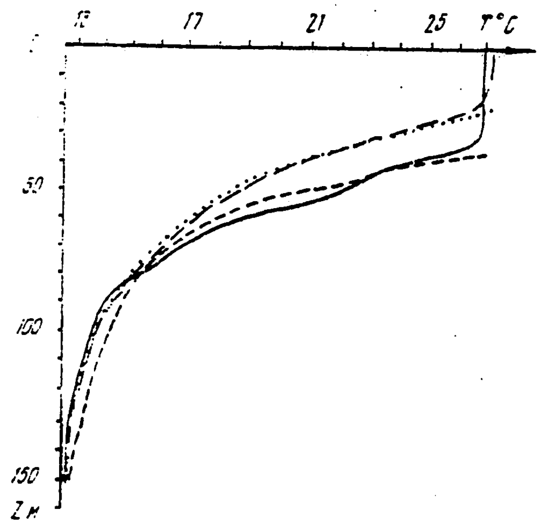

Fig. 1.

We will denote by $Z_T(T_j)$ and $Z_f(T_j)$ the depths corresponding to the temperature T_j on the basis of the dependences $T(Z)$ and $f(Z)$. For the isotherms 26, 24, 22, 20, 18, 16 and 14° we found the dispersions of the computed depth from the experimental value

$$\sigma_z^2 (T_j) = \frac{1}{30} \sum_{i=1}^{30} \left[z_{T,i} (T_j) - z_{f,i} (T_j) \right]^2, \tag{12}$$

the results are given in the table, where $\overline{Z}_T (T_j)$ is the mean depth of the isotherm; ΔZ_j is the experimentally registered range of change in depth of the isotherms; $\sqrt{\sigma_z^2}$ is the standard deviation of the evaluation. The distribution of the mentioned deviations is given in Fig. 2. Along the horizontal axis we have plotted the moduli of the deviations with an interval of one meter; along the vertical axis -- the mean probability of the deviations for the intervals.

The mean dispersion of the deviations $(Z_f - Z_T)$ for all the isotherms was $\sigma_z^2 = 12.4$ m^2 ($\sqrt{\sigma_z^2} = 3.5$ m); the mean value of the moduli of the deviations is 2.8 m, which is the characteristic of approximation accuracy. Since the displacements of the isotherms are ~25 m, it must be assumed that the registry of these displacements by the proposed method is accomplished with a mean accuracy 10-15%. The computed evaluation Z_0 was shifted by 3.2 m in the direction of greater depths in comparison with Z_{ou}. The dispersion of the evaluation is

$$\sigma_0^2 = \frac{1}{30} \sum_{i=1}^{30} \left[(z_0)_i - (z_{ou})_i \right]^2,$$

the standard deviation is 4.7 m.

The correlation coefficient

$$r(T_j,f_j)=\frac{\overline{[z_T(T_j)-\overline{z_T(T_j)}]\,[z_f(T_j)-\overline{z_f(T_j)}]}}{\sqrt{\overline{[z_T(T_j)-z_T(T_j)]^2}}\sqrt{\overline{[z_f(T_j)-\overline{z_f(T_j)}]^2}}} \tag{13}$$

is not dependent on the bias of the evaluations.

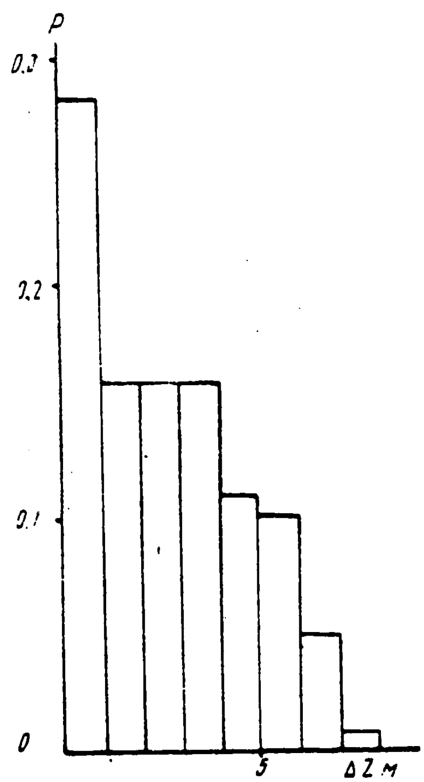

Fig. 2. Histogram of accuracy of evaluations of depth of isotherms.

The values of the correlation coefficients for different isotherms, indicated in the last column of the table, in 6 out of 7 cases exceed 0.9. The amplitudes of the changes in Z_T and Z_f are virtually identical. The correlation coefficient for Z_0 and Z_{ou} is equal to 0.834. These results give basis for assuming that the approximation (2) makes it easy to trace the changes in depth of the isotherms with time, especially internal waves.

We will proceed to an evaluation of the role of measurement accuracy

$$T_0,\, T_1,\, T_2,\, z_1,\, z_2 \tag{14}$$

under the assumption that the real temperature profile T(z) coincides with the function f(Z), determined by expression (2) with

$$T_0=\overline{T}_0=27{,}18^\circ,\ T_1=\overline{T}_1=14{,}67^\circ,$$
$$T_2-\overline{T}_2=12{,}46^\circ,\ (\overline{T})=17{,}82^\circ,$$
$$z_1=80 \text{ м},\ z_2=150 \text{ м}, \tag{15}$$

where averaging was taken for all 30 soundings taken into account. Then Z_0 = 33.5 m, b = 0.883, c = −15.9 m.

It is desirable to evaluate the error in determining the depth z of the isotherm T in dependence on the accuracy of information on the parameters (14). Taking into account the assumption T ≡ f and formulas (7)-(9), we solve (2) relative to Z

$$z=\frac{z_2 z_1 (T_0-T)(T-T_2)+z_2 z_0 (T-T_1)(T_0-T_2)-z_0 z_1 (T-T_2)(T_0-T_1)}{-z_0 (T_0-T)(T-T_2)-z_1 (T-T_1)(T_0-T_2)+z_2 (T-T_2)(T_0-T_1)}\,. \tag{16}$$

The results of measurement of the parameters can differ from their real values (14). Varying these parameters in (16), we obtain a formal evaluation Z_{inst} of the accuracy in determining the depth of the isotherm T in the first approximation.

Expression (16) contains both explicit and implicit (through Z_0) dependences on T_0, T_1, T_2, $\bar{T}$, Z_1, Z_2, and therefore in the computations we used the expression

$$\Delta Z_{\text{пр}} \approx \left(\frac{\partial Z}{\partial T_0} + \frac{\partial Z}{\partial Z_0}\frac{\partial Z_0}{\partial T_0}\right)\Delta T_0 + \left(\frac{\partial Z}{\partial T_1} + \frac{\partial Z}{\partial Z_0}\frac{\partial Z_0}{\partial T_1}\right)\Delta T_1 + \left(\frac{\partial Z}{\partial T} + \frac{\partial Z}{\partial Z_0}\frac{\partial Z_0}{\partial T_2}\right)\Delta T_2 + \\ + \frac{\partial Z}{\partial Z_0}\frac{\partial Z_0}{\partial \bar{T}}\Delta \bar{T} + \left(\frac{\partial Z}{\partial Z_1} + \frac{\partial Z}{\partial Z_0}\frac{\partial Z_0}{\partial Z_1}\right)\Delta Z_1 + \left(\frac{\partial Z}{\partial Z_2} + \frac{\partial Z}{\partial Z_0}\frac{\partial Z_0}{\partial Z_2}\right)\Delta Z_2 . \tag{17}$$

We will cite the result relating to the T(z) distribution corresponding to the adopted set of parameters (14)

[пр = inst]

$$\Delta Z_{\text{пр}} \approx \frac{1}{\{-0{,}073(T_0-T) - 1{,}162(T-T_1) + 1{,}841(T-T_2)\}^2} \times \\ \times \{[0{,}385(T-T_2)(T_0-T) - 0{,}751(T-T_1)(T-T_2)]\Delta Z_1 + \\ + [-0{,}073(T_0-T)(T-T_1) + 0{,}585(T-T_1)(T-T_2)]\Delta Z_2 + \\ + 3{,}591(T-T_1)(T-T_2)\Delta T + [5{,}727(T_0-T)(T-T_2) - \\ - 11{,}531(T-T_1)(T-T_2)]\Delta T_1 + [-4{,}836(T_0-T)(T-T_1) - \\ - 0{,}952(T-T_1)(T-T_2)]\Delta T_2 + 16{,}983(T-T_1)(T-T_2)\Delta \bar{T}\}. \tag{18}$$

In formulas (18) and (19) it is necessary to substitute the temperature values, measured in degrees, and the length of the segments is represented in meters. The instrument error ΔZ_{inst} is dependent on the T parameter, in particular, for the isotherm T = 24°

$$|\Delta Z_{\text{пр}}(24^\circ)| \approx 0{,}63|\Delta Z_1| + 0{,}57|\Delta Z_2| + 3{,}6|T_0| + \\ + 9{,}7|\Delta T_1| + 2{,}3|\Delta T_2| + 17{,}2|\Delta \bar{T}|. \tag{19}$$

With an accuracy in measurements $\Delta Z_1 \approx \Delta Z_2 \approx 0.5$ m, $\Delta T_0 \approx \Delta T_1 \approx \Delta T_2 \approx 0.01°$, $\Delta \bar{T} \approx 0.03°$ the instrument error does not exceed 1.2 m. For the other isotherms ΔZ_{inst} has close values.

Now we will discuss some peculiarities of measurement of T(Z) using sounding and distributed sensors. The possibility of approximating the real T(Z) distribution is analyzed by a comparison of f(T), stipulated by the formula (2), with the temperature profiles $T_I(Z)$ obtained during sounding with the ISTOK complex. This means that the error $|T(z) - f(Z)|$ in approximating the real T(Z) profiles by the functions f(Z) does not exceed the sums of the errors $|T(Z) - T_I(Z)|$ obtained during measurement with the ISTOK apparatus and the errors $|T_I(Z) - f(Z)|$ in representation of the results of measurements $T_I(Z)$ by the f functions

$$|T - f| \leqslant |T - T_I| + |T_I - f|. \tag{20}$$

An important and unmonitorable component of the error $|T - T_I|$ can be excluded if in place of the data obtained with the ISTOK complex, the parameters T_0, T_1, T_2, $\bar{T}$ are determined using measurements from drifting buoys made simultaneously at all horizons.

The use of sounding instruments has the advantage that the measurements are made at all horizons but these measurements are not simultaneous at different depths. The sounding time to a depth of 150 m is about 3 minutes, which is not always acceptable, in particular, in investigations of short-period internal waves.

In actuality, the internal waves can have a period 10-20 minutes and a height $\sim$15 m [5]. In such a case, coinciding with the instantaneous real T(Z) profile, for example, near the upper boundary of the thermocline, $T_I(Z)$ may be deformed by 5-10 m (with respect to the position of the isotherm) in the lower part of the seasonal thermocline. The drift of the vessel from which the soundings are made and the horizontal propagation of the internal waves lead to distortions of the same character. The noted errors in measurements with the sounding instrument are random; in individual cases they can lead to the registry of isotherms displaced both upward and downward relative to their position determined by the real instantaneous profile. The limitation on sounding frequency is also important.

Thus, for solution of a number of problems in oceanic physics associated with an investigation of the structure of intensive currents in the upper layer, transfer of heat and mass by synoptic eddies, direct measurements of heat content in the layer 0-150 m, determination of the position of the seasonal thermocline, investigation of the characteristics of internal waves, etc., the use of drifting buoys is virtually the only correct investigation method. The physical and methodological principles for determining the vertical temperature profile, set forth in the article, can serve as the basis for a sensor system on drifting buoys.

BIBLIOGRAPHY

1. Nelepo, B. A., Khmyrov, B. Ye., Terekhin, Yu. V., et al., PROBLEMY, VOZMOZHNOSTI I PERSPEKTIVY KOSMICHESKOY OKEANOGRAFII (Problems, Possibilities and Prospects of Space Oceanography), Preprint No 4, Sevastopol', Izd. MGI AN Ukrainskoy SSR, 1979, 52 pages.

2. Greku, R. Kh., Ostrepov, G. A., Puchkin, V. A. and Cherkasova, A. V., DREYFUYUSHCHIYE BUI DLYA ISSLEDOVANIYA TECHENIY V OKEANE (Drifting Buoys for Investigating Oceanic Currents), Preprint, No 2, Sevastopol', Izd. MGI AN Ukrainskoy SSR, 1978, 19 pages.

3. Isayev, I. L., Lomanov, Yu. P. and Paramonov, A. N., "Interpretation of Measurements Made With a Distributed Temperature Sensor," EKSPERIMENTAL'NYYE ISSLEDOVANIYA PO MEZHDUNARODNOY PROGRAMME "POLIMODE" (REZUL'TATY 17-go REYSA NIS "AKADEMIK VERNADSKIY" I 33-go REYSA NIS "MIKHAIL LOMONOSOV") (Experimental Investigations Under the International "POLYMODE" Program (Results of the (17th Voyage of the Scientific Research Ship "Akademik Vernadskiy" and the 33d Voyage of the Scientific Research Ship "Mikhail Lomonosov")), Sevastopol', Izd. MGI AN Ukrainskoy SSR, pp 166-170, 1978.

4. Kitaygorodskiy, S. A., FIZIKA VZAIMODEYSTVIYA ATMOSFERY I OKEANA (Physics of Interaction Between the Atmosphere and Ocean), Leningrad, Gidrometeoizdat, 1970, 284 pages.

5. Isayeva, L. S., Naumenko, M. F., Rotenberg, V. A. and Yachmenev, V. Ye., "Features of Structure of the Temperature Field of the Upper Layer of the Ocean in the Northeastern Part of the Tropical Atlantic," REZUL'TATY ISSLEDOVANIY SEVERNOY CHASTI TROPICHESKOY ZONY ATLANTICHESKOGO OKEANA PO PROGRAMME "DEKALANT" (Results of Investigations Carried Out in the Northern Sector of the Tropical Zone of the Atlantic Ocean Under the "DEKALANT" [illegible] Program), Sevastopol', Izd. MGI AN Ukrainskoy SSR, pp 66-81, 1975.

EFFECTIVENESS OF REMOTE METHODS FOR INVESTIGATING THE WORLD OCEAN

Sevastopol' SPUTNIKOVAYA GIDROFIZIKA in Russian 1980 (manuscript received 30 Jun 80) pp 142-147

[Article by I. K. Ivashchenko, A. S. Lezhen and N. I. Mavrenko]

[Text]

Abstract: A study was made of the problem of determining the effectiveness of remote methods for investigating the world ocean. It is proposed that a special efficiency criterion be formed using as a point of departure the generalized criterion of efficiency of large information systems, a class to which remote measurement complexes on different carriers belong. It is shown that the problem of evaluating efficiency is one of the fundamental tasks in the forming of promising optimum systems and oceanological research programs.

Remote methods for investigating the ocean are now coming into wide use in solution of different problems in oceanology, related to the necessity for obtaining regular operational information on the state of the world ocean and the dynamics of its development on a global scale. Their use is possible and desirable only with the broad introduction into sea research of automated oceanographic systems based on modern electronic computers carried aboard surface and underwater scientific research ships, with the use of apparatus for the remote sensing of the ocean on aircraft and artificial earth satellites. Satellites can be used both for carrying out direct measurements and in the collection and relaying of information from a network of buoy stations. Since the carrying out of such global experiments requires considerable expenditures of all types of resources the need arises for carrying out special investigations, as a result of which it should be possible to obtain evaluations of the alternatives for the development of remote methods and recommendations can be formulated concerning the rational spheres of their application. A special place is allocated to the problems of planning of an experiment and evaluating the anticipated efficiency of use of remote methods.

The great many such problems involved in evaluating the feasibility of creating and using noncontact research methods in general and with the employment of space technology, in particular, can be broken down into three classes.

Finally, a third class of problems which must be solved in the development of remote instrumentation for investigating the world ocean are the problems of validating the economically optimum structures of measurement (data) systems and evaluation of their operational efficiency.

It is already clear that not one of the known research methods independently is capable of ensuring solution of all oceanological problems in the required volume. This can be handled only using a complex system which includes both contact (traditional) and remote (nontraditional) instrumentation.

The central problem in the economic validation of use of any type of instrumentation is the choice of an economic evaluation criterion. In a general case the type of criterion is determined: purpose of the investigations; characteristics of the investigated object; stage of the life cycle in which the investigation is carried out; research problems. Since a complex system belongs to the class of large technical systems and the end product of its functioning is information with stipulated characteristics, such a system can be classified as a large information (data) system.

Since reference is to an evaluation of the efficiency of operation of instrumentation in the stage of its development, an integrated approach requires allowance for expenditures in all stages of the life cycle with the time reduction factor taken into account.

In order to evaluate a complex system it is necessary to have such a criterion as would reflect the principal characteristics of its structure and functioning; assignment to a class of information (data) systems; presence of different types of subsystems (scientific research ships, aerial and space carriers of instrumentation); interaction of different subsystems; features of determination of expenditures on elements of the system.

With allowance for the considerations cited above, the criterial function can be represented in the form

$$C_{opt} = \sum_{p_{ij}=1}^{k,l} C_{pj}^{N_1} \longrightarrow min,$$

where $C_{pj}^{N_1}$ is the cost of a unit of information supplied by different types of instrumentation for the j-th problem (task) or in the form [6]

$$\overline{C}_{opt} = \sum_{p_{ij}=1}^{k,l} \frac{C_{pj}^{R_1}}{N_{\Sigma pj} / A_{jp}^{year}} + E_H \cdot k \longrightarrow min \qquad \text{(in rubles/bit)}$$

where $C_{pj}^{R_1}$ (rubles/km^2) is the cost of obtaining information on a work unit (cost of a unit work) carried out by the ρ-th instrument for the j-th problem; $N_{\Sigma pj}$ (in bits) is the total annual volume of information supplied by the ρ-th instrument for the j-th problem; A_{jp}^{year} (km^2) is the annual volume of work carried out by the ρ-th instrument for the j-th problem; $N_{\Sigma jp}/A_{jp}^{year}$ is the information content of a work unit; $E_H \cdot k$ indicates that the formula takes into account expenditures in a reduced expenditures scheme.

As limitations we have:

operational: with respect to the number of carriers of information; with respect to the computation time for data collection; with respect to the number of types of information; with respect to the quality and quantity of collected information; with respect to work volumes;

resource: with respect to expenditures on transport, remote measurement instrumentation, control, interbranch and branch data processing.

The principal difficulty in use of the criterion "cost of a unit of information" in practical computations is usually a quantitative evaluation of the pragmatic information, but the form of the criterion proposed in [6] gives approximately such an evaluation through the index $C^{R1}_{p_j}$.

In order to adopt a decision concerning the feasibility of creating and operating a system it is necessary to have an evaluation of its efficiency. If the system belongs to the class of large information systems, as in our case, the generalized efficiency criterion can be represented as the minimax of the mean gain in the broad sense, represented as the excess of the positive effect over the negative effect [6],

$$\mathcal{E}(\bar{x}) = Q_{I\,mm}(\bar{x}) - Q_{II\,mm}(\bar{x}),$$

where $\mathcal{E}(\bar{x})$ is the generalized efficiency criterion; with $\mathcal{E}(\bar{x}) > 0$ it is desirable to create and use a new system; $\mathcal{E}(\bar{x}) = 0$ corresponds to the "threshold" of feasibility; Q_I is the positive component of the effect; Q_{II} is the negative component of the effect.

The great uncertainty caused by the absence of the necessary statistical data and peculiarities of the system do not make it possible to evaluate the economic effect for all research problems on the basis of available methods.

For some percentage of the problems involved in investigating the ocean, whose solution is possible by both traditional and nontraditional means, the economic effect can be determined in accordance with a standard method using the index "annual economic effect," determined from the difference in reduced expenditures and being a special case of the generalized efficiency criterion.

For problems not having an analogue, the author of [2] proposes an approach based on use of discrete analysis methods. It must also be remembered, first of all, that the use of remote methods for the solution of unique problems may not give a direct economic effect but their solution is sought for social, political or other reasons, and secondly, the total effect from the use of new instrumentation must be calculated for all spheres of use of the results of their functioning.

Thus, the development of predictions of the development of scientific research and measurement instrumentation and formation of optimum systems for investigating and evaluating the anticipated efficiency of their operation -- these are the principal tasks whose solution will make it possible to form optimum promising programs for oceanological research, including scientifically validated long-range space programs, and in the last analysis, solve the problem of increasing the efficiency of the investigations made and the quality of their control.

The first class of problems is related to the development and choice of promising directions in investigations of the ocean from the point of view of use of remote methods.

The basis of these studies is the development of a forecast of the development of oceanology, a component part of which is an analysis of promising means and methods for studying the world ocean.

For the formulation of a prediction of scientific research the authors of [1] proposed use of a combination of statistical and heuristic methods. In a probailistic model (information-logic scheme with "loops") the sequence of states of the object -- the scientific research process -- is represented in the form of levels of the "life cycle" of the project and forms a spatially-temporally discrete Markov chain. It is assumed that at any moment in time in state space there is determination of an n-dimensional vector of state whose coordinates are the quantitative and qualitative characteristics of the project stages. All the conditions necessary for use of analysis of the Markov chain are considered satisfied, that is, stochasticity and ergodicity of the process, uniqueness of presence in a state with a given set of vector coordinates, discreteness of transitions, etc. In some cases, in addition to these general assumptions, special simplifying assumptions can be introduced into the model: uniformity of the process (the matrix is not dependent on time), irreversibility (loopless model), presence of "absorbing" states, etc. The developed method for prediction on the basis of a dynamic-stochastic model, formulated using a combination of factographic and heuristic methods with subsequent verification of the forecast evaluations, makes it possible to make the necessary choice of alternatives of development and accomplish a redistribution of resources in the optimum way.

The problem of the choice of the range of problems (directions) in investigations of the ocean, for whose solution it is best to use remote methods, can be solved by the logical-substantive analysis method, and also with the use of formalized procedures -- discrete analysis methods [2].

A second class of problems involves the choice of an optimum (or quasioptimum) structure of technical research equipment. It should be noted that virtually all remote measurement equipment for investigating the world ocean (IR radiometers, SHF scatterometers, spectrophotometers, lasers, etc.) are multipurpose instruments, by means of which it is possible to solve a whole series of scientific-technical, national economic and other problems. In this connection it is proposed that a study be made of the real remote measurement instrumentation as a system having some ordered set of classification criteria, characterizing the system as a whole. As such criteria it is possible to propose energy consumption, autonomy, cost, inertia, universality, homogeneity, immanence, reliability, size, compatibility, etc. The "instrument-criteria" matrix table unambiguously describing the system is coded in a special way in a binary reckoning system and is processed in accordance with spectral or test algorithms proposed in [2, 4]. Such a procedure makes it possible to carry out an effective choice of the apparatus (on the basis of its characteristics) necessary for installation on artificial earth satellites or other carriers. At the same time, such a classification of the instrumentation makes it possible to group it with respect to types of statistical plans for experimental research [5].

BIBLIOGRAPHY

1. Ivashenko, I. K., Lezhen, A. S. and Mavrenko, N. I., "Methodological Principles for Developing a Prediction of Fundamental Scientific Investigations in the Academic Scientific Research Institutes With Specialization in Oceanography," MATERIALY KONFERENTSII "UPRAVLENIYE NAUCHNYMI ISSLEDOVANIYAMI I RAZRABOTKHAMI" (Materials of the Conference "Control of Scientific Research and Development"), Moscow, pp 38-42, 1979.

2. Mavrenko, N. I., "On Determining the Economic Effect Under Uncertainty Conditions," TRUDY MAI. VOPROSY UPRAVLENIYA RAZRABOTKAMI I PROIZVODSTVOM LETATEL'NYKH APPARATOV (Transactions of the Moscow Aviation Institute. Problems in Control of Development and Production of Flight Vehicles), No 393, Moscow, pp 34-37, 1977.

3. Berzhitskiy, M. L., SISTEMNYY ANALIZ I STATISTICHESKOYE PLANIROVANIYE EKSPERIMENTA V ISSLEDOVANIYAKH PRI SOZDANII OB"YEKTOV NOVOY TEKHNIKI (Systems Analysis and Statistical Planning of Experiments in Investigations for the Creation of New Instrumentation). Kiev, "Znaniye," pp 9-10, 1979.

4. Lezhen, A. S. and Mavrenko, N. I., "Spectral Approach to the Classification of Oceanological Investigations," AVTOMATIZATSIYA NAUCHNYKH ISSLEDOVANIY MOREY I OKEANOV (TEZISY DOKLADOV V VSESOYUZNOY SHKOLY) (Automation of Scientific Investigations of the Seas and Oceans (Summaries of Reports at the Fifth All-Union School)), Sevastopol', Izd-vo MGI AN UkSSR, pp 34-35, 1980.

5. Nalymov, V. V. and Chernova, I. A., STATISTICHESKIYE METODY PLANIROVANII EKSTREMAL'NYKH EKSPERIMENTOV (Statistical Methods in the Planning of Extremal Experiments), Moscow, "Nauka," pp 10-15, 1965.

6. Mavrenko, N. I., "Criteria and Methods for Evaluating the Efficiency of Space Vehicles and Methods for Investigating the Ocean," AVTOMATIZATSIYA NAUCHNYKH ISSLEDOVANIY MOREY I OKEANOV (TEZISY DOKLADOV V VSESOYUZNOY SHKOLY), Sevastopol', Izd-vo AN UkSSR, pp 161-162, 1980.

5303
CSO: 8144/1936

END